SKIN PERMEATION ENHANCEMENT BY TERPENES FOR TRANSDERMAL DRUG DELIVERY

KANG LIFENG

NATIONAL UNIVERSITY OF SINGAPORE
2005

Skin Permeation Enhancement by Terpenes for Transdermal Drug Delivery

Kang Lifeng
(MSc, China Pharmaceutical University)

A THESIS SUBMITTED FOR THE DEGREE OF DOCTOR OF PHILOSOPHY

Department of Pharmacy
National University of Singapore
2005

Acknowledgement

I would like to thank and acknowledge many people for their contributions to this thesis.

First of all, I am very grateful to my supervisor Associate Professor Chan Sui Yung. Thank you for your encouragement, enthusiasm, positive attitude, staunch support and guidance for my project which otherwise would not have accomplished.

To my co-supervisor Associate Professor Paul Ho Chi Lui, I express my thanks for his valuable suggestions and being always there for me. To Associate Professor Liu Xiang Yang, I thank you for sharing the cutting-edge knowledge in biophysical science and its application on pharmacy research. To his postdoctoral research fellow, Dr Prashant D Sawant, thank you for teaching me to do the routine research work. To Assistant Professor Fan Shenghua Kelly, thank you for the valuable comments on the experimental designs. I am so blessed to have taken the course you taught. To Dr Peter Johansson, thank you for teaching me the technique of using the microcalorimeter and for your continuous guidance. I would like to extend my sincere thanks to all the professors and lecturers in the Department of Pharmacy at NUS who offered their advices.

I thank all my seniors in NUS Pharmacy, especially Dr Vaddi Haranath Kumar who patiently showed to me the experiment skills. To Dr Wai-Johnn Sam, thank you for reminding me not to pollute the water sources of Singapore and to keep strictly to laboratory SOPs. And Dr Phan Toan-Thang, you showed me how much a PhD student

could achieve during four years. I wish to thank all juniors in our group. Anandaroop Mukhopadhyay, Choo Shiok Shyan, Lim Fung Chye Perry and together with all other friends, thank you for creating such a pleasant atmosphere for me in Singapore. I would like to take this opportunity to express my gratitude to Wong Pek Chuen Grace, Yeow Dingju Serene, Ang Hwee Ping, Poh Ai-Ling, Choo Qiuyi, Kan Shu Jun, Lee Hung Wah Sherry, Muhammed Taufiq Bin Jumah and Toh Tiong for the unforgettable time spent on your final year projects.

I would like to thank Chee Sze Nam,Wu Xiang, Chua Siang Meng, Lim Siok Lam and Ong Pei Shi, executives of the first Pharmacy Graduate Committee. I thank Ching Ai Ling, Soh Lay Peng Josephine, Han Yi, Lim Siok Lam, Chow Keat Theng, Zhang Wenxia, Hu Zeping, Liu Xiaohua, Liu Xin, and Yang Xiaoxia for their ardent support towards the inauguration of the AAPS-NUS Student Chapter.

All my friends for playing tennis, skating and diving with me. You helped me realize the importance of friendship and cooperation.

I thank my parents. Even as we are separated by 4000 miles I have always felt your love for me ever since I was a kid.

Table of Content

Summary

Terpenes are components of essential oils. Their enhancing effects on human skin and interactions with skin lipids were studied. **Firstly**, mathematical and statistical models for *in vitro* permeation studies using both Franz and flow-through cells were derived and tested. For Franz cells, the model allowed the accumulation of chemicals in the receptor compartment and gave comparable results as those obtained from infinite outflow methods. For flow-through cells, the proposed model provided more precise estimates than the existing models. **Secondly**, based on the models, the enhancing efficacies of 49 terpenes were studied. For monoterpenes and sesquiterpenes, the enhancing efficacies increased as their lipophilicities increased. Melting points and boiling points were negatively correlated with their enhancing effects. Monoterpenes, sesquiterpenes and diterpenes were found to be effective enhancers and sesquiterpenes were better compared to monoterpenes. Terpenes with ester and aldehyde functional groups were found to be better than the others. **Thirdly**, the enhancing effects of two terpenes on the skin were found to be reversible and the permeability of skin recovered once the enhancers were removed from the excised skin. **Fourthly,** the drug and enhancers were incorporated into Small Molecule Gelling Agents (SMGA) gels without affecting the aesthetic properties. The novel SMGA gels are suitable for topical or transdermal delivery. **Lastly**, the solubilities of Stratum Corneum (SC) lipids and ligand binding studies suggest that the enhancing mechanism of farnesol could be due to lipid extraction and/or lipid phase transition in the SC lamella. **In conclusion**, terpenes are effective skin penetration enhancers with reversible effects in both solutions and gels, that can bind and solubilize stratum corneum intercellular lipids.

List of Publications

Journal

1. **Kang L**, Liu XY, Sawant PD, Ho PC, Chan YW, Chan SY. 2005. SMGA gels for the skin permeation of haloperidol. ***Journal of Controlled Release*** 106:89-98.
2. **Kang L**, Ho PC,Chan SY. 2006. Interactions between a skin penetration enhancer and the main components of human stratum corneum lipids isothermal titration calorimetry study. ***Journal of Thermal Analysis and Calorimetry*** 83:27-30.
3. Lim FC P, Liu XY, **Kang L**, Ho PC, Chan YW, Chan SY. 2006. Organogel as a vehicle in transdermal drug delivery. ***International Journal of Pharmaceutics*** 311: 157-164.
4. **Kang L**, Fan SK, Ho PC, Chan YW, Chan SY. Improved data analysis and prediction of *in vitro* skin permeation study for drug penetration and chemical exposure. (Submitted).
5. **Kang L**, Poh AL, Fan SK, Ho PC, Chan YW, Chan SY. Reversible effects of permeation enhancers on human skin. (Submitted)
6. **Kang L**, Yeow DS, Fan SK, Ho PC, Chan YW, Chan SY. A statistical model for *In vitro* skin permeation study using Franz diffusion cell with finite outflow volume. (Submitted)
7. **Kang L**, Ho PC, Chan YW, Wong PG, Chan SY. Terpene skin penetration enhancers. (Submitted)
8. **Kang L**, Choo Q, Ho PC, Chan SY. Solubility of human stratum corneum intercellular lipids in propylene glycol and interactions with farnesol by isothermal titration calorimetry. (Submitted)

Patent

1. **Kang L**, Sawant PD, Liu XY, Chan SY. 2005. ***US patent*** application for invention "Transdermal drug delivery composition comprising an organogel and process for the preparation thereof". (Pub. No.: US 2005/0191338 A1)

Presentation

1. American Association of Pharmaceutical Scienctists Annual Meeting. 2003. Salt Lake City, USA.
2. Controlled Release Society Annual Meeting. 2004. Honolulu, USA.
3. Asia Association of School of Pharmacy Annual Meeting. 2004. Beijing, China.
4. American Association of Pharmaceutical Scienctists Annual Meeting. 2004. Baltimore, USA.
5. North American Thermal Analysis Society Annual Meeting. 2004. Williamsburg, USA.
6. Controlled Release Society Annual Meeting. 2005. Miami, USA.
7. The 17th Singapore Pharmacy Congress. 2005. Singapore
8. American Association of Pharmaceutical Scienctists Annual Meeting. 2005. Nashville, USA.

List of Tables

List of Figures

ampoule. The binding heat was derived from the measured heat subtracting the heat of the control as shown in Figure 3.6-2. The nonlinear regression model is based on $M + nL = ML_n + error$, which describes the binding reaction in this study between a host molecule M (the lipid), and a ligand molecule L (farnesol). Replicates were pooled for the nonlinear regression (replicates are 2, 3, 3 and 3 for **(a)**, **(b)**, **(c)** and **(d)**, respectively). Result of farnesol solution titrated into **(a)** cholesterol solution. Binding stoichiometry n = 1, binding constant $K = 6.79*10^4\ M^{-1}$ and ΔH = 1.40 kJ/mol, endothermic entropy-driven process. ΔG = -28.67 kJ/mol and ΔS = 97.02 J mol^{-1} K^{-1}, **(b)** behenic acid solution. Binding stoichiometry n = 2, binding constant $K = 7.62*10^3\ M^{-2}$ and ΔH = -112.93 kJ/mol, exothermic enthalpy-driven process. ΔG = -23.04 kJ/mol and ΔS = -289.98 J mol^{-1} K^{-1}, **(c)** ceramide 3 solution. Binding stoichiometry n = 2, binding constant $K = 3.10*10^6\ M^{-2}$ and ΔH = 44.81 kJ/mol, endothermic entropy-driven process. ΔG = -38.53 kJ/mol and ΔS = 268.81 J mol^{-1} K^{-1}, and **(d)** ceramide 9 solution. Binding stoichiometry n = 2, binding constant $K = 5.28*10^4\ M^{-2}$ and ΔH = 24.20 kJ/mol, endothermic entropy-driven process. ΔG = -28.03 kJ/mol and ΔS = 168.47 J mol^{-1} K^{-1}.

List of Abbreviations

Abbreviation	Full name
ANOVA	Analysis of Variance
ARES	Advanced Rheometric Expansion System
bp	boiling point
FDA	Food and Drug Administration
GP-1	N-lauroyl-L-glutamic acid di-n-butylamide
GRAS	Generally Recognized As Safe
h	hour
HP	Haloperidol
HPLC	High Performance Liquid Chromatography
ISA	IsoStearyl Alcohol
ITC	Isothermal Titration Calorimetry
LMGA	Low Mass Gelling Agent
mg	milligram
min	minute
ml	milliliter
MLR	Multiple Linear Regression
mp	melting point
MW	Molecular Weight
ng	nanogram
PDA	PhotoDiode Array
PG	Propylene Glycol
SC	Stratum Corneum
SD	Standard Deviation
SLR	Simple Linear Regression
SMGA	Small Molecule Gelling Agent
Sol	Solubility
TAM	Thermal Activity Monitor
TLC	Thin Layer Chromatography
VIF	Variance Inflation Factor
w/v	weight / volume
µl	micro liter
µm	micrometer

I Introduction

Transdermal drug delivery systems offer many advantages over conventional dosage forms such as sustained delivery, improved patient compliance, reduced side effects, elimination of first-pass effect, interruption or termination of treatment when necessary [1,2]. Haloperidol, an antipsychotic drug, is a suitable candidate for transdermal drug delivery [3]. It is a lipophilic compound with low molecular weight (375.9) and low daily maintenance dose (3 to 10 mg). There is a clinical need to develop a long-acting formulation for maintenance therapy to prevent the relapse of psychosis [4,5]. Haloperidol can only penetrate sub-therapeutically through the human skin *in vitro*, so that penetration enhancement is required for the drug to reach the therapeutic level. Chemical enhancers can increase the skin permeability by interacting with lipids and proteins in the stratum corneum, the top layer of the skin. Terpenes may increase the skin permeability by interacting with the skin lipid domains.

1.1 Human Skin Lipids and Transdermal Drug Delivery

Transdermal administration of drug has been exploited extensively in the past few years. In USA, out of 129 drug delivery candidate products under clinical evaluation, of which 51 are transdermal or dermal systems and 30% of 77 candidate products in preclinical development fall under this drug delivery category [6]. The value of market for transdermal delivery is $12.7 billion in the year 2005 and is expected to increase to $21.5 billion in 2010 and $31.5 billion in the year 2015 [7].

However, the major function of skin is as a rigid biological barrier protecting the interior milieu, rather than an amenable passage for chemicals to penetrate. Human skin is

composed of three layers, i.e., hypodermis, dermis and epidermis (Figure 1.1-1). Epidermis has five anatomical layers, which, from outermost to bottom, are stratum corneum, stratum lucidum, stratum granulosum, stratum spinosum and stratum basale (Figures 1.1-2). The stratum lucidum presents only in thick skins. All layers usually thinner in thin skin than in thick skin. Stratum corneum (SC) is the outermost layer that consists of keratin enriched dead cells, i.e., the corneocytes, surrounded by crystalline intercellular lipid domains (Figures 1.1-2 and 1.1-3). SC provides a permeability barrier that prevents desiccation and thereby permits life on dry land and at the same time prevents exogenous substances from entering our bodies so that a stable inner physiological condition can be maintained. In addition to the almost impermeable corneocytes, the barrier function is offered by the presence of a unique mixture of lipids in the intercellular spaces of the SC (Figure 1.1-4). These lipids, though acting as barriers, can provide a passage for permeation of exogenous chemicals, including drugs.

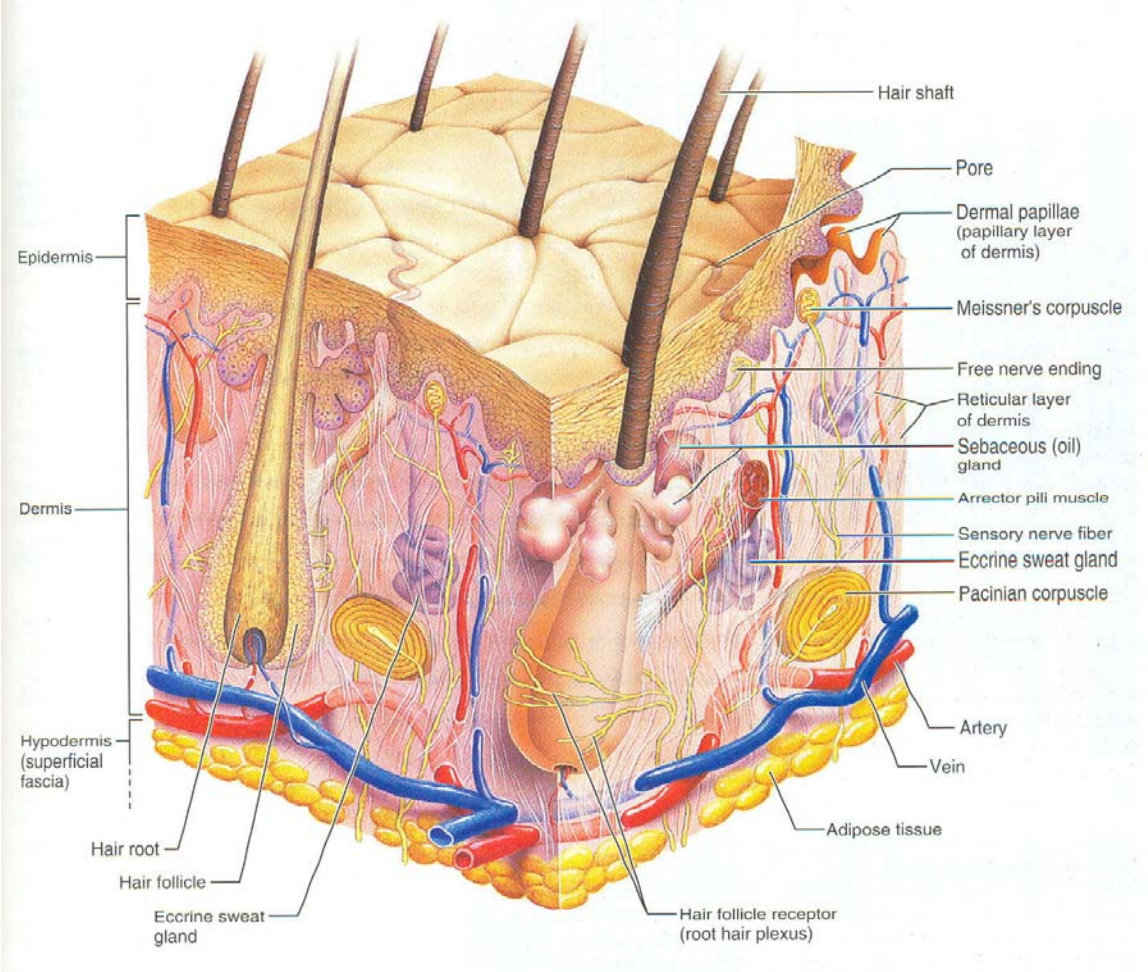

Figure 1.1-1 The human skin. Reproduced from Marieb E.N. (2003). Human Anatomy and Physiology. Pearson Education Inc.

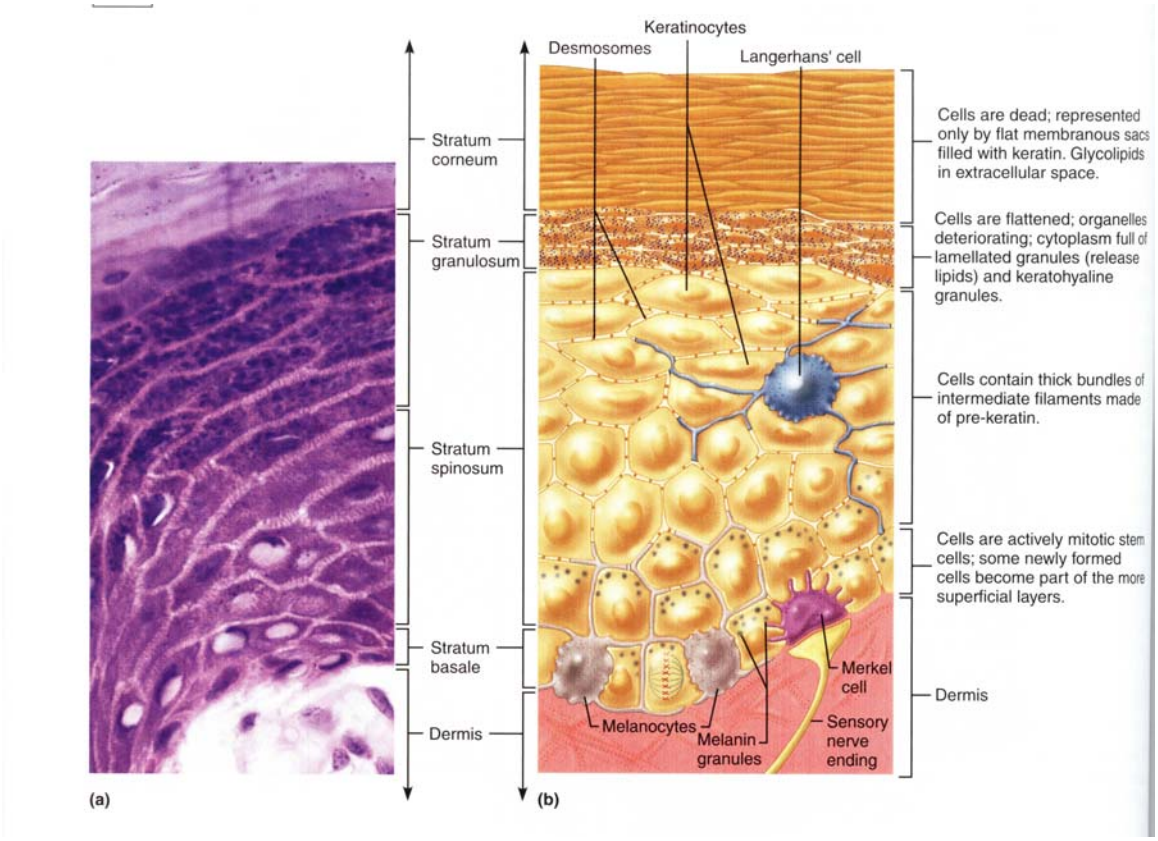

Figure 1.1-2 The human epidermis. Reproduced from Marieb E.N. (2003). Human Anatomy and Physiology. Pearson Education Inc.

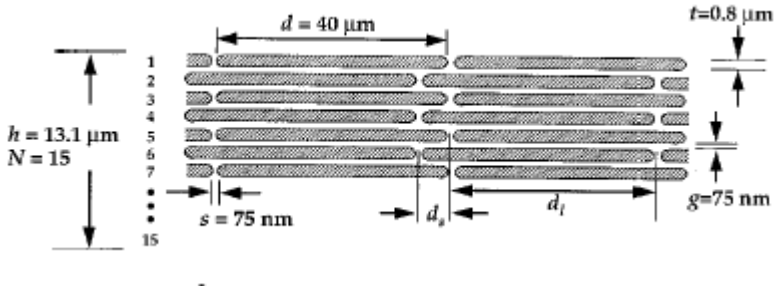

Figure 1.1-3 Stratum corneum diagram, reproduced from Mark E.J., Darnel B., Robert L. (1997). J. Pharm. Sci., 86, 1162-1172.

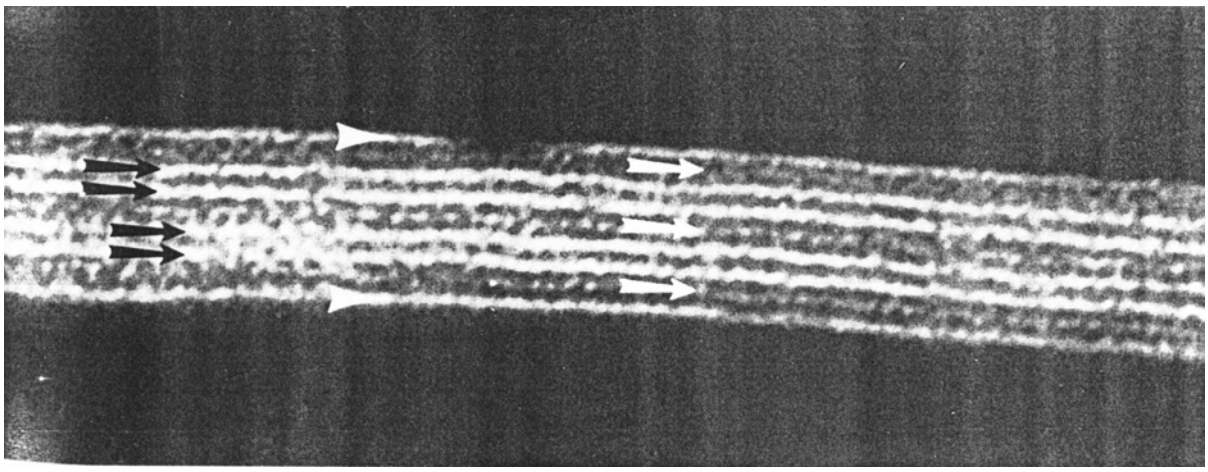

Figure 1.1-4 Stratum corneum intercellular lipids, transmission electron microscope image fixed by ruthenium tetroxide. Reproduced from Downing D.T. (1992). J. Lipid Res., 33, 301-312.

Lipids accumulate in small organelles known as lamellar granules as the epidermal keratinocytes differentiate, which occurs in the stratum granulosum, the layer just underneath the stratum corneum. The lamellar granules are extruded into the intercellular spaces where it undergoes enzymatic processing to produce a lipid mixture consisting of ceramides, cholesterol and fatty acids. The lipids are uniquely organized into a

mutilamellar complex that fills most of the intercellular space of the SC. The barrier properties of the SC are related to the phase behavior of the SC intercellular lipids. It has been proposed that a structurally unusual acylglucosylceramide is thought to be involved in assembly of the lamellar granules, and a related ceramide may have a major influence on the organization of the lamellae in the SC [8].

Intercellular lipids are organized in lamellar phases and these lamellae are oriented approximately parallel to the surface of the keratin-enriched cells. When visualized by transmission electron microscopy, the lamellae exist as broad and narrow bands (Figure 1.1-4). The broad bands are approximately 5 nm wide, and the narrow band is about 3 nm wide. Three patterns are identified as paired lipid layers, lipid monolayers and lipid envelopes.

At physiological temperature, lipids in lamellar bilayers of liposomes and membranes exist in either of two main states depending on their hydrocarbon chain lengths, a fluid crystalline state and a crystalline or gel state. If the temperature is lowered, the lipids are forced into a crystalline state. When such crystalline bilayers have water on both sides they are termed as the gel phase. A system containing aliphatic chain lengths in the range of C18-C34 is likely to be in a crystalline or a gel phase at normal skin surface temperature (approximately 28° to 32°C).

The major lipid classes that can be extracted from SC are ceramides, cholesterol and fatty acids, which make up approximately 50, 25, 10 percent of the stratum corneum lipid mass, respectively. At least 9 different subclasses of ceramide have been identified [9,10]. Each individual ceramide differs from the others in its head-group architecture and chain length distribution. The chain length of the fatty acids linked to

the (phyto) sphingosine backbone is approximately C24 and C26. The free fatty acids are straight-chained saturated species with chain lengths ranging from 16 through 30 carbons and the most abundant species are those with C24, C26 and C28. Cholesterol is a ubiquitous membrane lipid and is capable of either fluidizing membrane domains or of making them more rigid, depending on the physical properties of the other lipids and the proportion of cholesterol relative to the other components [11,12].

There are several models proposed for the arrangement of these lipids. The Singer-Nicholson model [13] has undoubtedly influenced many dermatologists and scientists who perceive the arrangement of these lipid units in the barrier as completely randomized. However, this is not compatible with the fact that there are very long hydrocarbon chains in the barrier lipids, i.e. a crystalline or gel phase, other than a liquid crystalline phase, would dominate the barrier. If the barrier lipids were in the crystalline/gel state, the mechanical properties of the lipid barrier would be compromised. This contradiction gives rise to the following two models that hypothesize the existence of a liquid crystalline sub-lattice, and another model that contradicts them. In the 'domain mosaic model' [11,14], lipids with very long chain lengths are segregated into domains in the crystalline/gel phase separated by grain borders populated by lipids with relatively short chain lengths in the liquid crystalline state. The liquid phase is a narrow continuous phase from the superficial SC layers down to the stratum granulosum-stratum corneum interface. In the 'sandwich model' [15,16], the fluid phase is mainly present in the narrow layer located in the center of the 13 nm repeating unit (Figure 1.1-5). This central lipid layer is not a continuous fluid phase as the amount of lipids forming the fluid phase in the SC is very limited. In 'single phase model' proposed by Norlen [17,18], no

phase separation between liquid crystalline and gel phases nor between different crystalline phases with hexagonal and orthorhombic chain packing, respectively, is present in the unperturbed barrier structure. The intercellular lipid within the stratum corneum exists as a single and coherent lamellar gel structure in the intercellular space of the stratum corneum. The latter two models do not adequately reconcile the proposed crystalline lamellae that would be rigid with the observed elasticity of the skin. An effective skin barrier also requires flexible and elastic lamellae to line the edge of the cell boundaries.

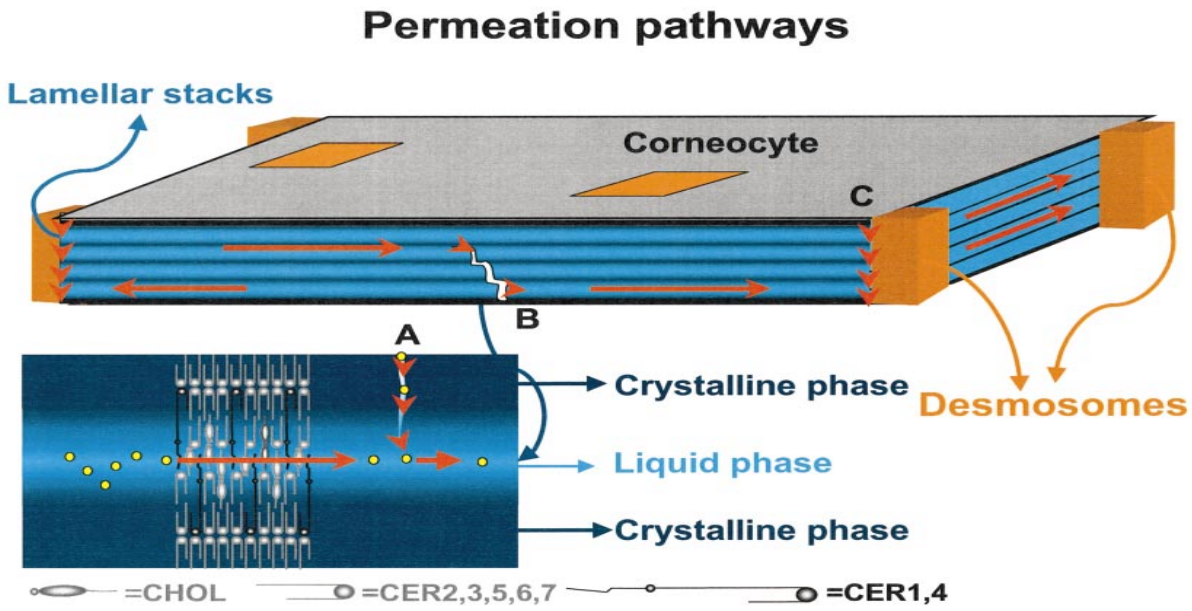

Figure 1.1-5 The 'sandwich model' of stratum corneum intercellular lipids. Reproduced from Bouwstra J.A. *et al* (2002). J. Invest. Dermatol., 118, 606-617.

From a pharmaceutical point of view, these proposed models provide general concepts of the barrier function and the permeation pathways found in the skin. It is conceivable that the fluid crystalline state sub-lattice is a region where lipids and corresponding hydrophobic molecules can permeate the barrier by diffusion forces. Penetration

enhancers, generally have short chain lengths, will preferentially reside in the fluid crystalline phase and to a certain extent, fluidize lipid units at the border of domains whereby the width of the grain border will increase and hence, permeability will increase perceivably. Terpenes are chemical skin penetration enhancers of natural sources.

1.2 Terpenes and Terpenoids

Plants contain many strong smelling components and since ancient times these components have been termed essential oils due to their volatility. Certain hydrocarbons were isolated from these essential oils. They are named 'terpenes' after 'turpentine' as turpentine oil is a mixture of these compounds [19,20]. They are usually named after the plants from which they were first isolated. Some terpenes share the same composition by percentage and some have even the same molecular weights and similar boiling points. However, they smell different, have different optical properties and behave differently in chemical reactions, therefore they are not identical.

The term 'terpene' is used to describe a compound, which is a constituent of an essential oil containing carbon and hydrogen or carbon atoms, hydrogen and oxygen atoms, and is not aromatic in character [21,22]. This definition is usually extended to include other compounds called terpenoids, which are not of natural occurrence, but are very closely related to the natural terpenes. In this report unless otherwise specified, the term terpene will refer to both the terpenes and terpenoids. Most terpenes are invariably hydrocarbons, alcohols, aldehydes, ketones, or oxides, and they may be solids or liquids. Terpene hydrocarbons are usually liquids, while terpenes of higher molecular weights,

mostly obtained from the natural gums and resins of plants and trees, are not steam-volatile.

Terpenes are defined and classified by the so-called 'isoprene rule', introduced by Wallach in 1887 [22]. Two isoprene units make one 'terpene unit'. Thus, isoprene unit number of two, three, four, five, six, and eight refers to monoterpene, sesquiterpene, diterpene, sesterterpene, triterpene and tetraterpene, respectively. A subsidiary classification is based on the number of carbon-rings present in the terpene; monoterpenes, for example, may be acyclic, monocyclic or bicyclic.

Terpenes are considered as less toxic compounds with low irritancy compared to surfactants and other skin penetration enhancers. Some are designated as generally recognized as safe (GRAS) by FDA [23,24]. These chemicals have been utilized for a number of therapeutic purposes, such as in antispasmodics, carminatives, and perfumery. Some terpenes have been reported to enhance the permeation of various drugs in transdermal drug delivery [24,25]. The permeation of drugs through human skin can be evaluated by *in vitro* methods. Franz cells and flow-through cells are among the most established cells for *in vitro* skin permeation studies. However, the mathematical and statistical models developed for them need further improvement to get more reliable estimation of the parameters such as permeability coefficient.

1.3 Modeling *In Vitro* Skin Permeation

1.3.1 Finite Outflow Volume Using the Franz Diffusion Cell

The SC, the viable epidermis and the upper layer of the papillae form the effective composite diffusion barrier layer of human skin. Subjacent are the capillaries of the microcirculation, where substances can easily diffuse into the blood stream [26].

Although the viable epidermis and the upper layer of the papillae can affect the diffusion of hydrophobic molecules, SC is the major rate-limiting barrier [26-28]. The thickness of SC is variable in different parts of the body [29,30], normally thicker in the sun-exposed areas, such as the outer forearm (12.96 ± 2.3 μm) and the inner forearm (9.58 ± 0.8 μm) [31]. The SC was generally regarded as a homogenous membrane in mathematical models of the skin permeation study. I*n vitro* skin permeation studies are used to evaluate *in vivo* skin absorption. Two types of diffusion cells commonly used are the flow-through cell [32] and static cell [33] with continuously-replaced and finite receptor solution, respectively. If the concentration of the receptor solution can be retained effectively at zero, a closed form of mathematical solution can be derived for the diffusion process [34-36], which was used for *in vitro* skin permeation study [5,26,37-39]. It is easy for the receptor solution concentration to be maintained effectively at zero with a flow-through cell by adjusting the flow rate. But with a static cells this appears to be more difficult. The aim here is to derive an equation of membrane diffusion based on finite outflow volume and to establish a statistical model to estimate the permeability coefficient. The method was exemplified by an *in vitro* skin permeation study.

Theory

The Fick's second law for one-dimensional diffusion is [35],

$$\frac{\partial C}{\partial t} = D\frac{\partial^2 C}{\partial x^2} \tag{1}$$

For a thin plane sheet or membrane of thickness l and diffusion coefficient D, almost all the diffusing substances will pass through the planar faces and only a negligible amount through the edges. With initial and boundary conditions stipulated as Eqs (2)-(4), the

solution is Eq (5) [35,40]. Eq (2) states that the concentration of the solute in the donor compartment is constant. Eq (3) stipulates that the membrane is absent of solute when permeation starts. Eq (4) describes the condition that the solution in the receptor compartment is well stirred so that the rate at which solute leaves the membrane is always equal to that at which it enters the solution. The parameters are *Q*, cumulative amount of permeated drug or chemical; *A,* the area of permeation; *K,* the partition coefficient between skin and donor solution; C_0, donor concentration of the solute; and time *t*. The dimensionless parameter *h* is given by $h = \frac{AlK}{V}$, where *V* is the outflow volume.

$$C = KC_0 \text{ at } x=0 \text{ for } t \geq 0, \tag{2}$$

$$C = 0 \text{ for } 0 < x \leq l \text{ when } t=0, \tag{3}$$

$$D\frac{\partial C}{\partial x} + \left(\frac{l}{h}\right)\frac{\partial C}{\partial t} = 0 \text{ for } x = l \text{ and } t \geq 0 \tag{4}$$

$$Q = VC_0\left\{1 - 2\sum_{1}^{\infty}\frac{h^2+\alpha_n^2}{h(h+1)+\alpha_n^2}\cdot\frac{\sin\alpha_n}{\alpha_n}\cdot e^{-\frac{\alpha_n^2}{l^2}\cdot D\cdot t}\right\} \tag{5}$$

The α_n is the *n*th positive root of Eq (6)

$$\alpha\tan\alpha = h \tag{6}$$

It follows that

$$0 < \alpha_1 \leq \pi/2,\ \pi < \alpha_2 \leq 3\pi/2,\ \ldots,\ (n-1)\pi < \alpha_1 \leq (n-0.5)\pi \tag{7}$$

For small *h*, [40]

$$\alpha_1 = \sqrt{h}(1 - h/6 + \cdots), \text{ and } \alpha_n = (n-1)\pi + h/(n-1)\pi + \cdots \tag{8}$$

With the parameter *D* unknown, Eq (5) can be developed into a nonlinear model to fit the data from *in vitro* skin permeation experiments. The model is shown as Eq (9), in which the expectation function is a nonlinear function of the parameter *D* [41,42].

$$Q_i = f(t_i, D) + \varepsilon_i \tag{9}$$

An observation Q_i can be expressed as the summation of a fixed part given by the nonlinear function $f(t_i, D)$ and the random error term ε_i. The error terms are assumed to be normal variables with zero expectation, constant variance and random distribution. Based on large-sample theory, the least squares estimators of the two parameters for the nonlinear regression model are approximately normally distributed, almost unbiased and with minimum variance. Therefore, the estimator of *D* has the *t*-distribution as follows:

$$\frac{\hat{D} - D}{s\left\{\hat{D}\right\}} \sim t(n - p) \tag{10}$$

Where $\hat{D}$ and $s\left\{\hat{D}\right\}$ are the estimator and its standard deviation, respectively, with a sample size of *n* and parameter number of *p*. Hence, the approximate $(1-\alpha)$ confidence interval for *D* is:

$$\hat{D} \pm t(1-\alpha/2; n-p)s\left\{\hat{D}\right\} \tag{11}$$

The prediction of a new observation Q_i, corresponding to a given level of *t*, can be derived similarly. The $(1-\alpha)$ confidence interval for Q_i is:

$$\hat{Q}_i \pm t(1-\alpha/2; n-2)s\left\{\hat{Q}_i\right\} \tag{12}$$

1.3.2 Infinite Outflow Volume Using Flow-through Diffusion Cell

Compared with the Franz type diffusion cells, the flow-though diffusion cells obviously make it much easier to retain the sink condition in the receptor compartment. Still the mathematical model can be derived from Fick's law [26,35]. When the donor concentration is kept constant at C_0 and receptor compartment maintains the sink condition, cumulative amount of permeated drug Q, is expressed as a function of time t. The mathematical expression relates Q to t in a nonlinear way with respect to the parameters. Therefore a nonlinear regression model has to be fitted to estimate the unknown parameters. The resultant estimates are used to calculate permeability coefficient and/or perform further hypothesis tests, but generally the error terms of the estimates from the nonlinear regression process are dropped arbitrarily, resulting in degradation of the information originally obtained from the permeation experiments [38,39,43].

This study is to establish a statistical model to encompass both the estimates and their error terms obtained from the nonlinear regression analysis, with which further pairwise comparisons can be made on the basis of all relevant information from the *in vitro* permeation. Furthermore, the prediction corresponding to a given level of t was also suggested. The method is exemplified by an *in vitro* skin permeation study with the use of chemical permeation enhancers, and the same method can be applied to exposure measurement to toxic chemicals.

Theory

The Fick's second law for one-dimensional diffusion is [35],

$$\frac{\partial C}{\partial t} = D\frac{\partial^2 C}{\partial x^2} \tag{13}$$

With initial and boundary conditions stipulated as Eqs (14)-(16), it has the solution of Eq (17) [35]. Eq (14) indicates that the membrane is absent of drug or chemical when permeation starts. Eq (15) and (16) state that the constant concentration of the drug in the donor compartment and the sink condition in the receptor compartment, respectively. The parameters are *Q*, cumulative amount of permeated drug or chemical, *A,* the area of permeation, *K,* the partition coefficient between skin and donor solution, *D,* the diffusion coefficient and *l*, path length of diffusion, C_0, donor concentration of the drug or chemical, and time *t*.

$C = 0$ for $0 < x < l$ when $t=0$, (14)

$C = KC_0$ at $x = 0$ for $t \geq 0$, (15)

$C = 0$ for $x = l$. (16)

$$Q = AlKC_0\left[\frac{D}{l^2}t - \frac{1}{6} - \frac{2}{\pi^2}\sum_{n=1}^{\infty}\frac{(-1)^n}{n^2}e^{\left(-\frac{D}{l^2}\pi^2 n^2 t\right)}\right] \tag{17}$$

Eq (17) basically describes the two stages of diffusion process, i.e., the initial transient diffusion corresponding to the exponential terms and as *t* increases the exponential terms become negligible so rapidly that *Q* becomes a linear function of *t*, showing the steady state diffusion. As *t* approaches infinity, it approaches to its asymptote as Eq (18).

$$Q = AlKC_0\left[\frac{D}{l^2}t - \frac{1}{6}\right] \tag{18}$$

The intercept of the curve on *t*-axis is defined as lag time, *Lt*. The so-named time-lag method [34] gives an easy solution to determine experimentally the diffusion coefficient, *D*, i.e. $D = l^2/6Lt$. However, it is difficult to find precisely the intercept of this

asymptote with the time axis. The pseudo-steady-state is achieved after a period of 3 times *Lt*. However, if the intercept of this pseudo-steady-state curve is used as the estimate of *Lt*, it will lead to a systematic over-estimation of the diffusion coefficient by 4%, without considerating all the other subjective errors involved to determine the intercept [35,40]. The measurement of diffusion path length *l*, on the other hand, causes even more difficulty because of the tortuous passages of the stratum corneum and its swelling behavior in water [44,45]. Values such as 10 μm [38], 13.1 μm [46], 15 μm [47], 20 μm [48], 30 μm [24] have been suggested by different authors. The application of time-lag method, originally designed for homogenous membrane like rubber, therefore, may not be suitable for the studies on skin permeation.

To circumvent the determination of diffusion path length, an alternative to diffusion parameter, the permeability coefficient K_p, also known as the permeance, is defined as Eq (19) [34,36,48-50]. Although K_p is a much less fundamental parameter than diffusion coefficient, it provides an easy solution for the skin permeation process, just as its other forms used in various diffusion applications [35].

$$K_p = K\frac{D}{l} \tag{19}$$

The slope of the asymptote as in Eq (18), divided by the permeation area, is the definition of the unit flux *J*, which intrinsically comply with Fick's first law.

$$J = \frac{dQ}{Adt} = KC_0\frac{D}{l} \tag{20}$$

Therefore, K_p can be calculated by Eq (21)

$$K_p = \frac{J}{C_0} \tag{21}$$

Eq (21) is the most frequently used method to calculate permeability coefficient [3,46,51-53]. In order to determine the permeability coefficient from Eq (21), it is necessary to find *J*. Generally, *J* is estimated from the linear portion of the permeation plot. By doing so the linear portion of the curve has to be determined subjectively and all the data on the curved region of plot, defined by Eq (17), are discarded. This can be improved by a statistical method using Eq (17) as the model to fit the full data set. Eq (17) includes both the transient and the linear portions, independent of the asymptote approximation. Since it is difficult to determine the diffusion path length, two intermediate parameters were defined as Eq (22) and (23), respectively [39].

$$K' = Kl \tag{22}$$

$$D' = \frac{D}{l^2} \tag{23}$$

As a result, Eq (17) and (19) can be re-parameterized as,

$$Q = AK'C_0\left[D't - \frac{1}{6} - \frac{2}{\pi^2}\sum_{n=1}^{\infty}\frac{(-1)^n}{n^2}e^{\left(-D'\pi^2n^2t\right)}\right] \tag{24}$$

$$K_p = K'D' \tag{25}$$

With the two unknown parameters *K'* and *D'*, Eq (24) is used as the nonlinear model to fit the data from *in vitro* skin permeation experiments. The estimates of *K'* and *D'* are then used to calculate K_p. Here the model is shown as Eq (26), in which the expectation function is a nonlinear function of the parameters *K'* and *D'* [41].

$$Q_i = f(t_i, K', D') + \varepsilon_i \tag{26}$$

An observation Q_i can be expressed as the summation of a fixed part given by the nonlinear function $f(t_i, K', D')$ and the random error term ε_i. The error terms are assumed to be normal variables with zero expectation, constant variance and random distribution. Based on large-sample theory, the least squares estimators of the two parameters for the nonlinear regression model are approximately normally distributed, almost unbiased and with minimum variance. Therefore, the estimators of *K'* have the *t*-distribution as follows.

$$\frac{\hat{K}' - K'}{s\{\hat{K}'\}} \sim t(n-p) \tag{27}$$

Where $\hat{K}'$ and $s\{\hat{K}'\}$ are the estimator and its standard deviation, respectively, with a sample size of *n* and *p* parameters. Hence, the approximate $(1-\alpha)$ confidence interval for *K'* is:

$$\hat{K}' \pm t(1-\alpha/2; n-p)s\{\hat{K}'\} \tag{28}$$

Similarly, estimates of *D'* are obtained and a $(1-2\alpha)$ confidence interval of K_p can be constructed as the product of the confidence intervals of *K'* and *D'*. Once confidence intervals of K_p from difference groups with or without enhancers are so obtained, pairwise comparisons would follow [54,55].

When large-sample theory applies, $\hat{K}'$ and $\hat{D}'$ are approximately normally distributed. If *X* and *Y* are bivariate normal random variables and the correlation between *X* and *Y* is ρ, the mean and variance of the product *XY* are [56]:

$$Mean(XY) = \mu_x\mu_y + \sigma_x\sigma_y\rho \tag{29}$$

$$Var(XY) = \mu_y^2\sigma_x^2 + \mu_x^2\sigma_y^2 + 2\mu_x\mu_y\sigma_x\sigma_y\rho + \sigma_x^2\sigma_y^2(1+\rho^2) \tag{30}$$

Therefore the point estimates of *K'* and *D'* can be calculated as Eq (29) and Eq (30), in which the estimates are obtained from the nonlinear regression.

Bootstrap sampling was employed to check the precision of sample estimates [41,57]. The method resamples from the observed data with replacement and calculates the estimated regression coefficients from the bootstrap samples with the same fitting procedure as the original fitting. The process is repeated many times to get the bootstrap estimates and their standard deviations, which are used to measure the precision of the large-sample estimates. In addition, the difference between the large-sample estimates and the mean of bootstrap sampling is an estimate of the bias of the regression coefficient estimate.

The prediction of a new observation Q_i, corresponding to a given level of *t*, can be derived similarly. The $(1-\alpha)$ confidence interval for Q_i is:

$$\hat{Q}_i \pm t(1-\alpha/2; n-2)s\left\{\hat{Q}_i\right\} \qquad (31)$$

Pairwise comparisons of the predictions of Q_i can be performed in the same way as the permeation coefficient.

The proposed statistical models formed the basis for *in vitro* skin permeation study. The efficacy and reversibility of skin penetration enhancers can be better evaluated by these models.

1.4 *In Vitro* Skin Permeation Study with Terpene Enhancers

1.4.1 Enhancing Efficacy of Terpenes

The efficacy of a skin penetration enhancer can be demonstrated by the permeability coefficient of the drug. It is interesting to establish the enhancing effects of terpene

enhancers of different categories with different functional groups. The relationship between the physicochemical properties of terpenes and their permeation enhancing effects of drugs through the skin can be investigated by statistical methods. Multiple linear regression (MLR) and other models can be used to determine relations between the permeability coefficient of the drug and the physicochemical properties of the enhancers [41]. The terpenes' properties were set as the predictor variables and the permeability coefficient (*Kp*) of HP was chosen as the response variable.

1.4.2 Reversible Effects of Terpenes

In addition to the evaluation of enhancer efficacy, the *in vitro* permeation method can also be used to test the reversibility of enhancers. An ideal skin penetration enhancer is effective, non-irritating, and reversible [58,59]. As stratum corneum (SC) regeneration takes 25 to 30 days, the loss of barrier function will persist [60]. Therefore, the effect of chemicals, in particular enhancers, on the skin is important. Some enhancers cause permanent epidermal damage that can only be repaired by SC regeneration [61-63]. On the other hand, the increased permeability of SC can return to its normal state when other enhancers are used and then removed. This temporary effect is attributed to the transient interactions between the enhancers and SC, mainly the SC lipids, which is the major diffusion passage of most small chemicals.

Carvone and eucarvone are ketone monoterpene and terpenoid, respectively. The hexagonal-ring carvone can be converted to heptagonal-ring eucarvone by a simple chemical process [64]. Carvone has two enantiomers, of which the (R)-form smells of spearmint and the (S)-form smells of caraway seeds [65]. The (S)-carvone is a skin-

irritant, so the (R)-form is a better candidate as a skin permeation enhancer [66]. Carvone is an important flavoring that is widely used in chewing gum, toothpaste, toiletries, food, drinks and other products [67]. It has been reported that carvone can enhance the skin permeation of 5-fluorouracil, tamoxifen and zidovudine [65,68-70]. Eucarvone is found in sugar mango, spearmint leaf, blackcurrant buds, Zieria and some Chinese medicinal plants like Asari Herba and Asiasari Radix [65,69,70] . Asari Herba was reported to be used as a skin penetration enhancer for administration of buprenorphine [71]. The aim of this study is to investigate the reversibility of their enhancing effects on excised human skin by *in vitro* permeation methods.

1.4.3 Incorporation of Terpenes in SMGA Gels

In all the precious permeation studies, only pure solutions of HP and enhancers in PG have been used. These form the basis for the development of semi-solid dosage forms. With similar functionality, supramolecular substances offer many advantages over traditional semi-solid dosage forms. Small molecule gelling agents (SMGA) or low-mass gelling agents (LMGA), of molecular weights less than 3000, can form supramolecular networks and immobilize water or organic solvents to yield SMGA gels [72-74]. The gelators for organic solvent are classified into five categories: fatty acids, steroids and their derivatives, anthracene derivatives, cyclo-(dipeptides), and sorbitols [74,75]. Hydrogelators consist mainly of four classes: conventional amphiphiles, bola amphiphiles, Gemini surfactants and sugar-based systems. SMGA can be used as gelling agents for almost all kinds of polar and non-polar liquids. The inherent physicochemical properties of gels, such as hardness, elasticity, clarity, and liquid-carrying capacity,

depend on the microstructure of the fiber network structure of SMGA, which in turn is determined by the mutual interactions between SMGA molecules and solvent, the degree of supersaturation, and branching agents [76-78]. The thermomechanical processing conditions such as the stress, strain, and temperature, would also influence the microstructure formation and macroscopic properties of the gels [79]. The gelation process is controlled by a crystallographic mismatch branching that leads to the formation of the Caley fractal-like interconnecting fiber network structures in the liquid [80]. These networks form highly porous superstructures and immobilize a large volume of liquid efficiently via capillary and other related forces. It is known that a SMGA can form a gel in one solvent, but may fail to form a gel in other isomeric solvents, or if formed, the network structures and properties may differ.

The gels are prepared by dissolving or dispersing the gelators in the organic solvents to prepare the sol phases which, on cooling, set to the gel state. Cooling the sol phase results in a self-assembly of the gelator molecules into 3-D permanent interconnecting nanocrystal fibrous networks, which immobilize the organic solvent. In contrast, systems consisting of nonpermanent or transient interconnecting fibers or needles can only form weak and viscous paste at low concentrations. The resultant organic gels are opaque or transparent in some cases, and thermoreversible in nature. On heating, the gel normally melts to the sol phase with an increase in the solubility of the gelator, but in some cases, complexes between gelator and solvent form at low temperature and the resulting solution will gelate with rising temperature [81]. The transition is thermoreversible in both cases.

SMGA gels are intrinsically different from microemulsions or polymeric gels. The essential components of microemulsion are oil, water and surfactant, which form circular units, stabilized by surfactant, dispersed in the leftover water or oil, i.e., the continuous phases [82]. The formation process is achieved by strong mechanical forces. Polymers immobilize bulk solvents by forming networks with their covalently connected long chains, such as the organogels formed by PG and Carbopol [83]. Some copolymers with relatively low molecular weights and narrow molecular-weight distributions possess self-assembly properties, but their molecular weights are generally two magnitude higher than that of SMGA, which is below 3000 [84-86]. For SMGA gels, the self-assembled three-dimensional fibrous network structures are formed by interconnecting nanosized fibers. The strands of SMGA gels are organized through noncovalent interaction, one of the reasons that make them thermoreversible. Apart from this, in the area of colloidal and nanoscale physics, the networks of aggregations are often found to have fractal geometry. These supramolecular materials find many applications in various fields, such as nanomaterials, lithography, biomaterial processing, tissue engineering, water purification and others [74,87-89]. In the fields of drug delivery, however, SMGA gels remain largely unexplored. The few cases that have been reported so far were briefly reviewed as follows. It is reported that a non-ionic surfactant, sorbitan monostearate, can gelate biodegradable oils and the SMGA gels formed may be suitable for a depot preparation for intramuscular administration [90]. Another study shows that L-alanine derivatives, as the gelling agent, immobilized soybean oil and medium-chain triglycerides, which can lead to *in situ* formation of an implant [91]. The most remarkable study is the antibiotic, vancomycin, which was derivatized into a hydrogelator by adding a pyrene group to its

molecule. The modified vancomycin, 11-fold more powerful than vancomycin, can dissolve in water to form a gel without additional heating. The novel mechanism of targeted delivery was attributed to the gelator-antibiotic molecules forming a lethal layer of SMGA gel which encapsulated the bacteria through self-assembly. The results could have led to a new area of drug design and delivery [92,93].

For topical or transdermal applications, only microemulsion-based organic gels have been previously reported [94-96]. The application of SMGA gels in transdermal drug delivery is thus investigated for the first time, to our best knowledge. Two SMGA gels are prepared by dissolving a small molecule gelling agent, N-lauroyl-L-glutamic acid di-n-butylamide (GP-1), into propylene glycol (PG) or isostearyl alcohol (ISA). While the ISA gels have already been extensively studied, PG is found to be gelated by GP-1 for the first time. Its rheological properties were studied by a rheological expansion system. A skin penetration enhancer, farnesol, is also incorporated. The effects of enhancer, gelator and solvent on skin permeability process are evaluated by means of *in vitro* skin permeation study with flow-though diffusion cells using a factorial design.

1.5 Actions of Terpenes on Skin Lipids

Apart from the *in vitro* permeation studies, which provide useful information at macroscopic level, the interactions between terpene enhancers and skin lipids can be studied in detail by isothermal titration method at microscopic level. The SC intercellular lipid composition differs markedly from that of typical biological membranes. The predominant extractable lipid classes are ceramides, cholesterol, and free fatty acids, the percentage (w/w) of which are about 50, 25 and 10, respectively. Nine subclasses of

ceramides have been identified in the human SC [9,10]. They are classified according to the different combinations of sphingosine and fatty acid moieties joined by an amide bond, and numbered by ascending polarity determined by TLC [97,98]. The three sphingosines are sphingosine (S), phytosphigosine (P) and 6-OH-sphingosine (H) and the three types of fatty acid are non-OH fatty acid (N), α-OH fatty acid (A) and acylated ω-OH fatty acid (O). Therefore, the 9 ceramides named as EOS, EOP, EOH, NS, NP, NH, AS, AP and AH, correspond to the ceramides 1, 9, 4, 2, 3, 6, 5, 7, 8 [9,99] (Figure 3.6-1). Ceramide 1, found in both human and pig SC, is essential for the formation of the 13-nm lamellar pattern in the X-ray diffraction study of SC lipids [100]. Ceramides 4, 6 and 8, with the 6-OH-spingosine moieties that are present only in human SC lipids, may not be essential for barrier formation [97,100,101]. The approximate ceramide composition (w/w) as determined by TLC was as follows: ceramide 1 (10%), ceramide 2 (30%), ceramide 3 (20%), ceramide 4 (10%), ceramide 5, ceramide 6, and ceramide 7 (together 15%), ceramide 8 (15%), re-numbered on ascending polarity [97,98]. Ceramide 3 was the most well characterized among all the SC ceramides [102,103]. Two artificial ceramides, i.e., ceramide 3A and ceramide 3B can also be classified as ceramide 3 although their origins in human SC have yet to be reported. Free fatty acid constituents in the human skin range from C14:0 to C28:0, and the predominant ones are palmitic acid (C16:0), stearic acid (C18:0), behenic acid (C22:0), lignoceric acid (C24:0) and cerotic acid (C26:0), which accounts for approximately of 10%, 10%, 15%, 25% and 10% (w/w) of the free fatty acids, respectively [104,105].

Farnesol is a sesquiterpene alcohol, widely distributed in the essential oils of rose and other plants [22], and is also produced in humans [106]. It has many applications in

cosmetic, food and pharmaceutical industry, for examples, food additives [107], antibacterial agents [108-110], antifungal agents [111,112], fragrance [113,114], and skin penetration enhancers for topical [115-118] or transdermal [53,119,120] delivery. As an activator of a nuclear receptor [121], farnesol can stimulate epidermal barrier and stratum corneum development [122,123]. Its interaction with lipid bilayers dimyristoylphosphatidylcholine (DMPC) revealed its preferable partitioning into and stabilizing of the liquid crystalline phase rather than the crystalline or gel phase [124,125]. The aim of this study is to investigate the interactions between farnesol and four SC intercellular lipids, i.e., cholesterol, behenic acid, ceramide 3 and ceramide 9, respectively, in propylene glycol (PG). PG is a common solvent for skincare products [126-128] and used here as the medium to dissolve farnesol and the lipids. When farnesol and the lipid interact with each other, heat is either generated or absorbed. Isothermal titration calorimetry (ITC) technique can monitor the heat flow in any physical or chemical reactions. Measurement of this heat allows the determination of reaction parameters [129,130]. Knowledge of these parameters is very helpful to elucidate the reaction of relatively weak binding [131], like the bindings in this study. The partition of the binding free energy ΔG into its enthalpy ΔH and entropy ΔS by ITC can provide information on structural changes and binding driving forces [132], while the determination of the binding stoichiometry enables the quantification of the process [133].

1.6 Objectives and hypotheses

Terpenes are promising skin penetration enhancers with low toxicity and irritancy profiles. Some terpenes have already been used in transdermal drug delivery. However, no systematic study has yet been done to address terpene skin penetration enhancement. This study, encompassing all the major terpenes from different subclasses, is to investigate systematically the efficacy, reversibility and dosage form compatibility of these chemicals, using *in vitro* skin permeation method and other techniques.

The **first part** of the study is to improve on the models of *in vitro* skin permeation experiments. Franz cells and flow-through cells are the most commonly used apparatus to investigate *in vitro* skin permeation of chemicals. However, the mathematical and statistical models of the permeation parameters derived from these experiments could be further improved. For Franz cells which feature finite outflow volumes, no mathematical models have been proposed. Models based on approximation methods are available but such models require the receptor solution to be maintained effectively at zero concentration, which, in some situations, is difficult to achieve, or very laborious if achievable. Therefore, an estimation method for the permeability coefficient of the membrane diffusion based on finite outflow volume could be developed and the resultant equation may offer a statistical solution, which allows the accumulation of chemicals in the receptor compartment. Mathematical models for flow-through cells have been proposed by other groups, but the statistical models for this experimental set-up need improvement. Statistical models that can include both the estimates together with their error terms and avoid the degradation of estimation from the nonlinear regression analysis would improve on the estimation and prediction of permeation parameters. With

these models, the permeation profiles of the drug and the terpene enhancers can be evaluated, which will form the basis of the second part of the study.

The **second part** of the study is to utilize the *in vitro* permeation method to study the efficacy and reversibility of terpenes across excised human skin, as well as their compatibilities within dosage forms. This is also an attempt to establish the relationship between the drug penetration-enhancing efficacy of each terpene with its physicochemical properties. Some useful relationships could be identified to allow the screening of other terpenes and chemicals as penetration enhancement candidates, thus avoiding laborious *in vitro* skin permeation studies and to conserve scarce human skin samples. It may also be possible to differentiate the penetration enhancing efficacies of terpenes with different functional groups. A desired characteristic of skin penetration enhancers is the reversibility of their effects on the skin so that the skin barrier function is restored upon the removal of such enhancers from the skin. An adaptation of the *in vitro* skin permeation studies could allow the reversibility effects of chemicals on skin to be evaluated. These terpene enhancers would have to be incorporated with the drug and other excipients into dosage forms for application on the skin. Their compatibilities with other excipients and the effects of novel SMGA gel formulations on the release and permeation profiles of the drug could be determined from *in vitro* skin permeation studies and rheological studies.

As it has been hypothesized that intercellular lipids of the human stratum corneum are the permeation passages for chemicals into the body, therefore extraction and/or phase transition of these lipids would affect permeation of drugs. **Lastly**, a mechanistic study of the thermal calorimetric interactions between terpenes and the intercellular lipids of

the human skin stratum corneum could offer the explanation for the underlying the kinetic investigations of terpenes on drug permeation via *in vitro* skin permeation method.

2. Materials and Methods

2.1 Materials

The following chemicals were purchased from Sigma-Aldrich Chemical Company (Steinheim, Germany): haloperidol, droperidol, DL-lactic acid, anitibiotic antimycotic solution (100 x), propylene glycol, terpinolene, α-phellandrene, ocimene, myrcene, (1R)-(-)-myrtenal, (S)-(-)-perillaldehyde, carvacrol, thymol, (R)-(-)-carvone, (1R)-(-)-myrtenol, (-)-α-thujone, (R)-(+)-pulegone, (+)-dihydrocarvone, (-)-carveol, citral, (-)-isopulegol, (+)-dihydrocarveol, (-)-dihydrocarveol, (S)-(-)-citronellal, geraniol, nerol, (±)-linalool, menthone, β-citronellol, L-(-)-menthol, cyclohexanemethanol, A-humulene, (-)-α-cedrene, (+)-β -cedrene, (+)-aromadendrene, (+)-longifolene, (-)-trans-caryophyllene, (-)-caryophyllene oxide, (-)-epiglobulol, (-)- guaiol, (+)-cedrol, (-)-isolongifolol, (-)-α-santonin, octisalate, (+)-cedryl acetate, retinol, phytol, squalene, cholesterol, palmitic acid, stearic acid, eicosanoic acid, behenic acid, lignoceric acid, cerotic acid. The following terpenes were purchased from TCI chemical company (Kyoto, Japan): (±)-α-bisabolol, farnesol, (±)-nerolidol, eucarvone, retinoic acid, β-carotene. Isostearyl alcohol (ISA) was purchased from Kishimoto Sangyo Asia Ltd (Singapore) and N-lauroyl-L-glutamic acid di-n-butylamide (GP-1) from Ajinomoto Co (Japan). Ceramide 9 (93%), ceramide 3 (94%), ceramide 3A (92.4%), ceramide 3B (98.5%) and ceramide 7 (95.6%) were provided as gifts from Cosmoferm BV (Delft, The Netherlands). All other chemical reagents were of at least reagent grade and used as supplied without further purification.

2.2 Preparation of Excised Human Epidermis

Abdominal skin was obtained from 3 different Chinese female donors with informed consent after plastic surgery at the Singapore General Hospital, Singapore. Epidermis was prepared by immersing the whole skin in 60 ^{0}C water for 2 min, followed by careful removal of the epidermis from the connective tissues [134]. Samples were stored in plastic bags at –80 ^{0}C until use. Prior to experiments, these membranes with the stratum corneum sides up were floated over 0.9% (w/v) sodium chloride solution containing antibacterial antimycotic solution (1 in 100 dilution) at 22 ± 1 ^{0}C for 2 h to equilibrate.

2.3 HPLC Method

Drug concentrations were determined by a reversed phase HPLC method (C_{18} column, Hewlett Packard) [3]. A photodiode array (PDA) detector was used to obtain the chromatographs corresponding to the wavelengths ranging from 170 to 800 nm. Mobile phase consisted of 0.05 M phosphate buffer (pH adjusted to 3) and acetonitrile with a ratio of 50:50. Droperidol was used as the internal standard. Flow rate was 1.3 ml/min and injection volume was 100 µl. Retention times of the internal standard and drug were approximately 4.9 and 6.7 min at 254 nm, respectively. Mean peak area ratios of the drug and internal standard in 0.03% (v/v) lactic acid were linearly related to the drug concentrations for the samples containing 20 to 1000 ng/ml (r^2 = 0.9990).

For the reversibility study the same HPLC method was used. Retention times of carvone and eucarvone were 5.1 and 5.6 min at 240 and 306 nm, respectively. External standard method shows the peak areas were linearly related to the enhancer concentrations in

0.03% (v/v) lactic acid ranging from 0.1 to 4 mg/ml (r^2 = 0.9999) for (R)-(-)-carvone and eucarvone, respectively.

2.4 Solubility Study of the Drug

30 mg of HP was added to 1 ml of 5% (w/v) terpene solution in PG in plastic cuvettes. The cuvettes were sonicated for 1 h in a water bath at 37 °C and kept in the water bath at 37 °C for up to 72 h. The solution was then centrifuged at 16000 rpm for 5 min and then 100 µl of the solution was carefully withdrawn from PG phase. The centrifuge time for β-carotene was 15 min to achieve better phase separation. The solution was diluted appropriately with mobile phase solution before HPLC assay.

2.5 Solubility Study of Terpenes

The enhancer was added to 1 ml of 0.03% (v/v) lactic acid in plastic cuvettes. Continuous stirring was performed for 72 h at 37 °C on a heater-stirrer (PermeGear, US). The solution was then centrifuged at 2000 rpm for 5 min and the aqueous phase was carefully withdrawn using a 1.2 x 38 mm metal needle attached to a gas tight syringe. The solution was diluted appropriately with 0.03% (v/v) lactic acid before the HPLC assay.

2.6 Solubility Study of Skin Lipids

The required amount of sample was weighed and solutions of various concentrations were made using PG as solvent in the receptor compartment of the Franz cell. A magnetic stirrer was placed into the flask which was stirred at 37 °C using a dry block for 3 days. The arms and mouth of the receptacle were sealed off with Parafilm® to avoid

contamination. At the appropriate time intervals, the sample was observed with naked eye to determine if the lipids were completely dissolved [135,136]. For the solubility of cholesterol in PG, the starting point was taken to be 1.8 mg/ml as reported [137]. The solubility of the rest of the lipids was largely determined via trial and error. A fixed amount of lipid was added in PG. The lipid concentration at which lipid particles cannot be detected by the naked eye was taken as its solubility. Tests were performed in triplicates.

2.7 *In Vitro* Skin Permeation Study

2.7.1 *In vitro* Skin Permeation Study Using Franz Diffusion Cell

In vitro permeation studies in the absence and presence of 5% w/v terpenes were carried out using amber glass Franz diffusion cells with a receptor compartment capacity of 6 ml. The receptor compartment was first filled with 0.03% v/v lactic acid containing 1% v/v antibiotic antimycotic solution. High vacuum silicone grease was then applied to both the donor and receptor compartments. The receptor solution was first degassed via sonication to ensure the absence of bubbles beneath the epidermis throughout the permeation study. Hydrated epidermis was then mounted between the donor and receptor compartments with the stratum corneum facing the donor compartment. Excess epidermis was scrapped off with forceps to minimize any lateral diffusion. The surface area of skin available for diffusion was approximately 0.79 cm^2. The epidermis was allowed to equilibrate with the receptor solution for about 0.5 h before the start of the permeation. A 1 ml of HP solution (3 mg/ml) in 100% v/v with or without enhancer was added to the donor compartment. Antibiotic antimycotic solution was added to the

receptor solutions at the concentration of 1% v/v to maintain the integrity of skin throughout the experiment and to minimize microbial contamination of samples. Both the donor compartment and sampling port were covered with parafilm and aluminium foil to prevent evaporation and minimize degradation of drug by light. The diffusion cells were maintained at the temperature of 37 ± 1°C over a dry block heater (PermeGear, USA). The contents of the receptor compartment were stirred throughout the experiment with a magnetic stirrer. Aliquots of 300 µl were withdrawn from the receptor compartment via the sampling port at predetermined time intervals for 48 h. After each sampling, the same volume of receptor solution was then replaced to maintain constant volume within the receptor compartment. Samples were then diluted appropriately with 0.03% v/v lactic acid containing 1% v/v antibacterial antimycotic solution and assayed using HPLC.

2.7.2 *In Vitro* Skin Permeation Study Using Flow-through Diffusion Cell

Flow-through type diffusion cells were used for permeation studies. Human epidermis was mounted between donor and receptor compartments and excessive skin at the sides was trimmed off to minimize lateral diffusion. Stratum corneum faced towards the donor compartment and the circular skin area for permeation was 0.785 cm^2. Since the solubility of HP in 0.03% (v/v) lactic acid solution is approximately 1 mg/ml, the receptor solution of 500 ml of 0.03% (v/v) lactic acid solution containing 1% (v/v) antibacterial antimycotic solution was placed in the reservoir bottle and allowed to flow through the receptor compartment at 0.75 ml/h. The pH of the receptor solution was approximately 3.3 but that did not affect the integrity of the epidermis [3,138]. Receptor

solution was thoroughly degassed to prevent the formation of bubbles beneath the membrane. An antibacterial and antimycotic solution was added to the receptor solutions to maintain the integrity of the skin throughout the experiment and to minimize the microbial contamination in samples during analysis. HP (3 mg/ml) in PG solutions with 5 %(w/v) of enhancer or without enhancer (control) were prepared. When the solubility of HP fell below 3 mg/ml, the solution used was at the actual concentration, for example, the concentration of HP in PG with 5 %(w/v) (R)-(-)-carvone is 2.43 mg/ml. A 1-ml solution was added to the donor compartment and covered with Parafilm® to minimize the contamination of the solution. Ambient temperature of the cells was controlled at 37 °C by a heater/circulator (Haake, Germany). The receptor solution is pumped by a 16-channel peristaltic cassette pump (Ismatec, Switzerland) continuously through the receptor compartment and drained into test-tube sitting in the fraction collector (ISCO Retriever IV, US). Cumulated receptor liquid samples were taken at 6-h intervals for HPLC assay.

2.8 *In Vitro* Skin Permeation Setup for Reversibility Study

Epidermis was cut into smaller pieces before treatment. An enhancer solution, 50 μl of 5%(w/v), or PG (as control) was applied onto the SC of the epidermis floating on 100 ml of 0.9%(w/v) sodium chloride solution containing 1 %(v/v) antibacterial antimycotic solution (hydration solution). The epidermis was then kept at room temperature for 24 h. The skin samples were rinsed five times with fresh hydration solution to remove excess enhancers left on the skin surface prior to *in vitro* permeation study. The donor solution

was 3 mg/ml HP in PG without enhancers. The rest of the permeation setup is similar to the study on untreated epidermis.

2.9 Preparation of the Terpene Solutions and Gels

Farnesol is easily miscible with PG or ISA. Clear solutions were obtained at 37 °C for all the formulae without GP-1. For the 4 gel formulae, GP-1 was weighed into a test tube and the organic solvent PG or ISA was added. The mixture was heated at $120\,^{0}C$ in an oven to dissolve GP-1 [76]. Upon dissolution, haloperidol or farnesol was added and the solution was vortexed until haloperidol was completely dissolved, normally within 30 min at about 60-120 ^{0}C. On cooling at room temperature of 22 ± 1 ^{0}C, the solution became a white, opaque or translucent organogel. For the 4 solution formulae, PG or ISA was heated to 60 ^{0}C to accelerate the dissolution of haloperidol and the solution was vortexed till haloperidol was dissolved completely. Haloperidol is photosensitive but very stable in solution [139,140]. The preparation of each of the 8 formulae was done in the dark. The first-order rate constant of drug degradation is 0.0248 day^{-1} at 110 ^{0}C [140]. Therefore approximately 0.0517% of the drug decomposed within the 30 min preparation period.

2.10 Factorial Design for the Gel Study

A 2^3 full factorial design is used to study the effect of three factors, i.e., the permeation enhancer, the gelator and the solvent, each at two levels, on the *in vitro* permeation profiles of the drug in solutions/gels, with specific focus on the permeability coefficient

K_p and lag-time Lt. For enhancer and gelator, the high level indicates their presence in the formulation and low level indicates their absence from the formula. The high and low levels of solvent are ISA and PG, respectively. Eight formulations were generated following the Yate's order [141,142]. Concentrations of haloperidol are 3 mg/ml in all the 8 formulations, respectively. The concentration of farnesol or GP-l was 5% (w/v) when applicable in the formulations. Data were analyzed by the statistical software Minitab®.

2.11 Gel Rheology Study by Advanced Rheometric Expansion System

A strain-controlled dynamic mechanical spectrometer with a temperature range from -150 to 600 ± 0.1 ^0C (ARES, Rheometric Inc., US) was used for the linear viscoelastic measurements [76,143]. A mixture of air and liquid nitrogen was used to control the cooling rate and the temperature. The sample was placed between two circular plates of diameter 25 mm having a gap of 1.5 mm between, and then subjected to sinusoidal oscillations by moving both the upper and lower plates. The frequency was set to 0.1 Hz. The amplitude of the oscillations was controlled to obtain a 0.1% maximum strain in the sample. Under this strain limit, the structure of supramolecular materials would not be destroyed by the measurements. The instant measurement of the applied stress and the resultant strain allowed the calculation of the storage modulus $G^{'}$ and the loss modulus $G^{"}$, and consequently the complex modulus G^* ($G^* = \sqrt{(G^{'})^2 + (G^{"})^2}$).

2.12 Ligand Binding Study by Isothermal Titration Calorimetry

The ITC experiments were done using a TAM2277 (Thermometric AB, Sweden) calorimeter, with 4-ml stainless steel ampoules [144]. Farnesol in PG solution was prepared at 71 or 20 mmol/L. PG solutions of cholesterol, behenic acid, ceramide 3 and ceramide 9 were prepared at 2 mmol/L, 0.667 mmol/L, 0.333 mmol/L and 0.333 mmol/L, respectively. A 0.12 ml solution of farnesol was titrated consecutively into 2.7 ml of lipid solutions in 15 aliquots. The lipid solution was stirred with a turbine at 60 rpm. The system's temperature was maintained at 37 °C. A control experiment was done by titrating farnesol solution into pure PG. ITC data were analyzed by Digitam® software (Scitech Software, Sweden) supplied with TAM2277 [43,145]. The measured heat of farnesol titrated into the lipid solution by ITC technique includes the binding heat of farnesol with the lipid, the dilution heat of farnesol, and other nonspecific heat. So the binding heat was derived from the measured heat subtracting the heat of the control experiment. The area under each peak is proportional to the fraction of the lipid that has reacted. The binding stoichiometry n, binding constant K, and enthalpy change ΔH were estimated from the nonlinear regression analysis procedure of Digitam®. The standard Gibbs free energy can be obtained from binding constant K, i.e., $\Delta G^{\circ} = -RT \ln K$, where R is the gas constant, 8.314 (J/mole.K), and T is the temperature (^{0}K). Since both ΔG and ΔH are known, the entropy change ΔS can be calculated from $\Delta G^{\circ} = \Delta H^{\circ} - T\Delta S^{\circ}$ [146].

3. Results and Discussions

3.1 Finite Outflow Volume Using Franz Diffusion Cell

Unpublished data from a study in our lab gave the value of D as approximately $1* 10^{-7}$ cm^2/h, determined by *in vitro* permeation experiments using the flow-through cell. In the study using flow-though cells, the donor solution is HP in PG and the concentration is 3 mg/ml (w/v). The diffusion coefficient D is calculated by measuring the permeability coefficient. Thus $1* 10^{-7}$ cm^2/h is chosen as the initial value for the nonlinear regression. Quick convergence of all the three groups, generally within 4 iterations indicates that large-sample theory is applicable [41]. The fitted curves and original data points are shown in Figure 3.1-2 to Figure 3.1-5. The fittings appear to be adequate. Normality plot of residuals, together with residuals against fits or order plots did not suggest any serious departures from the assumptions that the error terms are normal random variables with equal variances, though for the control group the variances moderately increased when the fit became larger. Weighted least square or transformation of the response variable Q can be used to stabilize the variances if necessary [147].

The diffusion path length l is difficult to measure because of the tortuous passages of the stratum corneum and its swelling behavior in water. In this study, the thickness of SC was assumed to be 10 μm from female abdominal skin sample [148,149] and for easy calculation. The partition coefficient was assumed to be unity, since PG is amphiphilic and to simplify the modeling process [35,50].

The estimates of the diffusion coefficient are shown in Table 3.1-1, together with the solubility results of HP. The 95% confidence interval of the control is (3.72, 5.09) $* 10^{-8}$ cm^2/h, which, according to $K_p = \frac{KD}{l}$ [36], gives the 95% confidence interval of the

permeability coefficient as (0.372, 0.509) * 10^{-4} cm/h. This interval estimate of the permeability coefficient is in agreement with the following one, (-0.000520, 3.23) * 10^{-4} cm/h, estimated from the model with infinite outflow volume (unpublished data from our lab). The confident interval of (0.372, 0.509) * 10^{-4} cm/h was more efficient than (-0.000520, 3.23) * 10^{-4} cm/h as the estimate of permeability coefficient. Comparisons of the 95% confidence intervals of the diffusion coefficients of all the 4 groups give the following results. The control, thymol and linalool group's confidence intervals overlapped with one another, but not with carvacrol. Therefore, compared with the control, only carvacrol significantly increased the permeation of HP.

Since $K_p = \frac{KD}{l}$, and Kp is assumed to be constant for a certain enhancer so that D is proportional to l/D. When the l is more than 10 μm, D will increase. On the other hand when K is bigger than unity, D will decrease. However, when both l and D are assumed to be constant then D is proportional to Kp, which can be useful to evaluate the relative enhancing abilities of the enhancers, especially to test if the addition of the enhancer will increase the drug permeation at all.

The model can be used to predict the cumulative permeation of HP for extended time period beyond the degradation of the excised SC when it does not represent the *in vivo* status (Eq 12). The model is useful for *in vitro* skin permeation study in transdermal drug delivery [150], cosmetics industry [151], and risk assessment on dermal exposure to toxic substances [152,153].

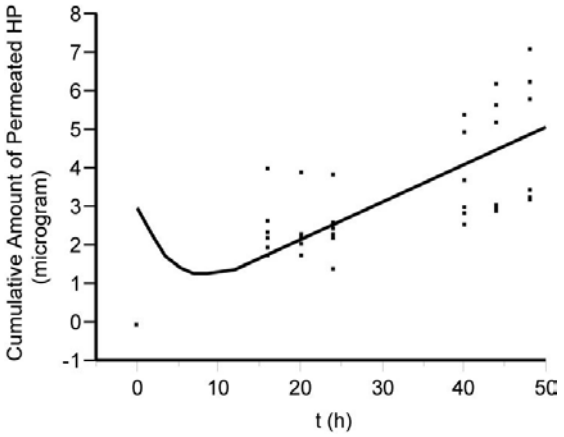

Figure 3.1-2 Control

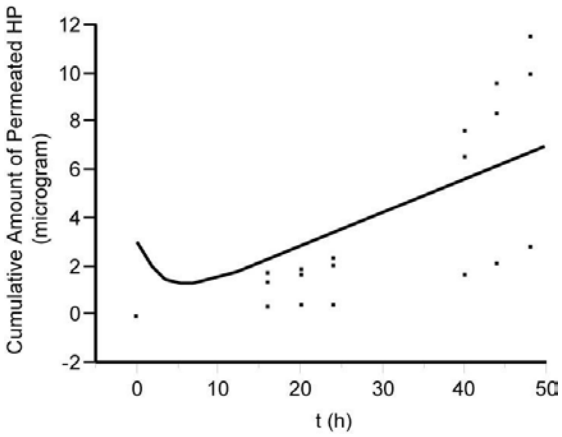

Figure 3.1-3 Linalool

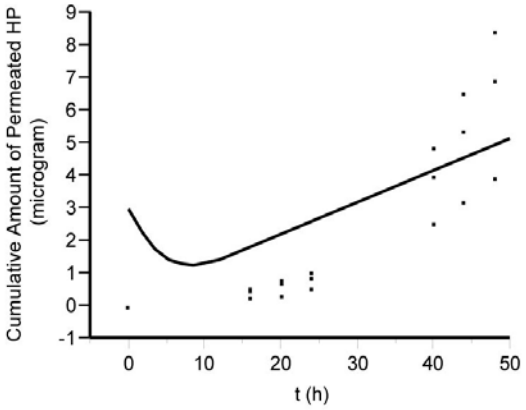

Figure 3.1-4 Thymol

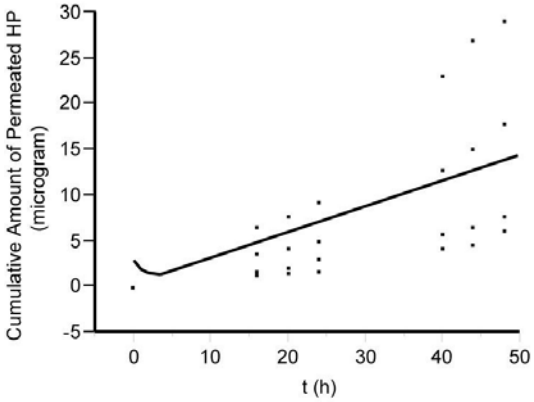

Figure 3.1-5 Carvacrol

Figure 3.1-2 to 3.1-5. Plot of the cumulative amount of permeated HP (μg) against time (h) without enhancer though a circular area of the epidermis of diameter of 1 cm. The fitted line is from the nonlinear regression (n = 48). Figure 3.1-2, without enhancer (n = 48). Figure 3.1-3, linalool (5%, w/v), (n = 24). Figure 3.1-4, thymol (5%, w/v), (n = 24). Figure 3.1-5, carvacrol (5%, w/v), (n = 36).

Enhancer	HP solubility in 5% (w/v) enhancer (mg/ml)	Diffusion coeff. $D*10^8$ (cm^2/h)	95% conf. interval $D*10^8$ (cm^2/h)
Control	3.08 ± 2.80	4.41 ± 0.337	(3.72, 5.09)
Thymol	3.56 ± 0.38	4.43 ± 0.579	(3.28, 5.58)
Linalool	3.59 ± 0.04	6.04 ± 0.824	(4.38, 7.70)
Carvacrol	3.85 ± 0.26	12.40 ± 1.59	(9.16, 15.6)*

Table 3.1-1 The solubility of HP in PG with or without 5% (w/v) enhancers. The point estimates of the diffusion coefficient, D, obtained from the nonlinear regression, and their 95% confidence interval. Data is given as Mean ± SD. * $p < 0.05$ (comparing treatment to the control)

3.2 Infinite Outflow Volume Using the Flow-through Diffusion Cell

Although the $Q(t)$ functions are derived from Fick's law, it cannot be applied in the strict mathematical sense to the skin permeation process because the actual diffusion process violates more or less the boundary and initial conditions with the changing of the diffusion path lengths, varying permeability coefficients, and imperfect sink conditions. But it can serve as a good statistical model to quantify skin permeability. Previous study shows the values of D' and K' are around 0.01 numerically [154]. Thus 0.01 is chosen as the initial value for the nonlinear regression. Quick convergence of all the three groups, generally within 10 iterations indicates that the large-sample theory is applicable [41]. The fitted curves and original data points are shown in Figures 3.2-1 to 3.2-3, and the fit appears to be adequate. Normality plot of residuals, together with residuals against fits or order plots, did not suggest any serious departures from the assumptions that the error terms are normal random variables with equal variances, though for the control group the variances moderately increased when the fit became larger.

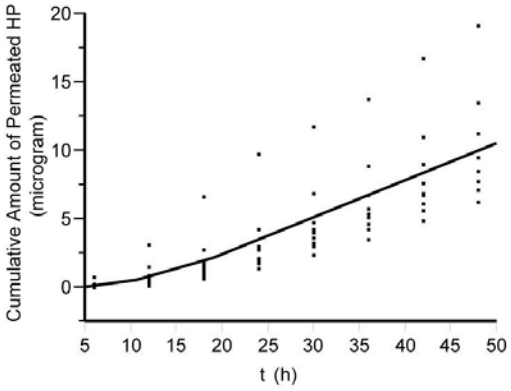

Figure 3.2-1 Control

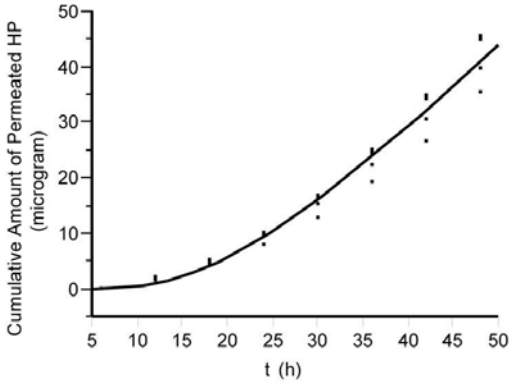

Figure 3.2-2 (+)-isolongifolol

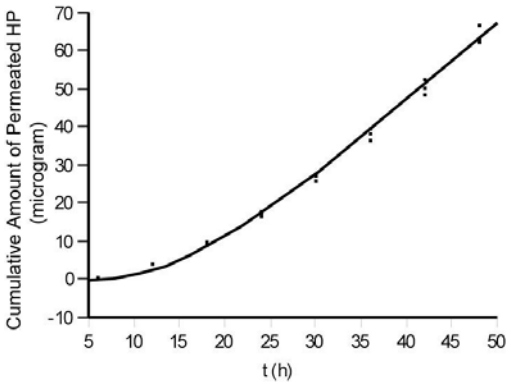

Figure 3.2-3 (-)-trans-caryophyllene

Figure 3.2-1 to 3.2-3. Plot of the cumulative amount of permeated haloperidol against time. The fitted line is from the nonlinear regression. Figure 3.2-1, no enhancer (n = 72). Figure 3.2-2, (+)-isolongifolol (5% w/v), (n = 32). Figure 3.2-3, (-)-trans-caryophyllene (5% w/v), (n = 24).

Weighted least square or transformation of the response variable Q can be used to stabilize the variances if necessary [147].

As the parameters of the nonlinear model, the inferences of D' and K' are based on Large-Sample theory. The sample sizes of control, (+)-longifolene and (-)-trans-caryophyllene groups are 72, 32 and 24, respectively, from 8, 4 and 3 replicated

permeation experiments, respectively. Point and interval estimates of *D'* and *K'* are given in Table 3.2-1, along with the bootstrapping estimates to confirm the approximateness of large-samples assumption, which are presented in columns 3 and 4. The chemical structures of the drug and enhancers are shown in Figure 3.2-4. One thousand bootstrap samples were generated for each of three groups. The histograms of bootstrapping distributions appear to be consistent with normal sampling distribution, with the bootstrap sampling distribution of control group slightly skewed to the right. The means, standard deviations and confidence intervals of bootstrapping estimates are very close to those of the large-sample's, again supporting the application of large-sample inference procedures here. The difference between the large-sample mean and the bootstrapping distribution estimate are small, which shows that the bias is negligible.

The 90% confidence intervals of permeability coefficient K_p are given in Table 3.2-2. The results carry an error rate of 10%, since the error rates of D' and *K'* are 5% each. Comparisons of the 90% large-sample confidence intervals of the permeability coefficients of the three groups give the following results. The control group's confidence interval overlaps with that of (+)-longifolene but not with (-)-trans-caryophyllene and the confidence intervals of (+)-longifolene and (-)-trans-caryophyllene overlap. Therefore, compared with the control, (-)-trans-caryophyllene significantly increased the permeation of the drug and, with an error rate of 10%, but there is no significant difference between the two enhancers with respect to the enhancement of skin permeation. The comparisons of bootstrapping confidence intervals yielded the same result. However, the overlapping part of control and (+)-longifolene is marginal, either for the large-sample confidence intervals (-0.00520, 3.23) vs. (2.78, 8.58) or for the

bootstrapping intervals, (0.167, 2.41) vs. (2.08, 8.49). Therefore, further studies are needed to obtain more effective confidence intervals for their comparisons.

Enhancer groups	K'	D'	K'^{*}	D'^{*}
Control	0.00708 ± 0.00360	0.0133 ± 0.00465	0.00872 ± 0.00626	0.0145 ± 0.00606
(n = 72)	-0.000130, 0.0143	0.00404, 0.0226	-0.0102, 0.0119	-0.00164,0.0203
(+)-longifolene	0.0741 ± 0.0130	0.00718 ±0.000662	0.0749 ± 0.0164	0.00729 ±0.000781
(n = 32)	0.0476, 0.101	0.00583, 0.00853	0.0380, 0.101	0.00547, 0.00843
(-)-trans-caryop-hyllene (n = 24)	0.0772 ± 0.00634	0.00913 ±0.000442	0.0766 ± 0.00746	0.00921 ±0.000497
	0.0641, 0.0904	0.00821, 0.0100	0.0546, 0.0877	0.00837, 0.0103

Table 3.2-1 The point estimates (Mean ± SD) of K' and D' obtained from the nonlinear regression, and their 95% confidence intervals. The bootstrapping estimates of K' and D', denoted by K'^{*} and D'^{*}, are obtained after 1000 resampling.

Enhancer groups	K_p **(cm/h) *10^4**	K_p^{*} **(cm/h) *10^4**
Control	0.777 ± 0.283	0.889 ± 0.660
	-0.00520, 3.23	0.167, 2.41
(+)-longifolene	5.23 ± 0.465	5.33 ± 0.643
	2.78, 8.58	2.08, 8.49
(-)-trans-caryophyllene	7.02 ± 0.245	7.01 ± 0.316
	5.26, 9.08	4.57, 9.04

Table 3.2-2 The point estimates (Mean ± SD) of permeability coefficient and their 90% confidence intervals, given by $K_p = K'D'$.

Enhancer groups	**After 72 h (μg)**	**After 168 h (μg)**
Control	16.84 ± 1.69	44.02 ± 6.18
	13.48, 20.21	31.69, 56.35
(+)-longifolene	78.13 ± 3.45	231.06 ± 16.06
	71.08, 85.18	198.26, 263.87
(-)-trans-caryophyllene	113.73 ± 2.19	316.68 ± 9.12
	109.17, 118.28	297.76, 335.60

Table 3.2-3 The point estimates (Mean ± SD) and the 95% confidence intervals of cumulative amount of permeated drug, after 72 hours and 168 hours, respectively.

The confidence intervals of *D'* overlapped for all three groups while for *K'*, only (+)-longifolene and (-)-trans-caryophyllene overlapped. Compared with the control, the enhancer, (+)-longifolene, increased *K'* significantly but not the permeability coefficient K_p, suggesting that it may have increased the diffusion coefficient *D* of the drug through skin. For (-)-trans-caryophyllene, the increased permeation could be due to the increase of the partition coefficient *K* between the donor solution and top layer of stratum corneum since both the *K'* and K_p increased significantly compared to the control.

The predicted cumulative amounts of permeated drug on days 3 and 7 are given in Table 3.2-3. None of the 6 confidence intervals overlapped, indicating cumulative permeated drugs among three study groups are significantly different at 5% level on days 3 or 7, respectively. The estimates of permeated drug/chemical are important in that, unlike *in vivo* environment where stratum corneum is replenished by the adjacent live stratum granulosum through keratinization, the excised stratum corneum, though composed of dead corneocytes, will deteriorate after days in contact with solvents, which will cause over-hydration of stratum corneum that can destroy the lamella and decomposition that will leave highly permeable passages in the stratum corneum. The predictions are relevant for transdermal drug delivery, for the cosmetic industry and for regulatory risk assessment on dermal exposure to toxic substances [152,155].

Although the interval estimate of permeability coefficient carries an error rate of 10% because of the error propagation, it is still accountable and it can be set at 5% by lowering the error rate of the two intermediate parameters to 2.5%. However, if the error terms from the nonlinear regressions are discarded and only 'clean' mean values are retained for further tests, the result could be misleading and the uncertainty is unforeseeable.

3.3 Enhancing Efficacy of Terpenes

Results. The permeability coefficients and solubilities of HP in PG and respective enhancers are listed with the physicochemical parameters of 49 terpenes, including terpene type (T), melting point, boiling point, LogP and molecular weight in Table 3.3-1. Octisalate is not a terpene but a UV-absorbent used in sunscreen compositions approved by US FDA (Figure 3.3-1) [156]. It is a promising skin penetration enhancer [157]. It consists of 15 carbon atoms, has similar structure to sesquiterpene and is included as one of the sesquiterpenes for model fitting. The MLR model is shown as Eq (2).

$$Y_i = \beta_0 + \beta_1 MW_i + \beta_2 mp_i + \beta_3 bp_i + \beta_4 LogP_i + \beta_5 Sol_i + \beta_6 X_{6i} + ... + \beta_{16} X_{16i} + \varepsilon_i \quad \text{Eq (2)}$$

Kp was set as the response variable (*Yi*). Seven potential predictor variables were chosen, five of which are quantitative predictors, i.e., solubility of HP in PG with 5% (w/v) terpene, mp, bp, logP and MW of each terpene. The two qualitative predictors are terpene type and functional group, requiring 11 indicator variables, as X variable inputs are shown in Tables 3.3-2 and 3.3-3, respectively. The coefficients of predictor variables are $\beta_1, \beta_2 ... \beta_{16}$, respectively. β_0 and ε_i are constant and error terms, respectively. Eq (2) was used to fit the data in Table 3.3-1. The resultant regression equation based on stepwise selection procedure is Eq (3), followed by fitting parameters.

$$K_p = 0.00337 - 0.000022mp - 0.00195X_6 - 0.00317X_9 + 0.00332X_{11} + 0.00197X_{12} \quad \text{Eq(3)}$$

(R^2 = 26.7%, Mallows C_p = 10.1, average VIF= 1.43, $P_{\text{residual normality}} < 0.05$)

Subsequently, diagnostic procedures were used to evaluate the fitting. The Box-Cox procedure indicated that a logarithmic transformation of the response variable *Kp* can improve the fitting ($\lambda = 0$). Therefore the Y_i in Eq(2) was changed to *LogKp* and the data

was fitted again with this revised model. The resultant regression equation based on stepwise selection is Eq (4), followed by the diagnostic parameters.

$$LogK_p = -8.31 - 0.0111mp - 0.00434bp + 1.08X_7 + 2.05X_8 + 1.80X_{10} + 3.74X_{11} + 3.47X_{12} + 2.23X_{13} + 1.59X_{14} + 2.79X_{15} \quad \text{Eq(4)}$$

(R^2 = 55.0%, Mallows C_p = 26.2, average VIF = 2.98, $P_{\text{residual normality}} > 0.05$)

For the 5 quantitative predictors, SLR models were used to fit the data with the full database and reduced database consisting of only monoterpenes and sesquiterpenes, respectively. The results are shown in Table 3.3-4. For the 2 qualitative predictors, ANOVA models were used to test the influence of terpene type and functional group on *Kp*, respectively.

No	Terpene Name, [CAS] and purity / %	T	MW	mp /^{o}C	bp /^{o}C	LogP	Sol /mg.ml^{-1}	Kp*10^{4} /cm.h^{-1}
0	Haloperidol	-	-	-	-	-	3.08± 0.28	1.19 ± 0.20
1	terpinolene [586-62-9] 97	1	136.2	liquid	182	4.67	2.30± 0.10	8.72 ± 4.01
2	α-phellandrene [99-83-2] 92	1	136.2	liquid	171	4.43	4.83± 0.21	59.39 ± 12.82
3	ocimene [3338-55-4] 70	1	136.2	liquid	175	4.70	7.74± 0.70	43.43 ± 10.37
4	myrcene [123-35-3] 95	1	136.2	liquid	167	4.58	6.03± 0.66	64.73 ± 12.82
5	(1R)-(-)-myrtenal [564-94-3] 98	1	150.2	liquid	216	2.52	7.27± 0.16	40.64 ± 17.21
6	(S)-(-)-perillaldehyde [18031-40-8]	1	150.2	liquid	238	2.81	6.34± 0.06	13.78 ± 1.21
7	carvacrol [499-75-2] 98	1	150.2	3.5	237	3.28	5.84± 0.26	1.69 ± 1.04
8	thymol [89-83-8] 98	1	150.2	51	233	3.28	6.69± 0.55	1.84 ± 1.17
9	eucarvone [503-93-5]	1	150.2	liquid	227	2.21	5.47± 0.02	4.71 ± 0.54
10	(R)-(-)-carvone [6485-40-1] 98	1	150.2	liquid	231	2.27	2.43± 0.19	4.77 ± 0.90
11	(1R)-(-)-myrtenol [515-00-4] 95	1	152.2	liquid	225	2.64	5.51± 0.05	23.71 ± 0.71
12	(-)-α-thujone [76231-76-0] 96	1	152.2	liquid	206	1.90	6.83± 0.08	1.78 ± 0.44
13	(R)-(+)-pulegone [89-82-7] 98	1	152.2	liquid	229	2.56	3.53± 0.07	13.47 ± 3.34
14	(+)-dihydrocarvone [7764-50-3] 98	1	152.2	liquid	222	2.47	6.92± 0.18	7.13 ± 1.00
15	(-)-carveol [99-48-9] 97	1	152.2	liquid	232	2.68	6.32± 0.59	12.31 ± 6.51
16	citral [5392-40-5] 96	1	152.2	liquid	229	3.17	6.33± 0.62	59.91 ± 17.88
17	(-)-isopulegol [89-79-2] 99	1	154.2	liquid	197	2.93	6.60± 0.49	1.91 ± 0.09
18	(+)-dihydrocarveol [22567-21-1] 97	1	154.2	liquid	220	2.92	6.28± 0.53	1.71 ± 0.38
19	(-)-dihydrocarveol [20549-47-7] 97	1	154.2	liquid	220	2.92	5.89± 0.45	1.28 ± 0.24
20	(S)-(-)-citronellal [5949-05-3] 96	1	154.2	liquid	208	3.48	9.43± 0.61	60.71 ± 33.73
21	geraniol [106-24-1] 98	1	154.2	liquid	230	3.28	6.11± 0.69	6.03 ± 1.42
22	nerol [106-25-2] 97	1	154.2	liquid	230	3.28	5.54± 0.20	4.10 ± 0.05
23	(±)-linalool [78-70-6] 96	1	154.2	liquid	199	3.28	5.05± 0.13	1.00 ± 0.60
24	menthone [14073-97-3] 90	1	154.2	liquid	209	2.63	7.53± 0.08	1.47 ± 0.28
25	β-citronellol [106-22-9] 95	1	156.2	liquid	225	3.38	5.29± 0.20	10.61 ± 10.14
26	L-(-)-menthol [2216-51-5] 98	1	156.2	43	215	3.20	5.11± 0.51	6.12 ± 0.66
27	cyclohexanemethanol [565-50-4] 99	1	172.7	117	265	1.07	5.16± 0.14	3.34 ± 1.75
28	α-humulene [6753-98-6] 99	2	204.3	liquid	276	7.03	5.28± 0.43	19.30 ± 1.96
29	(-)-α-cedrene [469-61-4] 99	2	204.3	liquid	263	6.38	4.62± 0.10	12.13 ± 3.31
30	(+)-β -cedrene [546-28-1] 97	2	204.3	liquid	263	6.37	4.72± 0.13	12.67 ± 5.31
31	(+)-aromadendrene [489-39-4] 97	2	204.3	liquid	258	6.41	4.77± 0.15	6.82 ± 1.29
32	(+)-longifolene [475-20-7] 99	2	204.3	liquid	252	6.39	4.55± 0.18	5.61 ± 0.67
33	(-)-trans-caryophyllene [87-44-5] 99	2	204.3	liquid	268	6.78	5.09± 0.02	7.07 ±0.34
34	(-)-caryophyllene oxide [1139-30-6] 99	2	220.3	63	280	4.57	4.49± 0.38	22.2 ± 17.35
35	(±)-α-bisabolol [515-69-5] 99	2	222.3	liquid	315	5.01	6.26± 0.48	66.48 ± 25.14
36	farnesol [4602-84-0] 97	2	222.3	liquid	283	5.31	5.65± 0.26	16.13 ± 7.15
37	(±)-nerolidol [7212-44-4] 97	2	222.3	liquid	276	5.31	5.10± 0.20	82.67 ± 32.96
38	(-)-epiglobulol [88728-58-9] 95	2	222.3	liquid	294	4.81	4.95± 0.38	110.34 ± 20.31
39	(-)- guaiol [489-86-1] 99	2	222.3	90	288	4.75	4.73± 0.31	2.9 ± 2.47
40	(+)-cedrol [77-53-2] 99	2	222.3	84	277	4.77	4.35± 0.12	3.76 ± 0.44
41	(-)-isolongifolol [1139-17-9] 99	2	222.3	112	-	4.05	4.63± 0.19	2.39 ± 0.60
42	(-)-α-santonin [481-06-1] 98	2	246.3	171	423	1.80	5.71± 0.38	3.66 ± 2.91
43	octisalate [118-60-5] 99	2	250.3	liquid	332	5.77	3.14± 0.34	55.86 ± 7.82
44	(+)-cedryl acetate [77-54-3] 95	2	264.4	45	292	5.67	5.76± 0.35	41.27 ± 13.22
45	retinol [68-26-8] 97	3	286.4	63	421	6.84	7.11± 0.23	13.94 ± 2.21
46	phytol [7541-49-3] 97	3	296.5	liquid	336	8.66	4.77± 0.31	61.29 ± 12.23
47	retinoic acid [302-79-4] 98	3	300.4	146	463	6.83	8.79± 1.46	0.20 ± 0.18
48	squalene [111-02-4] 97	4	410.7	liquid	429	13.09	3.91± 0.16	2.25 ± 0.60
49	β-carotene [7235-40-7] 102.8	5	536.8	181	655	15.51	18.6± 1.60	0.24 ± 0.17

Table 3.3-1 The solubilities of HP in PG with terpene enhancers 5% (w/v). In the first column No, '0' stands for HP in PG 5% (w/v) without terpene enhancer and numbers 1 to 49 are assigned to the 49 terpenes. The second column is the name of each terpene,

followed by its CAS entry and purity. The third column T indicates the terpene category. Key: 1 monoterpene, 2 sesquiterpene, 3 diterpene, 4 triterpene, 5 tetraterpene. From the fourth to seventh column is the molecular weight, melting point, boiling point and LogP of each terpene, respectively. The data were from SciFinder Scholar® and original product information. The melting points of liquid terpenes are set as –1 ^{0}C for those liquid terpenes that do not have published melting points. The boiling point of (-)-isolongifolol is not available and is estimated at 300 ^{0}C, similar to the boiling points of other sesquiterpenes. The eighth column, Sol, is the solubility of HP in PG at 37 °C without or with 5% (w/v) enhancer. The last column *Kp* is the permeability coefficient of HP though human skin. Data are given as Mean ± SD.

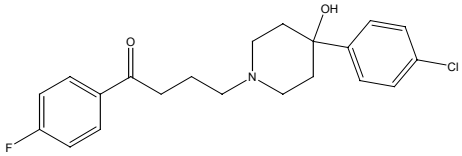

haloperidol

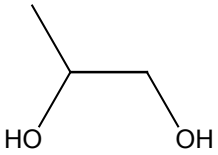

propylene glycol

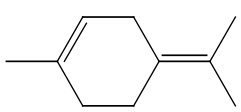
1 terpinolene

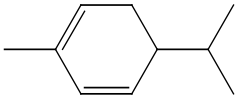
2 α-phellandrene

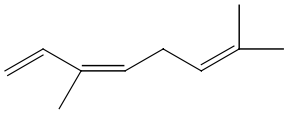
3 ocimene

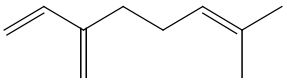
4 myrcene

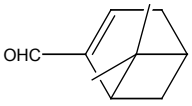

5 (1R)-(-)-myrtenal

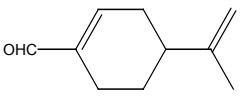

6 (S)-(-)-perillaldehyde

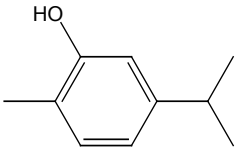

7 carvacrol

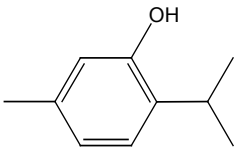

8 thymol

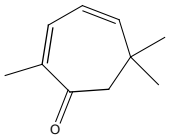

9 eucarvone

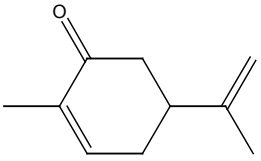

10 (R)-(-)-carvone

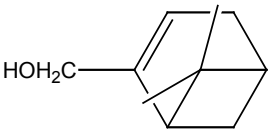

11 (1R)-(-)-myrtenol

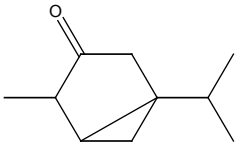

12 (-)-α-thujone

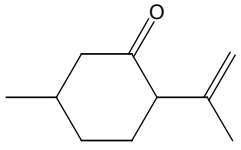

13 (R)-(+)-pulegone

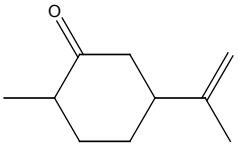

14 (+)-dihydrocarvone

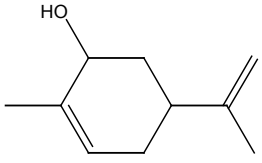

15 (-)-carveol

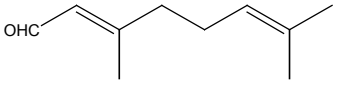

16 citral

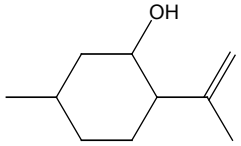

17 (-)-isopulegol

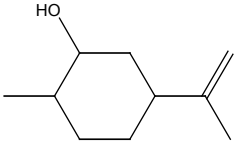

18 (+)-dihydrocarveol

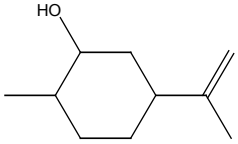

19 (-)-dihydrocarveol

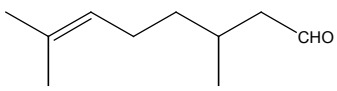

20 (S)-(-)-citronellal

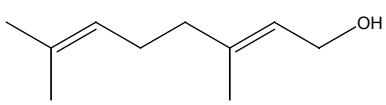

21 geraniol

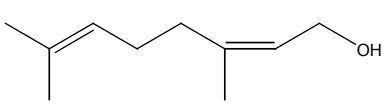

22 nerol

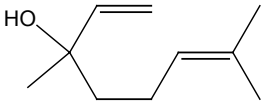

23 (±)-linalool

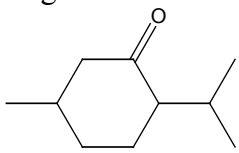

24 menthone

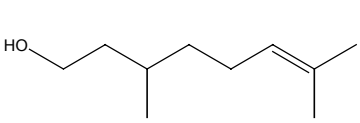

25 β-citronellol

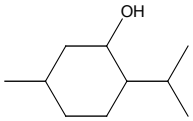

26 L-(-)-menthol

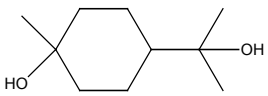

27 cyclohexanemethanol

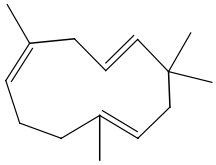

28 α-humulene

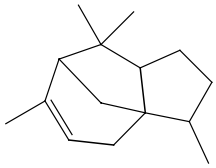

29 (-)-α-cedrene

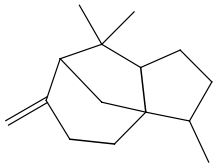

30 (+)-β –cedrene

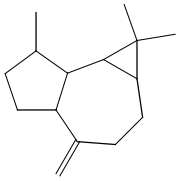

31 (+)-aromadendrene

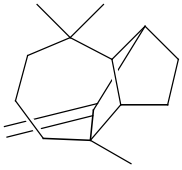

32 (+)-longifolene

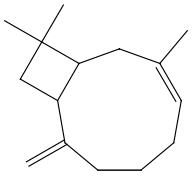

33 (-)-trans-caryophyllene

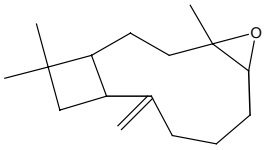

34 (-)-caryophyllene oxide

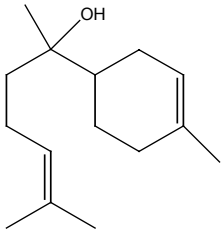

35 (±)-α-bisabolol

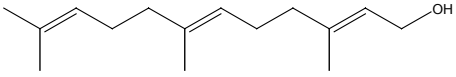

36 farnesol

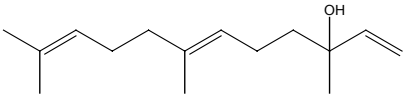

37 (±)-nerolidol

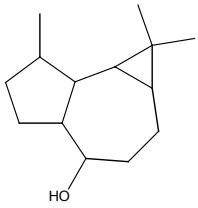

38 (-)-epiglobulol

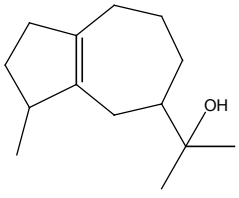

39 (-)- guaiol

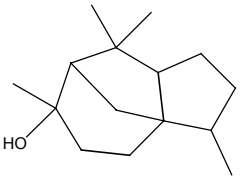

40 (+)-cedrol

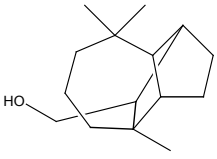

41 (-)-isolongifolol

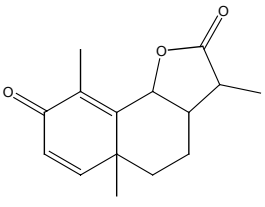

42 (-)-α-santonin

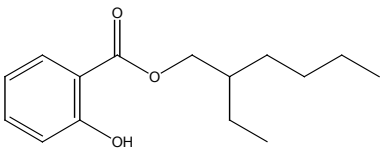

43 octisalate

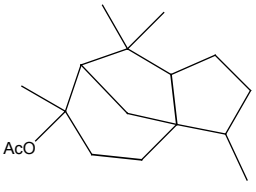

44 (+)-cedryl acetate

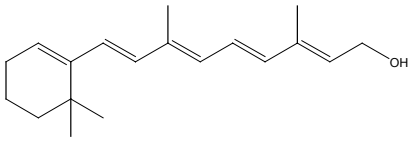

45 retinol

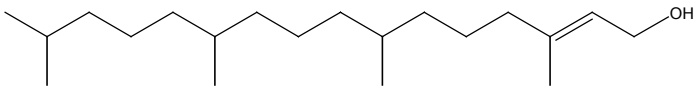

46 phytol

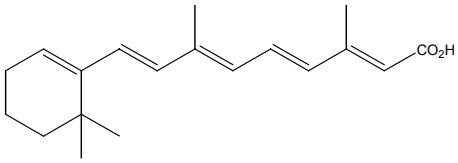

47 retinoic acid

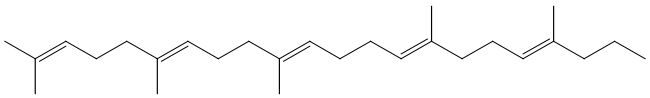

48 squalene

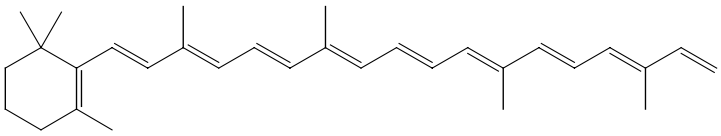

49 β-carotene

Figure 3.3-1 The molecular structures of haloperidol, propylene glycol and the 49 terpenes.

Terpene type	**MW**	**mp**	**LogP**	**Sol**	X_6	X_7	X_8	X_9
Monoterepne	MW_i	mp_i	$LogP_i$	Sol_i	1	0	0	0
Sesquiterpene	MW_i	mp_i	$LogP_i$	Sol_i	0	1	0	0
Diterpene	MW_i	mp_i	$LogP_i$	Sol_i	0	0	1	0
Triterpene	MW_i	mp_i	$LogP_i$	Sol_i	0	0	0	1
Tetraterpene	MW_i	mp_i	$LogP_i$	Sol_i	0	0	0	0

Table 3.3-2 The data input for X variables, indicating terpene type.

Terpene type	**MW**	**mp**	**LogP**	**Sol**	X_{10}	X_{11}	X_{12}	X_{13}	X_{14}	X_{15}	X_{16}
Alcohol	MW_i	mp_i	$LogP_i$	Sol_i	1	0	0	0	0	0	0
Aldehyde	MW_i	mp_i	$LogP_i$	Sol_i	0	1	0	0	0	0	0
Ester	MW_i	mp_i	$LogP_i$	Sol_i	0	0	1	0	0	0	0
Hydrocarbon	MW_i	mp_i	$LogP_i$	Sol_i	0	0	0	1	0	0	0
Ketone	MW_i	mp_i	$LogP_i$	Sol_i	0	0	0	0	1	0	0
Oxide	MW_i	mp_i	$LogP_i$	Sol_i	0	0	0	0	0	1	0
Phenol	MW_i	mp_i	$LogP_i$	Sol_i	0	0	0	0	0	0	1
Acid	MW_i	mp_i	$LogP_i$	Sol_i	0	0	0	0	0	0	0

Table 3.3-3 The data input for X variables, indicating functional group of each terpene.

Row	Variable (X_i)	Database	Fitted line	R^2	p-value
1	LogP	Full	Logkp = -7.037 – 0.03449 LogP	0.3%	0.491
2	LogP	Reduced	Logkp = -.8.578 + 0.3742 LogP	15.9%	**0.000**
3	MW	Full	Logkp = -6.208 – 0.005003 MW	4.5%	**0.006**
4	MW	Reduced	Logkp = -8.158 + 0.006095 MW	2.3%	0.081
5	mp	Full	Logkp = -6.830 – 0.01614 mp	22.6%	**0.000**
6	mp	Reduced	Logkp = -6.905 – 0.01026 mp	8.1%	**0.001**
7	bp	Full	Logkp = -5.622 – 0.005897 bp	9.9%	**0.000**
8	bp	Reduced	Logkp = -7.160 – 0.000350 bp	0.0%	0.895
9	Sol	Full	Logkp = -5.952 – 0.2121 Sol	8.7%	**0.000**
10	Sol	Reduced	Logkp = -7.511 + 0.07833 Sol	0.5%	0.423

Table 3.3-4 Simple linear regression *LogKp* against each predictor respectively. The p-value of less than 0.05 indicates the two variables are correlated. The column, 'database' indicates either 'full', indicating that all the 149 data points would be fitted, or 'reduced', indicating only data points of monoterpenes and sesquiterpenes would fitted.

Discussion. The results showed that *LogKp*, the monotonic increasing function of *Kp*, is a better response variable than *Kp* itself in the MLR model, for the following three reasons. First, the coefficient of determination, i.e., R^2, increased from 26.7% to 55%, indicating that the predictors in Eq(4) explained more of the variances than those in Eq(3). Second, the Anderson-Darling test showed that the residuals in Eq(3) did not follow normal distribution ($P_{\text{residual normality}} < 0.05$) while those in Eq(4) did ($P_{\text{residual normality}} > 0.05$). The test was substantiated by the residual plots. The residuals generated in Eq(3) were random, approximately with equal variance, but did not follow normal distribution very well. But the histogram of the residuals generated in Eq(4) showed satisfactory bell-shape normal distribution pattern. Third, Mallows C_p did not suggest any substantial bias in Eq(4). Furthermore, considering that the number of predictors was 10 in Eq(4) and 5 in Eq(3), the Mallows C_p of 10.1 in Eq(3) and of 26.2 in Eq(4) were comparable. Similar

to Mallows C_p, the average of the variance inflation factor (VIF) did not indicate any serious multicollinearity problems in both models. Hence, Eq(4) was chosen as the final MLR model. Similarly, it was shown that *LogKp* was a better response variable than *Kp* in SLR and ANOVA models. Therefore *LogKp* was used to fit the models. *Kp* is referred to in following discussions since *LogKp* is a monotonic increasing function of *Kp*.

The MLR model provided a preliminary screening tool to evaluate terpene enhancers based on human skin. It is valuable because human skin samples are not readily available and *in vitro* permeation studies are time-consuming. It is not as informative as SLR models for the evaluation of relations between two variables. SLR regressions were conducted between *LogKp* and other 5 quantitative predictors, respectively.

Table 3.3-4 showed 10 regression results, in which *LogKp* was regressed against LogP, MW, mp, bp and Sol, respectively, with either the full or the reduced database consisting of only monoterpenes and sesquiterpenes. The reduced database was used because monoterpenes and sesquiterpenes were identified as more promising enhancer candidates. Diterpenes, triterpenes and tetraterpenes were not as efficient as monoterpenes and sesquiterpenes probably due to the following reasons. First, they contain 20, 30 and 40 carbon atoms respectively, which makes most of them biologically active and not suitable as pharmaceutical excipients. They were included in this study for the purpose of testing the relationship between the enhancement abilities and physicochemical properties of different types of terpenes. Second, there is a large number of monoterpenes and sesquiterpenes available but the numbers of diterpenes, triterpenes and tetraterpenes are

limited. However, it should be noted that phytol, a diterpene, showed remarkable penetration enhancement.

Row 1 of Table 3.3-4 showed that LogP did not correlate with *Kp*. In row 2, however, they were positively related for monoterpenes and sesquiterpenes only. Compared with the total number of data points, which is 149, the number of monoterpenes and sesquiterpenes, which is 132, accounts for most of the data points. But the 17 data points from diterpenes, triterpenes and tetraterpenes did exert an influential effect on the regression, which masked the positive relation between *Kp* and LogP of monoterpenes and sesquiterpenes. The positive relation between *Kp* and LogP may be an indication of the lipid passage in the stratum corneum barrier [46,100]. Terpenes with higher lipophilicity may solubilize more stratum corneum intercellular lipids into the vehicle. As a result the permeation rate of the drug increased.

The relation between *Kp* and MW was similar to that of *Kp* and LogP since MW and LogP were positively correlated (Pearson correlation is 0.880 for the full database, and 0.569 for the reduced database). For the reduced database, from row 4 of Table 3.3-4 monoterpenes and sesquiterpenes with larger MW may lead to better enhancing effects, although the p-value indicates that more samples are required to verify the significance. For the full database, *Kp* and MW should not be correlated if their relation was consistent with that of *Kp* and LogP as shown in row 1 of Table 3.3-4. However, from row 3 it appears that *Kp* is negatively related to MW, i.e., as terpene molecules became bigger, their enhancing abilities decreased regardless of their increased lipophilicities. Therefore MW, other than LogP, may be a suitable predictor for terpenes of all categories. So for

all terpenes, their enhancing abilities decreased as MW increased but for monoterpenes and sesquiterpenes, their enhancing abilities increased as LogP or MW increased.

Rows 5 to 8 show the influence of mp and bp on *Kp*. It is shown in rows 6 and 7 that *Kp* decreases as the melting point increases. The main reason was because the mp of all liquid terpenes was set to be –1, which put too much weight on regression. However it can be demonstrated that apart from those data points with a mp of –1, the rest of the points still showed a trend that lower mp correlated with greater *Kp*. Similar patterns were identified with the boiling point. For the full database, the enhancing ability correlated negatively with bp. But for the reduced database, it shows that enhancing abilities did not correlate with bp. This may be because most monoterpenes and sesquiterpenes share similar bp so that *Kp* cannot be differentiated by bp.

The relationship between *Kp* and solubility of HP in PG with 5% (w/v) terpene is shown in rows 9 and 10. Although row 9 shows that *Kp* decreased as the solubilization effect of the terpenes increased, it can be proven that the trend is dictated by outliers, i.e., the last three data points of carotene. Once these three points are removed, *Kp* did not correlate with Sol ($p = 0.389$). In fact, row 10 shows that *Kp* may be positively related to Sol, though the correlation is not significant. However, greater solubilizatoin is advantageous in transdermal drug delivery since a higher drug concentration will create a higher concentration gradient across the skin, which may result in greater drug permeation.

While the relation between the enhancing effects and quantitative variables can be addressed by SLR models, its relation with qualitative variables can be better explained by ANOVA models. When 'terpene type' is assumed to be the only factor that influences *Kp*, one-way ANOVA shows that terpenes had different enhancing effects ($p < 0.05$).

The pairwise comparison with Tukey's method showed that compared with tetraterpene, monoterpene, sesquiterpene and diterpene were better enhancers but no significant difference was detected among the three. For the reduced database, the two-sample *t*-test showed that the *Kp* of sesquiterpene is significantly greater than that of monoterpene ($p < 0.05$). This indicates that terpene enhancers with 15 carbon atoms are better than those with 10 carbon atoms. Apart from terpene type, it is also interesting to find out by one-way ANOVA that there are significant differences among various function groups ($p < 0.05$). The overall ranking of enhancing ability is as follows: ester > aldehyde > oxide > hydrocarbon > alcohol > ketone > phenol > acid. Tukey's tests showed that not all pairwise comparisons are significant. For example, the effect of ester and aldehyde are not significantly different from one another, but aldehyde's enhancing effect is significantly greater than that of alcohol, hydrocarbon, ketone, phenol and acid.

3.4 Reversible Effects of Terpenes

Results. The solubility results are shown in Table 3.4-1. With the addition of 5 % (w/v) (R)-(-)-carvone, the solubility of HP in PG dropped from 3.08 to 2.43 mg/ml and when 5 % (w/v) eucarvone was added, it increased to 5.47 mg/ml. Eucarvone should have greater permeation enhancing potential than (R)-(-)-carvone. For the enhancers in 0.03 %(v/v) lactic acid, (R)-(-)-carvone has a higher solubility of 0.729 mg/ml than that of eucarvone at 0.566 mg/ml. Both enhancers have relatively lower solubility compared to HP with a solubility of approximately 1 mg/ml in 0.03 %(v/v) lactic acid.

The permeation profiles of both drugs and enhancers, from permeation studies using either normal or pretreated epidermis, are shown in Figure 3.4-2. For the permeation

study using pretreated epidermis, the permeation profile of eucarvone was obtained but that of (R)-(-)-carvone was not, since (R)-(-)-carvone was presumably washed away prior to the permeation. The permeation profile of eucarvone was distinctly different from other exponential curves because, for all the others, the donor concentration was constant but, for eucarvone, its amount was finite in the epidermis. The estimated values and confidence intervals of the permeability coefficient of K_p are given in Table 3.4-2, except for the finite-dosed eucarvone. It was demonstrated that the K_p of HP with 5% w/v (R)-(-)-carvone, HP with 5% w/v eucarvone, and (R)-(-)-carvone 5% w/v in PG (50mg/ml) were comparable to one another but significantly larger than the rest. (One-way ANOVA and Tukey's method comparing all pairs, $p < 0.05$).

In the extraction study, 3.82 ± 0.0521 μg of eucarvone was extracted from the eucarvone-treated epidermis but no (R)-(-)-carvone was extracted from the (R)-(-)-carvone-treated epidermis after the 48-h permeation period. HP of 295.27 ± 60.62, 242.45 ± 31.98 and 48.94 ± 13.90 μg were extracted from the control, (R)-(-)-carvone-pretreated and eucarvone-pretreated epidermis, respectively.

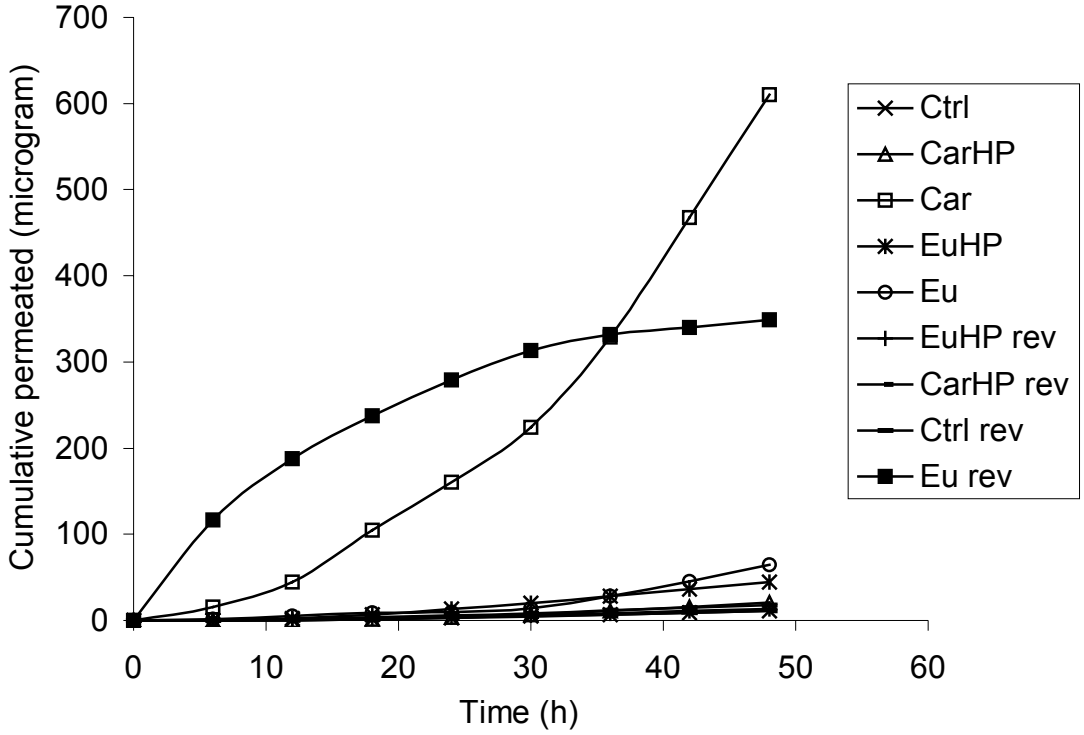

Figure 3.4-2 Time course of mean cumulative amounts of HP permeated through 0.786 cm^2 of human epidermal membrane in the PG solutions. Each point represents mean value (n = 3). In the study using normal epidermis, three permeation experiments with different donor solutions gave five permeation curves: (a) the control of which HP (3 mg/ml) was in pure PG gave the permeation profile of HP (**Ctrl**), (b) HP (3 mg/ml) in PG with 5% (w/v) of eucarvone solution gave the permeation profiles of HP (**EuHP**) and eucarvone (**Eu**), and (c) HP (2.43 mg/ml) in PG with 5% (w/v) of (R)-(-)-carvone gave the permeation profiles of HP (**CarHP**) and (R)-(-)-carvone (**Car**). In the study using pretreated epidermis, the three permeation experiments using the same donor solutions (HP in PG, 3 mg/ml, w/v) gave 4 permeation curves: (a) the epidermis treated with pure PG gave the permeation profile of HP (**Ctrl rev**), (b) the study with eucarvone solution (5%, w/v)-pretreated epidermis gave the permeation profiles of HP (**EuHP rev**) and eucarvone (**Eu rev**), and (c) the study with (R)-(-)-carvone (5%, w/v)-pretreated epidermis gave the permeation profile of HP (**CarHP rev**).

Discussion. In the study using normal epidermis, three permeation experiments with different donor solutions gave five permeation curves (Figure 3.4-2). Both enhancers can

enhance the permeation of HP to similar level, about 4-folds higher than the control (Table 3.4-2). The permeability coefficient of (R)-(-)-carvone was also 4 times higher than that of eucarvone. It appears that the permeation of HP was independent of enhancer's permeability through the skin. In the study using pretreated epidermis, three permeation experiments using the same donor solutions (HP 3 mg/ml, w/v in PG) yielded four permeation curves (Figure 3.4-2). For the three HP permeation results, their K_p were not significantly different from one another, nor different from the control resulting from the untreated epidermis (One-way ANOVA, $p > 0.05$).

Combined with the results from skin extraction study, it was found that only about 1% (w/w) of the trapped eucarvone remained in the epidermis after the 48-h permeation, which infers that eucarvone could have been washed away by PG. Unlike eucarvone, (R)-(-)-carvone was not detected in the receptor solution or in the epidermis under the same conditions. Most of the R-(-)-carvone in epidermis was probably rinsed off by the vehicle prior to the permeation study. This is consistent with the findings from the solubility study, which shows that the solubility of eucarvone is lower than (R)-(-)-carvone in 0.03% lactic acid and eucarvone permeates much slower than (R)-(-)-carvone (Table 3.4-2).

Solute and solvent	**Concentration (mg/ml)**
HP in PG	3.08 ± 0.280
HP in PG with 5% (w/v) (R)-(-)-carvone	2.43 ± 0.185[a]
HP in PG with 5% (w/v) eucarvone	5.47 ± 0.0189[a]
(R)-(-)-carvone in 0.03% (v/v) lactic acid	0.729 ± 0.0510[b]
Eucarvone in 0.03% (v/v) lactic acid	0.566 ± 0.0171

Table 3.4-1 Solubility study of HP in PG and enhancers in 0.03% (v/v) lactic acid at 37 °C. [a]One-way ANOVA, Tukey's method comparing to control, $p < 0$ .05.
[b]2-sample *t*-test comparing (R)-(-)-carvone with eucarvone, $p < 0.05$.

Enhancer groups	K'	D'	K_p (cm/h) *10^4
HP without enhancer	0.0128 ± 0.00404	0.00932 ± 0.00175	1.12 ± 0.185
	0.00656, 0.0246	0.00651, 0.0143	0.546, 2.70
			1.19 ± 0.199
HP with 5% w/v	0.0863 ± 0.0533	0.00519 ±0.00144	3.72 ± 1.88
(R)-(-)-carvone	0.0356, 0.225	0.00353, 0.00806	1.26, 18.1
			4.77 ± 0.896[a]
HP with 5% w/v	0.0471 ± 0.00484	0.00997 ±0.000627	4.67 ± 0.196
eucarvone	0.0381, 0.0582	0.00879, 0.0114	3.34, 6.63
			4.71 ± 0.544[a]
(R)-(-)-carvone 5% w/v	0.0591 ± 0.0267	0.00811 ±0.00233	3.59 ± 1.31
in PG (50 mg/ml)	0.0192, 0.141	0.00494, 0.0152	1.58, 7.83
			4.40 ± 0.217[a]
Eucarvone 5% w/v	0.0247 ± 0.0064	0.00387 ±0.00038	0.932 ± 0.158
in PG (50 mg/ml)	0.0153, 0.038	0.00312, 0.0046	0.732, 1.24
			0.966 ± 0.121
HP without enhancer	0.0134 ± 0.0102	0.0127 ± 0.0065	1.04 ± 1.03
Skin pretreated with PG	0.00522, 0.0301	0.00775, 0.0257	0.404, 7.74
			1.71 ± 0.729
HP without enhancer	0.0187 ± 0.0154	0.0076 ± 0.00339	0.902 ± 0.916
Skin pretreated	0.00775, 0.0462	0.00489, 0.0119	0.379, 5.96
with carvone			1.44 ± 0.614
HP without enhancer	0.0142 ± 0.00175	0.01 ± 0.000757	1.41 ± 0.0716
Skin pretreated	0.0108, 0.0185	0.00853, 0.0119	0.921, 2.20
with eucarvone			1.42 ± 0.262

Table 3.4-2 The point estimates (Mean ± SD) of K' and D' obtained from the nonlinear regression, and their 90% confidence intervals. The point estimate (Mean ± SD) of permeability coefficient and its 90% confidence interval, given by $K_p = K'D'$. For the column K_p, each cell contains three estimates, of which the first and second are the point and interval estimates from pooled data (n = 24) with estimation errors generated by the nonlinear regression, respectively, and the third is the point estimate from individual data set (n = 8) discarding the estimation errors generated by the nonlinear regression. ([a]One-way ANOVA, Tukey's method comparing all the pairs, $p < 0.05$).

From the two studies, it was found that when the enhancers were removed, the HP permeability coefficients returned to normal from a 4-fold increase in the presence of enhancers. In addition, results from the permeation study with pretreated epidermis also showed that the permeability coefficients of HP were comparable among all groups. Therefore, the effects of both enhancers on skin permeability to HP were reversible.

After 48-h permeation study, the amount of HP extracted from the epidermis pretreated with PG, (R)-(-)-carvone and eucarvone was 295.27 ± 60.62, 242.45 ± 31.98 and 48.94 ± 13.90 μg, respectively. The eucarvone-pretreated epidermis retained less HP than that treated with (R)-(-)-carvone or PG (One-way ANOVA, Tukey's method, $p < 0.05$). If all the eucarvone were rinsed off from the epidermis prior to it being mounted for the permeation study, then it should not have much influence on HP deposition in epidermis. This is not the case as the eucarvone-pretreated epidermis retained only about 20% of the amount in the PG-pretreated or the 5% (w/v) (R)-(-)-carvone-pretreated epidermis. As the permeability coefficients of HP through the three types of pretreated skin were similar, the trapped eucarvone probably did not facilitate the permeation of HP and may have decreased the diffusion path length and partition coefficient proportionally.

To estimate K_p, two different methods were used. In the first method, all replicates were pooled for nonlinear regression, which gave point and interval estimates. In the second method, each replicate was used as individual data set for nonlinear regression. Consequently, one point estimate was obtained from each replicate and the error term was dropped. These clean estimates, therefore, became the sampled K_p, subject to further statistical comparisons. In the first method, K_p was estimated from the original permeation data, but in the second method, the quality of estimation was compromised because of the arbitrary omission of the error term. When the data variance is small, effective confidence interval can be obtained by the first method and pairwise comparisons can be conducted by comparing the variable's confidence intervals. But when the data variation is large the confidence intervals tend to be so wide that

comparisons become too conservative. In this case, the second method will be an alternative at the expense of reduced data quality.

3.5 Incorporation of Terpenes in SMGA Gels

Results

SMGA gels. The PG gels start to gelate almost immediately as the ambient temperature changed from 120 ^{0}C to room temperature (22 ± 1) whereas the ISA formulation began to gel an hour later and the process was much slower than for the PG gels. For both ISA and PG gels, the formulae without farnesol gelated faster than those with farnesol. Flake-like white spots appeared ubiquitously in the clear solution and intensified slowly until a uniform gel was formed. The PG gels (formula 'b' and 'ab') are opaque and white in color while the ISA gels are translucent, indicating that PG gels possess thicker fibers and a lower degree of network branching than the ISA gels. The improved clarity of ISA gels is due to the formation of thinner fibers and more densely branched three dimensional network structures [79].

The structure of interconnecting fiber networks is directly associated with the rheological properties. As shown in Figure 3.5-2, where the moduli were recorded as a function of time, the elastic and viscous moduli gels formed at 0.01% of strain, $20\,^0C$ and 1 Hz frequency and are almost parallel to each other; therefore the gels possess the mesh-like interconnecting networks of micro/nano structures. Figure 3.5-3 shows the change of the moduli of the gels as functions of various oscillating strain amplitudes, γ. The strain corresponds to the deformation of the networks caused by the applied shear stress. The storage modulus, $G^{'}$, remains stable under small strains and decreases abruptly when γ

exceeds a certain value γ_0, which corresponds to the breakage of the junctions in the networks. The gels can withstand up to 0.25% of the strain. Below this strain, the mesh-like micro/nanostructure is intact and above this, it crumbled.

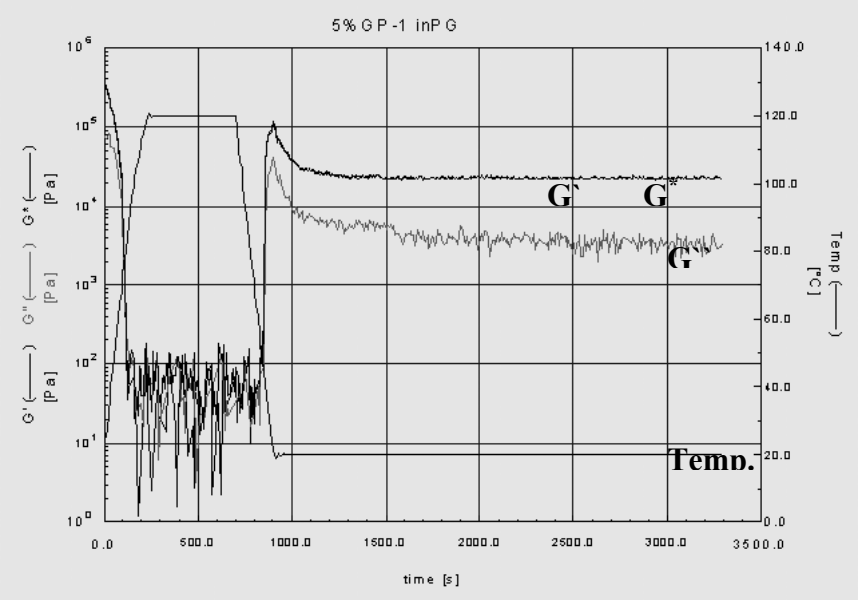

Figure 3.5-2 Dependence of the storage modulus $G^{'}$, the loss modulus $G^{"}$, and the complex modulus G^{*} on time. Time sweep method for formula 'ab' gel at $20\,^{0}C$.

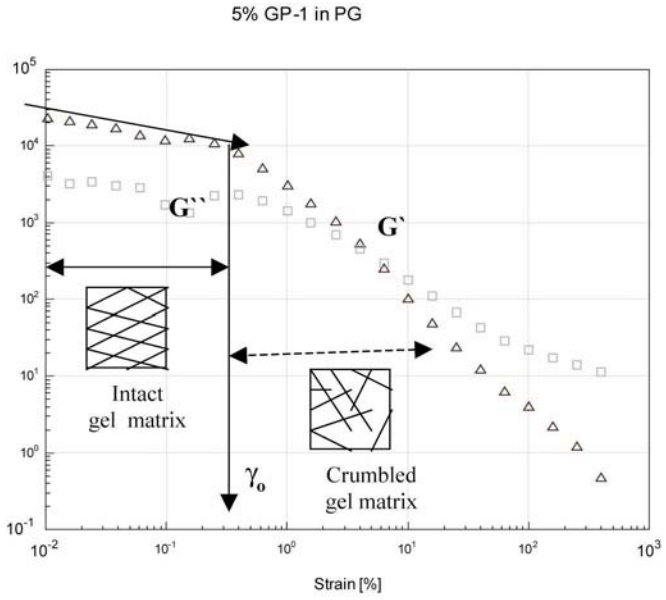

Figure 3.5-3 Dependence of the storage modulus $G^{'}$, the loss modulus $G^{"}$, and the complex modulus G^{*} on strain. Dynamic strain method for formula 'ab' gel at $20\,^{0}C$.

***In vitro* permeation study**. The original permeation data are shown in Figure 3.5-4. The estimated values of K_p and Lt are given in Table 3.5-1, and as the response variables for the three factors, their changes in response from low levels to high levels of the factors were analyzed with a statistical model and the results are shown in Table 3.5-2.

For the permeability coefficient K_p, factors A and C are significant, indicating that the enhancer and solvent exerted their influences upon K_p when changing from low level to high level, but the gelator did not. The effect of enhancer farnesol is positive, showing it can increase K_p when present in the formula. The factor C, solvent, shows a negative effect, which indicates that when the solvent changed from low level (PG) to high level (ISA), the permeability coefficient K_p decreased. Therefore PG delivered haloperidol at

a faster rate than ISA on average. One of the two-way interactions, A*C, also showed significant negative effect. This can be due to the enhancer being less effective in ISA than in PG. The three-way interaction term is not significant.

Unlike K_p, the lag-time, Lt, is sensitive to all the three factors, as well as, their combinations. The enhancer and gelator increased lag-time, while ISA decreased the lag-time compared to PG. The positive two-way interaction term shows that when the gelator was present, the enhancer increased lag-time to a larger extent than when there was no gelator in the formula and vice versa. The other two negative two-way interactions showed that ISA can counteract the elongation effect of the enhancer or the gelator on drug permeation. The three-way interaction is negative, for which the most intuitive explanation is that when the solvent is ISA, the A*B interaction is not as strong as when the solvent is PG, therefore the enhancer/gelator will not increase the lag-time much more than when the gelator/enhancer is absent.

Foumula Name	**Enhancer (factor A)**	**Gelator (factor B)**	**Solvent (factor C)**	**Permeability coefficient K_p *10^4 (cm/h)**	**Lag-time Lt (h)**
1	-	-	PG	1.35 ± 0.21	17.98 ± 1.37
a	+	-	PG	16.13 ± 7.15	32.27 ± 6.77
b	-	+	PG	0.52 ± 0.09	38.52 ± 7.50
ab	+	+	PG	40.69 ± 27.32	98.27 ± 11.24
c	-	-	ISA	5.52 ± 0.09	11.52 ± 0.49
ac	+	-	ISA	4.19 ± 0.46	10.69 ± 0.63
bc	-	+	ISA	5.28 ± 1.73	9.14 ± 2.70
abc	+	+	ISA	4.71 ± 0.66	9.41 ± 0.63

Table 3.5-1 The formulae of the 8 solutions/gels, the permeability coefficient K_p and the lag-time Lt of the drug haloperidol. Factor A refers to farnesol and factor B refers to GP-1. The plus sign stands for presence (high level) and minus sign for absence (low level). The low and high levels of factor C are propylene glycol (PG) and isostearyl alcohol (ISA), respectively (n = 3 or 4).

Factors	Effect on K_p	p, effect on K_p	Effect on Lt	p, effect on Lt
A	13.388	0.006*	18.36	0.000*
B	6.016	0.180	20.74	0.000*
C	-9.738	0.036*	-36.55	0.000*
A*B	6.583	0.144	11.63	0.000*
A*C	-14.167	0.004*	-18.65	0.000*
B*C	-5.931	0.186	-22.53	0.000*
A*B*C	-6.029	0.179	-11.10	0.000*

Table 3.5-2: The effects and levels of significance of the factors and their interaction terms. The results were confirmed by ANOVA tests ($p < 0.05^*$).

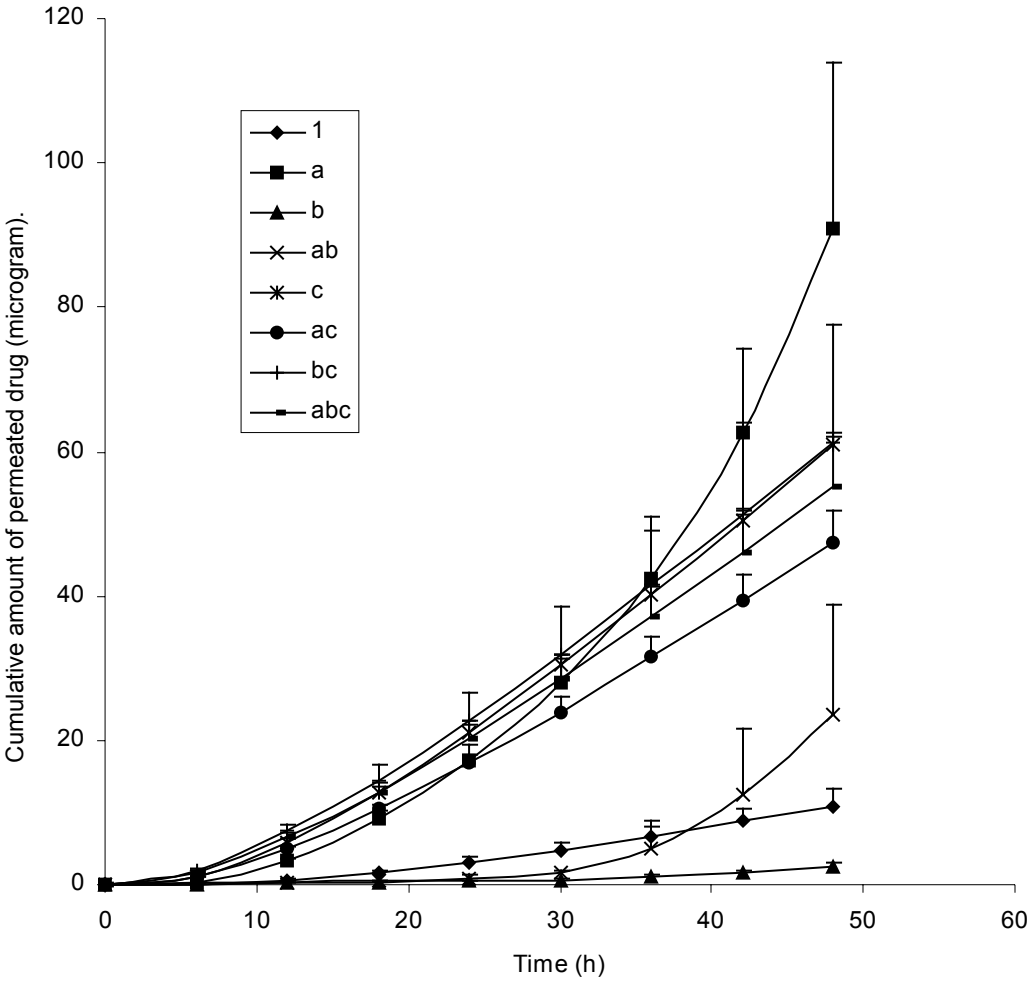

Figure 3.5-4 Time course of mean cumulative amounts of haloperidol permeated through 1 cm^2 of human epidermal membrane in the solutions/gels formulated according to Table 1. Each point represents Mean ± SD (n = 3 or 4).

Discussion. The gels accommodated both the drug and the permeation enhancer while still retaining their rheological and aesthetic properties, demonstrating that the SMGA gels have the potential to deliver drugs through the skin. The *in vitro* permeation study was then conducted to evaluate the transdermal delivery of the drug, haloperidol, by the SMGA gels.

The permeability coefficient, K_p, and the lag-time, Lt, defined a permeation curve of the cumulative permeated drug against time with all the other parameters constant. Pseudo-steady permeation with a flux of K_pC_0 is expected after a transitional period of 3 times Lt [35,40]. Both parameters can be influenced by the three factors and their interaction terms, all of which are estimated in the factorial design as shown in Table 3.5-2.

The factor A, a skin penetration enhancer, may increase K_p by modifying the lipid compositions and structures. The factor C is the solvent. PG is an established solvent for transdermal delivery, miscible with water. It can dissolve many essential oils, but is immiscible with fixed oils. ISA is a saturated fatty alcohol, clear and viscous. It is a biocompatible solvent widely used in cosmetic industry. Factor B is the gelator, the SMGA, also being used for cosmetics, such as lipstick, eyeliner, deodorant and makeup lotions [158-161]. It may retard the permeation process by its steric supramolecular structure, reducing the permeation area on the skin and by Fick's law this is linearly related to K_p.

On average, however, as the results have shown, the gelator did not influence K_p significantly as it did with Lt. This is also shown in Figure 3.5-4, where the curve 'a' is well above curve 'ab', but the slopes of their linear parts are quite similar to each other.

The definitions of permeability coefficient and lag-time are $K_p = K\frac{D}{l}$ and $Lt = \frac{l^2}{6D}$, respectively. The partition coefficient between the donor solution and the top layer of the stratum corneum, *K,* is difficult to define as there are no distinct lipid interfaces as the vehicle passed through the stratum corneum. If *K* is assumed to remain constant with the introduction of the gelator into the delivery system, a plausible explanation is that both the diffusion path length, *l*, and the diffusion coefficient, *D*, increased while their ratio remains constant. The lipophilic gelator GP-1 (MW = 453.70, Log P = 5.02) could have posed some extra spatial hindrance to propylene glycol (MW = 76.09, Log P = -0.81), which literally increased the path length. The increased *D* could be due to the synergistic effect between the enhancer, farnesol (MW = 222.37, Log P = 2.47), and the gelator, both lipids in nature. As for the other solvent, ISA, the scenario is partially different as the gelator present did not affect either the K_p or Lt values significantly. As shown in Figure 3.5-4, compared with the formula 'ac', the presence of the gelator in formula 'abc' did not cause any significant effect on the permeation profile (two-sample *t*-test, $p > 0.05$). The solvent ISA (MW = 270.49, Log P = 7.19) is similar to GP-1 structurally as well as sizeably, and they are both lipophilic. The aliphatic long-chain gelator, GP-1, thus presented a lesser permeation barrier to the drug in ISA than to that in PG. This ISA-controlled permeation was in line with the statistical result that ISA could significantly counteract the delayed effect of the enhancer or gelator on drug permeation. Some other interaction effects among the three factors were also revealed by the statistical analysis, of which the most prominent one is that, the enhancer performed much better in PG than in ISA, judging by K_p. In fact, the enhancer in ISA did not exert

any significant effect (two-sample *t*-test, $p > 0.05$). Since the main barriers are caused by the stratum corneum intercellular lipids, the penetration of PG is retarded, to some extent, due to its hydrophilicity [11,162,163]. The situation was changed with the addition of farnesol, which bridged the lipids and PG so that the solutions moved faster as a whole through the lamella of the intercellular lipids.

The main components of these intercellular lipids, i.e., cholesterol, free fatty acids and ceramides, are more compatible with ISA than with the enhancer, due to their lipophilic properties [97]. Thus the combination of ISA and farnesol did not facilitate drug permeation further as much as ISA alone. In PG formulation, the gelator and enhancer increased lag-time to a larger extent in combination than individually. The synergistic effect could be due to the fact that the gelator GP-1 is lipid in nature and it reinforced the diffusion barrier of the SC lipids.

In summary, ISA-based delivery systems are robust, less susceptible to effects of the enhancer or gelator, which is preferable for dosage form design, but not for permeation enhancement. The four formulae of ISA share almost identical permeation profiles (two-sample *t*-tests, $p > 0.05$). Solvent PG-based systems are sensitive to the level change of the three factors. With the addition of farnesol, the permeation coefficient increased 12 times. Further addition of the gelator results in a 3-fold increase of lag-time, but the increase of permeation coefficient is not significant due to the large variances involved (two-sample *t*-tests, $p > 0.05$).

3.6 Terpenes Bind and Solubilize Skin Lipids

Results. The complete array of structures of major SC intercellular lipids is shown in Figure 3.6-1. The 9 extractable ceramides are arranged in a manner such that the molecular moieties of sphingosine, phytosphingosine and 6-OH-sphingosine appear periodically, matching the corresponding moieties of acylated ω-OH fatty acid, non-OH fatty acid, and α-OH fatty acid, respectively [97].

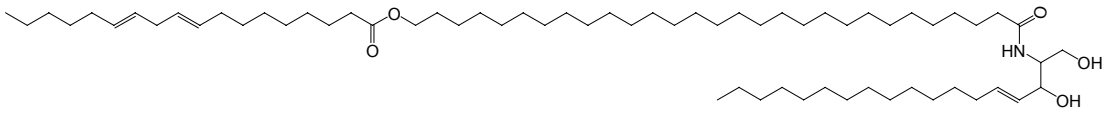

Ceramide 1, EOS ($C_{65}H_{123}NO_5$, MW = 998.68)

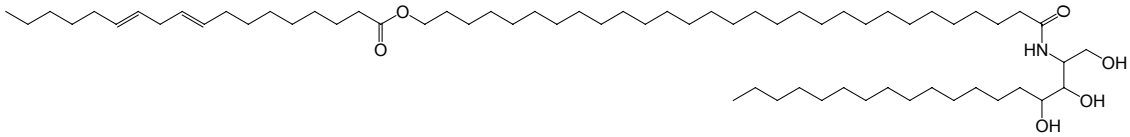

Ceramide 9, EOP ($C_{65}H_{125}NO_6$, MW = 1016.69)

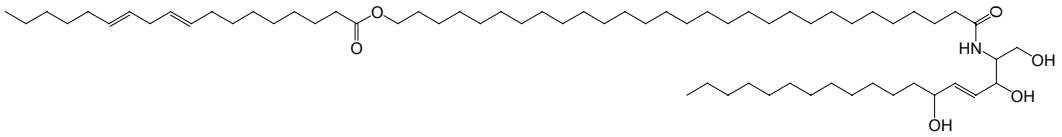

Ceramide 4, EOH ($C_{65}H_{123}NO_6$, MW = 1014.68)

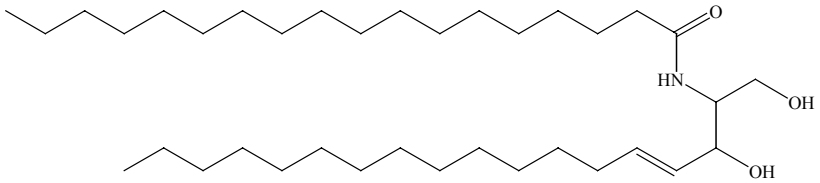

Ceramide 2, NS ($C_{36}H_{71}NO_3$, MW = 565.95)

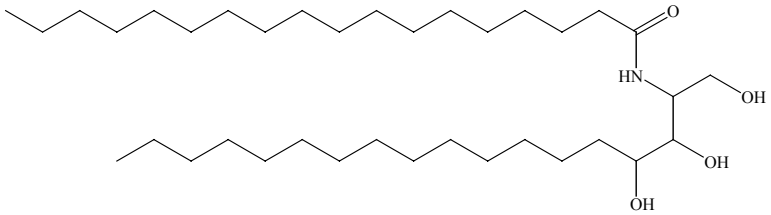

Ceramide 3 (N-stearyolphytosphingosine), NP ($C_{36}H_{73}NO_4$, MW = 583.97, Log P = 13.38)

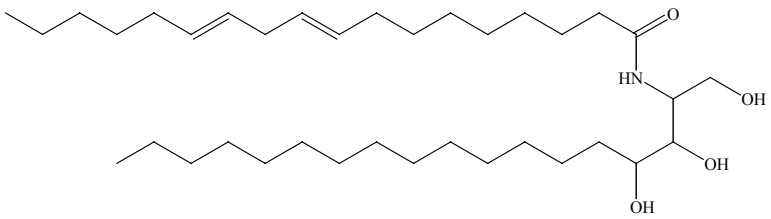

Ceramide 3A, N-linoleoyl-phytosphigosine, ($C_{36}H_{69}NO_4$, MW = 579.94)

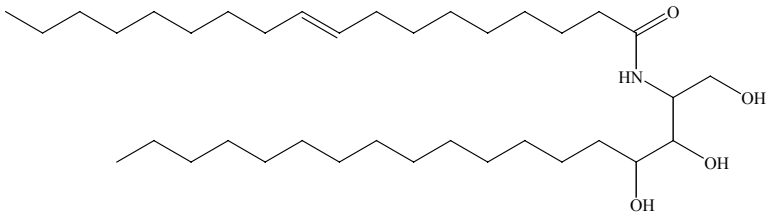

Ceramide 3B, N-oleoyl-phytosphigosine ($C_{36}H_{71}NO_4$, MW = 581.95)

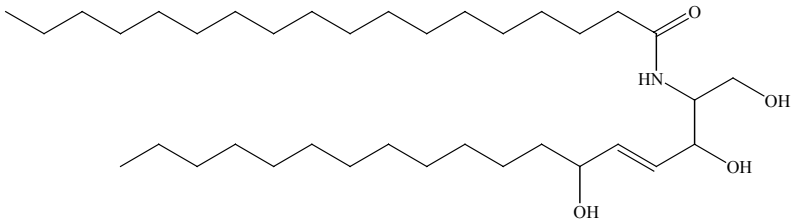

Ceramide 6, NH ($C_{36}H_{71}NO_4$, MW = 581.95)

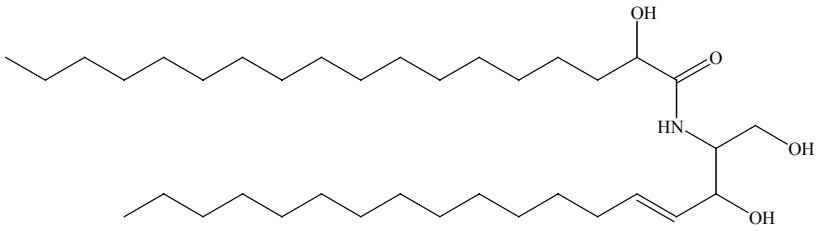

Ceramide 5, AS ($C_{36}H_{71}NO_4$, MW = 581.95)

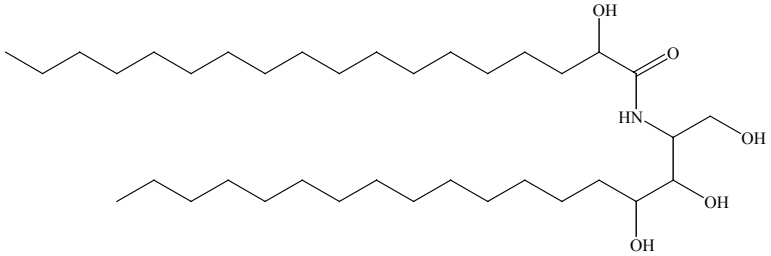

Ceramide 7, AP ($C_{36}H_{73}NO_5$, MW = 599.97)

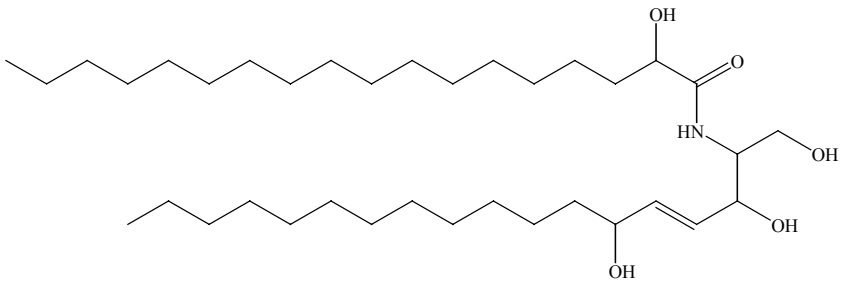

Ceramide 8, AH ($C_{36}H_{71}NO_5$, MW = 597.95)

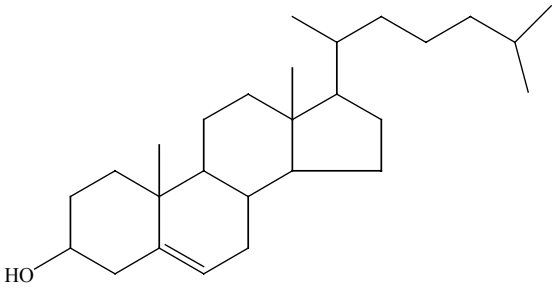

Cholesterol [57-88-5] ($C_{27}H_{46}O$, MW= 386.65, Log P = 9.85)

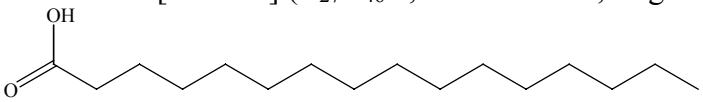

Palmitic acid [57-10-3] ($C_{16}H_{32}O_2$, MW= 256.42, Log P = 7.15, mp 61-64 ^{0}C)

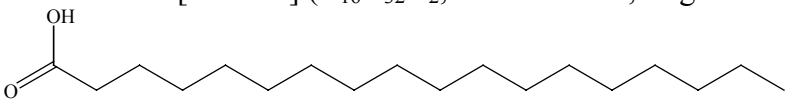

Stearic acid [57-11-4] ($C_{18}H_{36}O_2$, MW= 284.48, Log P = 8.22)

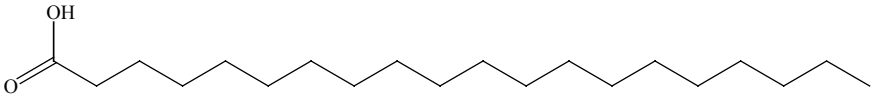

Arachic (eicosanoic) acid [506-30-9] ($C_{20}H_{40}O_2$, MW= 312.53, Log P = 9.28)

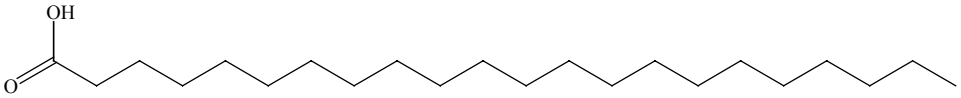

Behenic (docosanoic) acid [112-85-6] ($C_{22}H_{44}O_2$, MW= 340.58, Log P = 10.34)

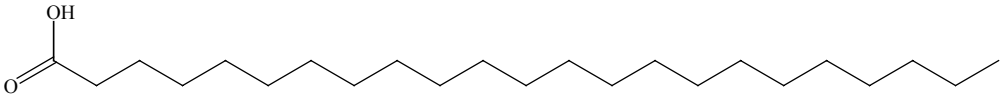

Tricosanoic acid [2433-96-7] ($C_{23}H_{46}O_2$, MW= 354.61, Log P = 10.87, mp=70-80^{0}C)

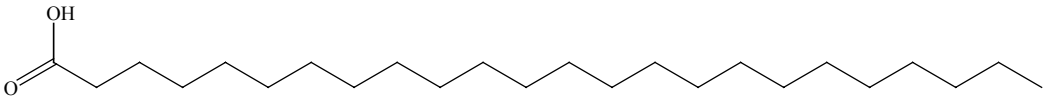

Lignoceric (tetracosanoic) acid [557-59-5] ($C_{24}H_{48}O_2$, MW= 368.64, Log P = 11.40)

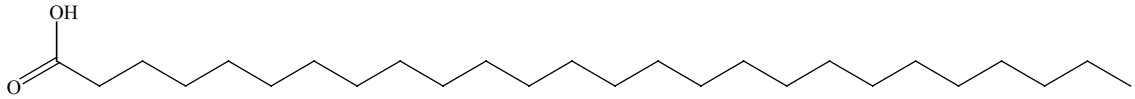

Cerotic (hexacosanoic) acid [506-46-7] ($C_{26}H_{52}O_2$, MW= 396.69, Log P = 12.47)

Figure 3.6-1. The molecular structure of ceramides 1-8 including ceramide 9, cholesterol and free fatty acids (C16:0, C18:0, C20:0, C22:0, C23:0, C24:0, C26:0).

Solubilities of SC intercellular lipids in PG are in Table 3.6-1. Cholesterol, palmitic acid and stearic acid were the most soluble among all the lipids in PG. With the addition of 5% (w/v) farnesol, the three lipids were further solubilized to a significant extent. This suggests that the loss of these three lipids may enhance skin permeability while the other lipids and the highly impermeable corneocytes of SC remain as the intact skin barrier.

Lipid	In pure PG	In PG with 5% (w/v) farnesol	Increase % with 5% (w/v) farnesol
Cholesterol	1.84 ± 0.01	*4.88 ± 0.03	165.0
Palmitic acid	3.53 ± 0.02	*15.03 ± 0.06	326.0
Stearic acid	2.04 ± 0.02	*6.31 ± 0.02	209.0
Arachic acid	0.71 ± 0.01	*1.21 ± 0.04	70.5
Behenic acid	0.51 ± 0.01	*0.91 ± 0.02	76.5
Tricosanoic acid	0.30 ± 0.02	*1.60 ± 0.05	430.0
Ligonoceric acid	0.21 ± 0.01	0.22 ± 0.01	4.7
Cerotic acid	0.11 ± 0.00	0.11 ± 0.01	7.9
Ceramide 9	0.61 ± 0.01	0.61 ± 0.01	0.0
Ceramide III	0.91 ± 0.01	*1.21 ± 0.02	33.7
Ceramide IIIA	0.71 ± 0.01	*0.90 ± 0.02	26.9
Ceramide IIIB	1.11 ± 0.01	1.10 ± 0.01	0.0
Ceramide VII	0.24 ± 0.06	*0.40 ± 0.01	65.3

Table 3.6-1. Solubility (mg/ml) of skin lipids in PG and PG with 5% (w/v) farnesol. Data is Mean ± SD (n = 3). * Two-sample *t*-test ($p < 0.05$) comparing the lipid solubility in 5% (w/v) farnesol to the solubility in pure PG.

Interaction between the lipids and farnesol by ITC follows. Figure 3.6-2 shows the isothermal titration results of farnesol solutions titrated into cholesterol, behenic acid, ceramide 3 and ceramide 9 solutions, respectively. Figure 3.6-3 summarizes the binding parameters fitted by nonlinear regression analysis. The energy (integral) of each peak was plotted as a function of the ratio between the moles of farnesol added to the moles of the lipid in the ampoule (Figure 3.6-2). It was shown in Figure 3.6-3 that one farnesol molecule bound one cholesterol molecule while two farnesol molecules bound one molecule of each of the other lipids, respectively. These four interactions were spontaneous processes with negative free energy change. For cholesterol, ceramide 3 and ceramide 9, the positive entropy changes showed their interactions with farnesol were entropy-driven but for behenic acid, the binding was enthalpy-driven with decreased entropy after binding. The negative enthalpy-change of the latter indicated it was exothermic while the former three binding processes were all endothermic with increased entropy.

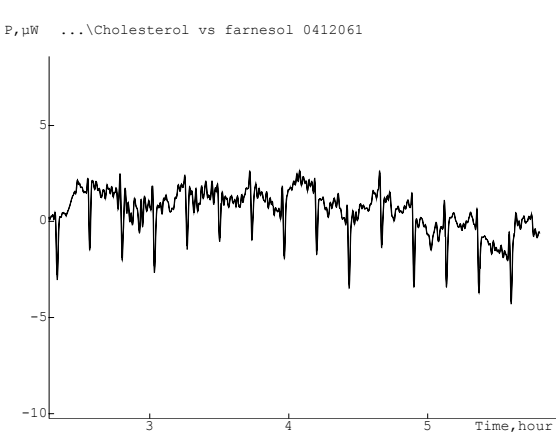

(a)

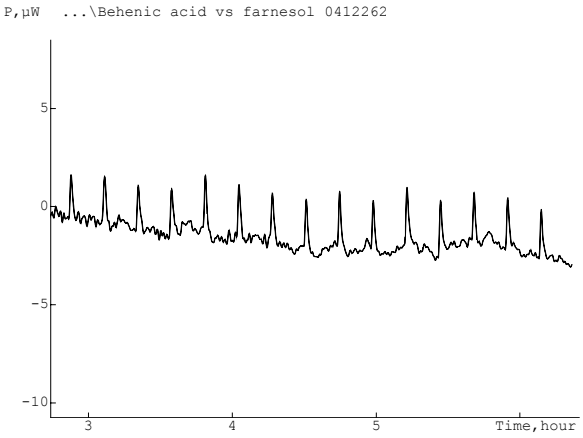

(b)

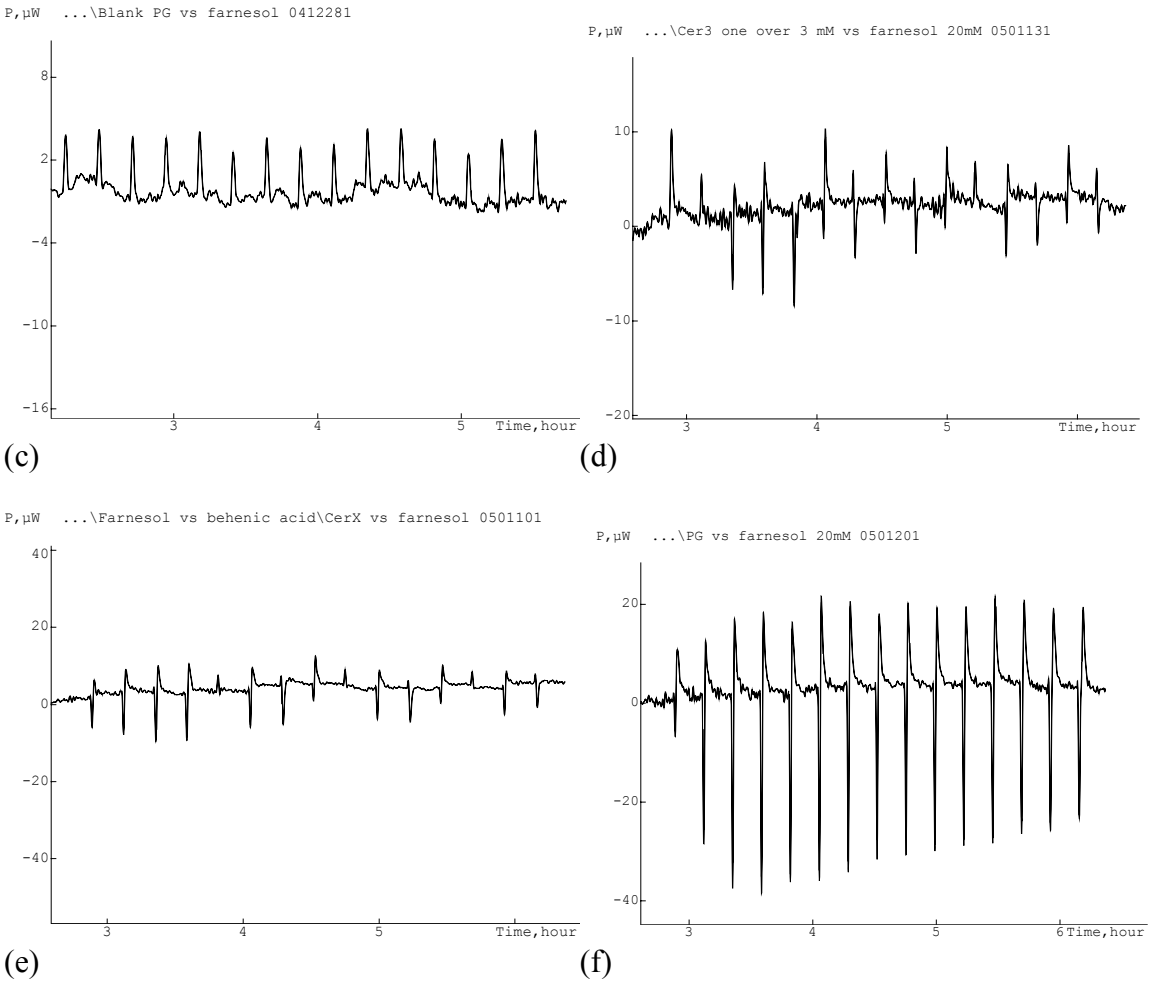

Figure 3.6-2. Results obtained from ITC. The positive heat peak indicates an exothermic process, i.e., the heat flows from the system to the surroundings and the negative heat flow-rate indicates an endothermic process whereby heat flows in the opposite direction. 0.12 ml of farnesol solution (71 mmol/ml) was titrated consecutively by 15 aliquots into 2.7 ml of **(a)** cholesterol solution (2 mmol/ml), **(b)** behenic acid solution (0.667 mmol/ml), and **(c)** pure PG. 0.12 ml of farnesol solution (20 mmol/ml) was titrated consecutively by 15 aliquots into 2.7 ml of **(d)** ceramide 3 solution (0.333 mmol/ml), **(e)** ceramide 9 solution (0.333 mmol/ml), and **(f)** pure PG.

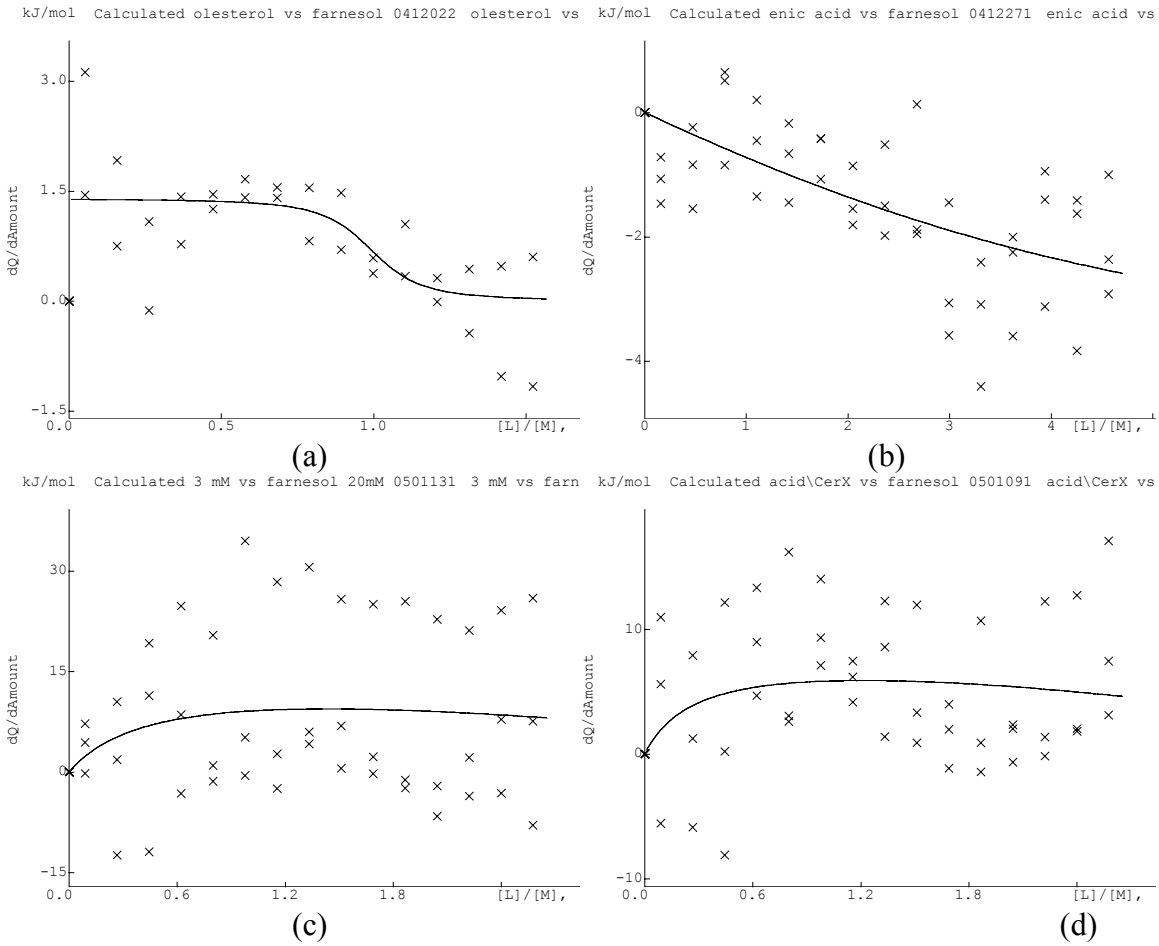

Figure 3.6-3. Nonlinear regression analyses to estimate the binding stoichiometry, n, the binding constant K, and the enthalpy change ΔH using software Digitam®. The energy (integral) of each peak as in Figure 3.6-2 was plotted as a function of the ratio of the moles of farnesol added to the moles of the lipid in the ampoule. The binding heat was derived from the measured heat subtracting the heat of the control as shown in Figure 3.6-2. The nonlinear regression model is based on $M + nL = ML_n + error$, which describes the binding reaction in this study between a host molecule M (the lipid), and a ligand molecule L (farnesol). Replicates were pooled for the nonlinear regression (replicates are 2, 3, 3 and 3 for **(a)**, **(b)**, **(c)** and **(d)**, respectively). Result of farnesol solution titrated into **(a)** cholesterol solution. Binding stoichiometry n = 1, binding constant K = $6.79*10^4$ M^{-1} and ΔH = 1.40 kJ/mol, endothermic entropy-driven process. ΔG = -28.67 kJ/mol and ΔS = 97.02 J mol^{-1} K^{-1}, **(b)** behenic acid solution. Binding stoichiometry n = 2, binding constant K = $7.62*10^3$ M^{-2} and ΔH = -112.93 kJ/mol, exothermic enthalpy-driven process. ΔG = -23.04 kJ/mol and ΔS = -289.98 J mol^{-1} K^{-1}, **(c)** ceramide 3 solution. Binding stoichiometry n = 2, binding constant K = $3.10*10^6$ M^{-2} and ΔH = 44.81 kJ/mol, endothermic entropy-driven process. ΔG = -38.53 kJ/mol and ΔS = 268.81 J mol^{-1} K^{-1}, and **(d)** ceramide 9 solution. Binding stoichiometry n = 2, binding constant K = $5.28*10^4$ M^{-2} and ΔH = 24.20 kJ/mol, endothermic entropy-driven process. ΔG = -28.03 kJ/mol and ΔS = 168.47 J mol^{-1} K^{-1}.

Discussion. For cholesterol, ceramide 3 and ceramide 9, the increased entropy indicated that the final state (after binding) became more disordered than the original state. Since the dilution heat of farnesol has been discounted and the dilution effect of the lipid was negligible due to the limited volume of the titrant, the increased entropy resulted from the binding between farnesol and the lipid molecules. The original aggregation state of the lipid in PG solution was more ordered than afterwards with the intrusion of farnesol, which bound the lipids and rearranged the lipid aggregates. For behenic acid, however, the binding decreased the entropy. The binding happened only because it released heat and decreased the system energy. It showed that the aggregates of behenic acid in PG were more ordered than the binding complexes with farnesol. The introduction of farnesol into the behenic solution, therefore, aligned the behenic acid molecules in PG.

The solubility results showed that cholesterol, behenic acid and ceramide 3 were significantly solubilized by farnesol while ceramide 9 was not (Table 3.6-1). Therefore, for cholesterol and ceramide 3, their formed complexes were more disordered and have higher solubilities in PG with farnesol than in PG alone. Although the formed complexes of behenic acid were more ordered, they have higher solubilities in PG with farnesol than behenic acid in PG alone. For ceramide 9, its solubility was not affected by farnesol, but its aggregation state was disturbed. The results suggest that the skin penetration enhancing mechanism of farnesol is most likely due to lipid extraction and/or triggering lipid phase transition of the SC lamella, where the lipid molecules are in crystalline or liquid crystalline phases [100]. For cholesterol and ceramides with non-acylated ω-OH fatty acids, farnesol may increase their solubilities and disrupt their structures. For ceramides with long chain acylated ω-OH fatty acids such as ceramides 1 and 4, farnesol

could have bind to them and disturb the crystalline phase. For free fatty acids, with the exception of lignoceric acid and cerotic acid, farnesol increased their solubilities significantly. Some binding complexes of fatty acids with farnesol could pose as a permeation barrier, but much less impervious than the compact crystalline or liquid crystalline phases of SC lipids.

Inter- and intra-molecular hydrogen bonds could be the driving forces for the bonds. Between cholesterol and farnesol, the binding ratio is unity, suggesting that they were mutual bond donors and acceptors. The carboxyl group of behenic acid could accommodate two farnesol molecules via hydrogen bonds. It is plausible that an intra-molecular hydrogen bond was formed within the ceramide 3 or the ceramide 9 molecule, between the hydroxyl and the neighboring carboxyl groups whereas the other hydroxyl groups of each ceramide formed hydrogen bonds with the two farnesol molecules.

Compared with the physical enhancing methods of circumventing the SC barrier by piercing multiple micro-sized passages in it, chemical enhancement may be safer. Chemical enhancers would disturb only some of the SC lipids, leaving the highly impermeable corneocytes unchanged, so that the SC can still be functional as an effective biological barrier [2,51].

4. Conclusion

The modeling of drug permeation process through excised skin using both Franz cell and flow-through cell facilitated the studies on the efficacies and reversibilities of enhancers, and also from the SGMA gels. The permeation behaviors of the model drug and the enhancers are further investigated by studying the interactions between skin lipids and terpene enhancers.

4.1 Models for Franz and Flow-through Cells

Mathematical and statistical models for Franz cell with finite outflow volume and flow-through cell with infinite outflow volume have been derived.

A mathematical solution based on finite outflow volume was derived from the Fick's law. It can serve as a statistical model to estimate the permeability coefficient from *in vitro* skin permeation study with the accumulation of penetrants in the receptor compartment of the static diffusion cells. The model is suitable to describe the *in vitro* drug or chemical permeation studies using Franz cells.

However, the flow-though cells have infinite outflow volume, so a different model that enables the parameter estimation without impairing the integrity and quality of the original permeation data was proposed. The nonlinear regression model derived from Fick's law is appropriate. Bootstrap sampling is useful for checking the precision of parameter inference based on the large-sample theory. For the *in vitro* permeation study that we conducted with flow-through cells, the method proved to be robust. The estimates of permeated drug/chemical are important in that, unlike *in vivo* environment where stratum corneum is replenished by the adjacent live stratum granulosum through

keratinization, the excised stratum corneum, though composed of dead corneocytes, will deteriorate after days in contact with solvents, which will cause over-hydration of stratum corneum that can destroy the lamella and decomposition that will leave highly permeable passages in the stratum corneum. The predictions are relevant for transdermal drug delivery, the cosmetic industry and regulatory risk assessment on dermal exposure to toxic substances.

4.2 Enhancing Efficacy of Terpenes

The enhancing effects of 49 terpenes are compared by *in vitro* drug permeation studies through excised human epidermis. The results are tabulated and analyzed by statistical methods. The derived multiple linear regression (MLR) models can be used for the estimation of permeability coefficients of haloperidol in the presence of terpene enhancers. Models which can provide an estimation of drug or chemical permeability coefficient though human skin are useful for the preliminary screening of enhancers. For monoterpenes and sesquiterpenes, the permeability coefficients of haloperidol increased as the lipophilicities of terpenes increased. For terpenes of all categories, their enhancing abilities decreased as their MW increased. Melting points and boiling points of terpenes were negatively correlated with the permeability coefficients of haloperidol. Sesquiterpenes were better than monoterpenes when only the enhancing effects were considered. The overall ranking of enhancing ability is as follows: ester > aldehyde > oxide > hydrocarbon > alcohol > ketone > phenol > acid.

4.3 Reversible Effects of Terpenes

In addition to the enhancing effects, the reversibility of the effects of terpenes on the skin is also an important characteristic of an ideal enhancer. From the results of this study, the permeability of the pre-treated epidermis was comparable to that of the control, so the insult to the barrier function of the skin caused by the enhancers was restored. As an *in vitro* study was performed, the recovery of the epidermal barrier function could not be due to the cellular regeneration at the horny layer restoring its physical barrier. The mechanism for this reversible enhancement would be attributed to the insertion of these enhancers within the SC intercellular lipid lamella. The disruptions in the lipid lamella eased the permeation of the lipophilic drug through the tortuous pathway, hence resulting in enhancement of drug permeation. Likewise, once the enhancers were removed, bonds between the lipids could start to re-form and the depletion of the enhancers could allow the packing of the lipids to revert back to its original alignment. (R) - (-) carvone had a much faster elution profile out of the epidermis than eucarvone. The results also showed that (R) - (-) carvone, rather than eucarvone, retained more HP within the epidermis. This suggests that (R) - (-) carvone could be useful as an enhancer for depot HP therapy. In conclusion, both (R) - (-) carvone and eucarvone were shown to be effective and reversible enhancers for the *in vitro* permeation of HP through human epidermis.

4.4 Incorporation of Terpenes in SMGA Gels

The enhancing effect of a selected enhancer, farnesol, incorporated into gels containing small molecule gelling agents (SMGA), was evaluated. The SMGA gels developed for application on the skin retained their characteristic aesthetic and rheological properties

with the incorporation of the drug and enhancer. These *in vitro* human skin permeation studies showed that the gels possessed desirable properties for both topical and transdermal delivery. The translucent lipophilic gels with ISA were stable and the permeation of the drug reached the pseudo steady state in less time compared to the PG-based gel. The latter, opaque white in color, delivered the drug at a faster rate with the addition of the enhancer. The gelator, GP-1, did not influence the drug permeation rate but increased its permeation lag-time.

4.5 Terpenes Bind and Solubilize Skin Lipids

To better understand the effects of the terpenes on drug permeability through the skin, their interactions with SC intercellular lipids were studied using isothermal titration (ITC) method. Cholesterol, palmitic acid and stearic acid were the most soluble among all the lipids in propylene glycol and they were further significantly solubilized upon the addition of farnesol. The interactions between farnesol and four representative lipids, i.e., cholesterol, behenic acid, ceramide 3 and ceramide 9 were studied using the ITC method. The binding ratios of farnesol to cholesterol, behenic acid, ceramide 3 and ceramide 9 were found to be 1, 2, 2 and 2, respectively. All were endothermic and entropy-driven except for that between farnesol and behenic acid, which was exothermic and enthalpy-driven. Hydrogen bonding may be the driving force of these interactions. The results suggest that the skin penetration enhancing mechanism of farnesol could be due to lipid extraction and/or triggering lipid phase transition of the SC lamella.

The result is consistent with the permeation study results, which showed the permeability coefficient of the drug increased as the lipophilicities of monoterpene and sesquiterpenes

increased. It is perceivable that terpenes with high lipophilicities will have more interactions with skin lipids.

In summary, this thesis has contributed the following new knowledge on the use of penetration enhancers as a chemical approach to breach the human skin barrier. (1) Mathematical and statistical models for *in vitro* permeation studies using both Franz and flow-through cells were derived and tested. (2) A scheme to relate the enhancing efficacies of 49 terpenes to their physiochemical properties. The approach may be relevant for assessment of other chemicals as enhancers. (3) The enhancing effects of two terpenes on excised skin were demonstrated to be reversible. (4) The novel SMGA gels are suitable for topical or transdermal drug delivery. (5) The enhancing mechanism of farnesol could be due to lipid extraction and/or lipid phase transition in the SC lamella.

4.6 Future Work

This study shows that monoterpenes and sesquiterpenes with ester or aldehyde function groups are the most promising candidates. However, it should be noted that the drug used in this study, i.e., haloperidol, is a hydrophobic compound and the finding may not apply to other drugs, in particular the hydrophilic drugs. Further studies may be conducted as follows. First, the relationship between permeability coefficient and the amount of SC lipids extracted can be studied by testing the solubilities of the SC lipids in different enhancers. It is useful to find out if the complete removal of SC lipids is a feasible penetration enhancement method. Second, it is important to determine if the terpene is in the monomer or aggregated state in the skin. Existence of a hydrophobic micelle core can entrap the lipids, and therefore, solubilization may occur only above the

critical micelle concentration (CMC). The CMC of terpenes can be determined by ITC method. Third, the relationship between pore-size of membrane and its permeability may be studied to explain the enhancing effects resulting from lipid extraction. Fourth, the transport of therapeutic doses of the haloperidol, safety and stability of the delivery systems may also be studied.

References

[1] B.W. Barry, Breaching the skin's barrier to drugs, Nat. Biotechnol. 22 (2) (2004) 165-167.

[2] M.R. Prausnitz, S. Mitragotri, R. Langer, Current status and future potential of transdermal drug delivery, Nat. Rev. Drug. Discov. 3 (2) (2004) 115-124.

[3] H.K. Vaddi, P.C. Ho, S.Y. Chan, Terpenes in propylene glycol as skin-penetration enhancers: Permeation and partition of haloperidol, Fourier transform infrared spectroscopy, and differential scanning calorimetry, J. Pharm. Sci. 91 (7) (2002) 1639-1651.

[4] A.C. Altamura, F. Sassella, A. Santini, C. Montresor, S. Fumagalli, E. Mundo, Intramuscular preparations of antipsychotics: Uses and relevance in clinical practice, Drugs 63 (5) (2003) 493-512.

[5] H.K. Vaddi, L.Z. Wang, P.C. Ho, S.Y. Chan, Effect of some enhancers on the permeation of haloperidol through rat skin in vitro, Int. J. Pharm. 212 (2) (2001) 247-255.

[6] B.W. Barry, Is transdermal drug delivery research still important today?, Drug Discovery Today 6 (19) (2001) 967-971.

[7] Jain-PharmaBiotech. Transdermal Drug Delivery - Technologies, Markets, and Companies. http://www.pharmabiotech.ch/reports/tdd/. Accessed on July 1, 2005.

[8] P.W. Wertz, Lipids and barrier function of the skin, Acta Derm. Venereol. Suppl. (Stockh). 208 (2000) 7-11.

[9] M. Ponec, A. Weerheim, P. Lankhorst, P. Wertz, New acylceramide in native and reconstructed epidermis, J. Invest. Dermatol. 120 (4) (2003) 581-588.

[10] M. Ponec, Skin constructs for replacement of skin tissues for in vitro testing, Adv. Drug Deliv. Rev. 54 Suppl 1 (2002) S19-30.

[11] B. Forslind, A domain mosaic model of the skin barrier, Acta Derm. Venereol. 74 (1) (1994) 1-6.

[12] D.T. Downing, Lipid and protein structures in the permeability barrier of mammalian epidermis, J. Lipid Res. 33 (3) (1992) 301-313.

[13] S.J. Singer, G.L. Nicolson, The fluid mosaic model of the structure of cell membranes, Science 175 (23) (1972) 720-731.

[14] B. Forslind, S. Engstrom, J. Engblom, L. Norlen, A novel approach to the understanding of human skin barrier function, J. Dermatol. Sci. 14 (2) (1997) 115-125.

[15] J. Bouwstra, G. Pilgram, G. Gooris, H. Koerten, M. Ponec, New aspects of the skin barrier organization, Skin Pharmacol. Appl. Skin Physiol. 14 Suppl 1 (2001) 52-62.

[16] J.A. Bouwstra, F.E. Dubbelaar, G.S. Gooris, M. Ponec, The lipid organisation in the skin barrier, Acta Derm. Venereol. Suppl. (Stockh). 208 (2000) 23-30.

[17] L. Norlen, Skin barrier structure and function: The single gel phase model, J. Invest. Dermatol. 117 (4) (2001) 830-836.

[18] L. Norlen, Skin barrier formation: The membrane folding model, J. Invest. Dermatol. 117 (4) (2001) 823-829.

[19] O. Wallach. Alicylic compounds, Nobel Lecture, December 12, 1910. http://nobelprize.org/chemistry/laureates/1910/wallach-lecture.pdf. Accessed on July 1, 2005.
[20] O. Montelius. The Nobel Prize in Chemistry 1910. http://nobelprize.org/chemistry/laureates/1910/press.html. Accessed on July 1, 2005.
[21] A.A. Newman, Chemistry of terpenes and terpenoids, Academic Press, London and New York, 1972.
[22] A.R. Pinder, The Chemistry of the Terpenes, Chapman & Hall, London, 1961, pp. 223.
[23] FDA. Part 182 substances generally recognized as safe. http://www.cfsan.fda.gov/~lrd/fcf182.html. Accessed on July 1, 2005.
[24] A.C. Williams, B.W. Barry, Terpenes and the lipid-protein-partitioning theory of skin penetration enhancement, Pharm. Res. 8 (1) (1991) 17-24.
[25] V.R. Sinha, M.P. Kaur, Permeation enhancers for transdermal drug delivery, Drug Dev. Ind. Pharm. 26 (11) (2000) 1131-1140.
[26] R.J. Scheuplein, Properties of the skin as a membrane, Adv. Biol. Skin 12 (1972) 125-152.
[27] B.M. Magnusson, Y.G. Anissimov, S.E. Cross, M.S. Roberts, Molecular size as the main determinant of solute maximum flux across the skin, J. Invest. Dermatol. 122 (4) (2004) 993-999.
[28] R.L. Bronaugh, In vitro percutaneous absorption models, Ann. N. Y. Acad. Sci. 919 (2000) 188-191.
[29] J. Sandby-Moller, T. Poulsen, H.C. Wulf, Epidermal thickness at different body sites: Relationship to age, gender, pigmentation, blood content, skin type and smoking habits, Acta Derm. Venereol. 83 (6) (2003) 410-413.
[30] A.J.P. Klein-Szanto, Stereologic baseline data of hormal human epidermis, J. Invest. Dermatol. 68 (2) (1977) 73-78.
[31] M. Huzaira, F. Rius, M. Rajadhyaksha, R.R. Anderson, S. Gonzalez, Topographic variations in normal skin, as viewed by in vivo reflectance confocal microscopy, J. Invest. Dermatol. 116 (6) (2001) 846-852.
[32] C.A. Squier, M. Kremer, P.W. Wertz, Continuous flow mucosal cells for measuring the in vitro permeability of small tissue samples, J. Pharm. Sci. 86 (1) (1997) 82-84.
[33] T.J. Franz, Percutaneous absorption on the relevance of in vitro data, J. Invest. Dermatol. 64 (3) (1975) 190-195.
[34] H.A. Daynes, The process of diffusion through a rubber membrane, Proceedings of the Royal Society of London, Series A: Containing papers of a mathematical and physical character 97 (685) (1920) 286-307.
[35] J. Crank, The Mathematics of Diffusion, 2nd Ed, Clarendon Press, Oxford, 1975, pp. 44-52.
[36] E.L. Cussler, Diffusion: Mass Transfer in Fluid Systems, Cambridge University Press, Cambridge, UK, 1996, pp. 18-27.
[37] O. Diez-Sales, A. Copovi, V.G. Casabo, M. Herraez, A modelistic approach showing the importance of the stagnant aqueous layers in in vitro diffusion studies, and in vitro-in vivo correlations, Int. J. Pharm. 77 (1) (1991) 1-11.

[38] M.I. Foreman, I. Clanachan, I.P. Kelly, The diffusion of nandrolone through occluded and non-occluded human skin, J. Pharm. Pharmacol. 30 (3) (1978) 152-157.
[39] H. Okamoto, H. Komatsu, M. Hashida, H. Sezaki, Effects of b-cyclodextrin and di-O-methyl-b-cyclodextrin on the percutaneous absorption of butylparaben, indomethacin and sulfanilic acid, Int. J. Pharm. 30 (1) (1986) 35-45.
[40] R.C.L. Jenkins, P.M. Nelson, L. Spirer, Calculation of the transient diffusion of a gas through a solid membrane into a finite outflow volume, Trans. Faraday Soc. 66 (1970) 1391-1401.
[41] J. Neter, M.H. Kntner, C.J. Nachtsheim, W. Wasserman, Applied Linear Statistical Model, WCB/McGraw-Hill, Boston, 1996, pp. 531-555.
[42] D.M. Bates, D.G. Watts, Nonlinear Regression Analysis and Its Applications, John Wiley & Sons, New York, 1988, pp. 32-39.
[43] D. Hallen, Data treatment: Considerations when applying binding reaction data to a model, Pure Appl. Chem. 65 (7) (1993) 1527-1532.
[44] R.R. Warner, K.J. Stone, Y.L. Boissy, Hydration disrupts human stratum corneum ultrastructure, J. Invest. Dermatol. 120 (2) (2003) 275-284.
[45] J.A. Bouwstra, A. de Graaff, G.S. Gooris, J. Nijsse, J.W. Wiechers, A.C. van Aelst, Water distribution and related morphology in human stratum corneum at different hydration levels, J. Invest. Dermatol. 120 (5) (2003) 750-758.
[46] M.E. Johnson, D. Blankschtein, R. Langer, Evaluation of solute permeation through the stratum corneum: Lateral bilayer diffusion as the primary transport mechanism, J. Pharm. Sci. 86 (10) (1997) 1162-1172.
[47] G.B. Kasting, Kinetics of finite dose absorption through skin 1. Vanillylnonanamide, J. Pharm. Sci. 90 (2) (2001) 202-212.
[48] R.J. Scheuplein, Mechanism of percutaneous absorption. II. Transient diffusion and the relative importance of various routes of skin penetration, J. Invest. Dermatol. 48 (1) (1967) 79-88.
[49] G.L. Flynn, S.H. Yalkowsky, T.J. Roseman, Mass transport phenomena and models: Theoretical concepts, J. Pharm. Sci. 63 (4) (1974) 479-510.
[50] R.J. Scheuplein, I.H. Blank, Permeability of the skin, Physiol. Rev. 51 (4) (1971) 702-747.
[51] B.W. Barry, Novel mechanisms and devices to enable successful transdermal drug delivery, Eur. J. Pharm. Sci. 14 (2) (2001) 101-114.
[52] R.L. Bronaugh, R.F. Stewart, Methods for in vitro percutaneous absorption studies IV: The flow-through diffusion cell, J. Pharm. Sci. 74 (1) (1985) 64-67.
[53] P.A. Cornwell, B.W. Barry, Sesquiterpene components of volatile oils as skin penetration enhancers for the hydrophilic permeant 5-fluorouracil, J. Pharm. Pharmacol. 46 (4) (1994) 261-269.
[54] T. Wonnacott, Confidence intervals or hypothesis tests, J. Appl. Stat. 14 (3) (1987) 195-201.
[55] J.A. Rice, Mathematical Statistics and Data Analysis, Duxbury Press, Belmont, California, 1994, pp. 306-308.
[56] D.N. Anderson, S.R. Taylor. Application of Regularized Discrimination Analysis to Regional Seismic Event Identification. 2000; New Orleans. US Department of Defense and US Department of Energy.

[57] N.R. Draper, H. Smith, Applied Regression Analysis, John Wiley & Sons, New York, 1998, pp. 585-591.
[58] J. Hadgraft, Modulation of the barrier function of the skin, Skin Pharmacol. Appl. Skin Physiol. 14 Suppl 1 (2001) 72-81.
[59] M.B. Haberkamp, in: D.S. Hsieh, Drug Permeation Enhancement: Theory and Applications, Mercel Dekker, New York, 1994, pp. 43-58.
[60] W.S. Pray, Nonprescription Product Therapeutics (2nd ed), Lippincott Williams & Wilkins, Philadelphia, 2003.
[61] B.W. Barry, S.L. Bennett, Effect of penetration enhancers on the permeation of mannitol, hydrocortisone and progesterone through human skin, J. Pharm. Pharmacol. 39 (7) (1987) 535-546.
[62] M. Goodman, B.W. Barry, Action of penetration enhancers on human skin as assessed by the permeation of model drugs 5-fluorouracil and estradiol. I. Infinite dose technique, J. Invest. Dermatol. 91 (4) (1988) 323-327.
[63] H. Okamoto, M. Ohyabu, M. Hashida, H. Sezaki, Enhanced penetration of mitomycin C through hairless mouse and rat skin by enhancers with terpene moieties, J. Pharm. Pharmacol. 39 (7) (1987) 531-534.
[64] E.E. Van Tamelen, J. McNary, F.A. Lornitzo, Mechanism of the carvone hydrobromide-eucarvone transformation, J. Am. Chem. Soc. 79 (1957) 1231-1236.
[65] J.A. Pino, J. Garcia, M.A. Martinez, Comparison of solvent extract and supercritical carbon dioxide extract of spearmint leaf, J. Essent. Oil Res. 11 (2) (1999) 191-193.
[66] The Combined Chemical Dictionary: Chemical Database Online, Chapman & Hall, London, 2005, pp. JSX52-Q.
[67] J.Y. Mo, D.W. Frank, assignee. Topical stabilized prostaglandin E compound dosage forms. US Patent 6,841,574, January 11, 2005.
[68] J. Pino, A. Rosado, R. Sanchez, Volatile components of three cultivars of mango from Cuba, Nahrung 33 (8) (1989) 709-715.
[69] S.-J. Kim, assignee. Composition containing Asiasari Radix extracts for protecting brain cells and improving memory. US Patent 6,737,087, May 18, 2004.
[70] S.G. Griffin, D.N. Leach, J. Markham, R. Johnstone, Antimicrobial activity of essential oils from Zieria, J. Essent. Oil Res. 10 (2) (1998) 165-174.
[71] O.Y.-P. Hu, assignee. Transdermal delivery of buprenorphine preparations. U.S. patent 6,004,969, December 21, 1999.
[72] L.A. Estroff, A.D. Hamilton, Water gelation by small organic molecules, Chem. Rev. 104 (3) (2004) 1201-1218.
[73] D.J. Abdallah, R.G. Weiss, Organogels and low molecular mass organic gelators, Adv. Mater. 12 (17) (2000) 1237-1247.
[74] P. Terech, R.G. Weiss, Low molecular mass gelators of organic liquids and the properties of their gels, Chem. Rev. 97 (8) (1997) 3133-3160.
[75] Y.C. Lin, R.G. Weiss, Liquid-crystalline solvents as mechanistic probes. Part 34. Evidence for random parallel and antiparallel packing between neighboring cholesteryl 4-(2-anthryloxy)butyrate (CAB) molecules in the cholesteric liquid-

crystalline phase. Identification of the four photodimers from CAB, Liq. Cryst. 4 (4) (1989) 367-384.
[76] X.Y. Liu, P.D. Sawant, Formation kinetics of fractal nanofiber networks in organogels, Appl. Phys. Lett. 79 (21) (2001) 3518-3520.
[77] X.Y. Liu, P.D. Sawant, Micro/Nanoengineering of the self-organized three-dimensional fibrous structure of functional materials, Angew. Chem. Int. Ed. Engl. 41 (19) (2002) 3641-3645.
[78] X.Y. Liu, P.D. Sawant, W.B. Tan, I.B. Noor, C. Pramesti, B.H. Chen, Creating new supramolecular materials by architecture of three-dimensional nanocrystal fiber networks, J. Am. Chem. Soc. 124 (50) (2002) 15055-15063.
[79] P.D. Sawant, X.Y. Liu, Formation and novel thermomechanical processing of biocompatible soft materials, Chem. Mater. 14 (9) (2002) 3793-3798.
[80] N. Vandewalle, M. Ausloos, R. Cloots, Formation of nick instabilities due to particle clustering along crystal interfaces, Physical Review E: Statistical Physics, Plasmas, Fluids, and Related Interdisciplinary Topics 56 (4) (1997) 4042-4047.
[81] K. Kuroiwa, T. Shibata, A. Takada, N. Nemoto, N. Kimizuka, Heat-set gel-like networks of lipophilic Co(II) triazole complexes in organic media and their thermochromic structural transitions, J. Am. Chem. Soc. 126 (7) (2004) 2016-2021.
[82] M. Kreilgaard, Influence of microemulsions on cutaneous drug delivery, Adv. Drug Deliv. Rev. 54 Suppl 1 (2002) S77-98.
[83] J.S. Chu, R. Chandrasekharan, G.L. Amidon, N.D. Weiner, A.H. Goldberg, Viscometric study of polyacrylic acid systems as mucoadhesive sustained-release gels, Pharm. Res. 8 (11) (1991) 1408-1412.
[84] J. Kopecek, Polymer chemistry: Swell gels, Nature 417 (6887) (2002) 388-389, 391.
[85] T.J. Deming, Facile synthesis of block copolypeptides of defined architecture, Nature 390 (6658) (1997) 386-389.
[86] A.P. Nowak, V. Breedveld, L. Pakstis, B. Ozbas, D.J. Pine, D. Pochan, T.J. Deming, Rapidly recovering hydrogel scaffolds from self-assembling diblock copolypeptide amphiphiles, Nature 417 (6887) (2002) 424-428.
[87] S. Bhattacharya, Y. Krishnan-Ghosh, First report of phase selective gelation of oil from oil/water mixtures. Possible implications toward containing oil spills, Chem. Comm. (2) (2001) 185-186.
[88] Y. Ono, K. Nakashima, M. Sano, Y. Kanekiyo, K. Inoue, S. Shinkai, J. Hojo, Organic gels are useful as a template for the preparation of hollow fiber silica, Chem. Comm. (14) (1998) 1477-1478.
[89] K. Yabuuchi, E. Marfo-Owusu, T. Kato, A new urea gelator: Incorporation of intra- and intermolecular hydrogen bonding for stable 1D self-assembly, Org. Biomol. Chem. 1 (19) (2003) 3464-3469.
[90] S. Murdan, G. Gregoriadis, A.T. Florence, Novel sorbitan monostearate organogels, J. Pharm. Sci. 88 (6) (1999) 608-614.
[91] A.C. Couffin-Hoarau, A. Motulsky, P. Delmas, J.C. Leroux, *In situ*-forming pharmaceutical organogels based on the self-assembly of L-alanine derivatives, Pharm. Res. 21 (3) (2004) 454-457.

[92] J.C. Tiller, Increasing the local concentration of drugs by hydrogel formation, Angew. Chem. Int. Ed. Engl. 42 (27) (2003) 3072-3075.
[93] B. Xing, C.W. Yu, K.H. Chow, P.L. Ho, D. Fu, B. Xu, Hydrophobic interaction and hydrogen bonding cooperatively confer a vancomycin hydrogel: A potential candidate for biomaterials, J. Am. Chem. Soc. 124 (50) (2002) 14846-14847.
[94] S. Bhatnagar, S.P. Vyas, Organogel-based system for transdermal delivery of propranolol, J. Microencapsul. 11 (4) (1994) 431-438.
[95] Y.A. Shchipunov, E.V. Shumilina, W. Ulbricht, H. Hoffmann, The branching of reversed polymer-like micelles of lecithin by sugar-containing surfactants, J. Colloid Interface Sci. 211 (1) (1999) 81-88.
[96] H. Willimann, P. Walde, P.L. Luisi, A. Gazzaniga, F. Stroppolo, Lecithin organogel as matrix for transdermal transport of drugs, J. Pharm. Sci. 81 (9) (1992) 871-874.
[97] M.E. Stewart, D.T. Downing, A new 6-hydroxy-4-sphingenine-containing ceramide in human skin, J. Lipid Res. 40 (8) (1999) 1434-1439.
[98] K.J. Robson, M.E. Stewart, S. Michelsen, N.D. Lazo, D.T. Downing, 6-Hydroxy-4-sphingenine in human epidermal ceramides, J. Lipid Res. 35 (11) (1994) 2060-2068.
[99] S. Motta, M. Monti, S. Sesana, R. Caputo, S. Carelli, R. Ghidoni, Ceramide composition of the psoriatic scale, Biochim. Biophys. Acta 1182 (2) (1993) 147-151.
[100] J.A. Bouwstra, P.L. Honeywell-Nguyen, G.S. Gooris, M. Ponec, Structure of the skin barrier and its modulation by vesicular formulations, Prog. Lipid Res. 42 (1) (2003) 1-36.
[101] T.J. McIntosh, M.E. Stewart, D.T. Downing, X-ray diffraction analysis of isolated skin lipids: Reconstitution of intercellular lipid domains, Biochemistry 35 (12) (1996) 3649-3653.
[102] S. Raudenkolb, W. Hubner, W. Rettig, S. Wartewig, R.H. Neubert, Polymorphism of ceramide 3. Part 1: An investigation focused on the head group of N-octadecanoylphytosphingosine, Chem. Phys. Lipids 123 (1) (2003) 9-17.
[103] S. Raudenkolb, S. Wartewig, R.H. Neubert, Polymorphism of ceramide 3. Part 2: A vibrational spectroscopic and X-ray powder diffraction investigation of N-octadecanoyl phytosphingosine and the analogous specifically deuterated d(35) derivative, Chem. Phys. Lipids 124 (2) (2003) 89-101.
[104] P.W. Wertz, D.T. Downing, in: L.A. Goldsmith, Physiology, Biochemistry, and Molecular Biology of the Skin, 2nd ed., Volume 1, Oxford University Press, New York, 1991, pp. 205-231.
[105] P.W. Wertz, D.C. Swartzendruber, K.C. Madison, D.T. Downing, Composition and morphology of epidermal cyst lipids, J. Invest. Dermatol. 89 (4) (1987) 419-425.
[106] A.G. Staines, P. Sindelar, M.W.H. Coughtrie, B. Burchell, Farnesol is glucuronidated in human liver, kidney and intestine in vitro, and is a novel substrate for UGT2B7 and UGT1A1, Biochem. J. 384 (3) (2004) 637-645.
[107] L.U. Franklin, J.L. Pimentel, (Ximed Group PLC, USA), assignee. Terpene-containing food preservatives and antimicrobials. WO Patent 2003070181, 2003.

[108] B.F. Brehm-Stecher, E.A. Johnson, Sensitization of Staphylococcus aureus and Escherichia coli to antibiotics by the sesquiterpenoids nerolidol, farnesol, bisabolol, and apritone, Antimicrob. Agents Chemother. 47 (10) (2003) 3357-3360.
[109] Y. Inoue, A. Shiraishi, T. Hada, K. Hirose, H. Hamashima, J. Shimada, The antibacterial effects of terpene alcohols on Staphylococcus aureus and their mode of action, FEMS Microbiol. Lett. 237 (2) (2004) 325-331.
[110] G. Ramage, S.P. Saville, B.L. Wickes, J.L. Lopez-Ribot, Inhibition of Candida albicans biofilm formation by farnesol, a quorum-sensing molecule, Appl. Environ. Microbiol. 68 (11) (2002) 5459-5463.
[111] D. Bockmuehl, R. Breves, M. Weide, H.-M. Hoehne, M. Heinzel, (Henkel Kommanditgesellschaft Auf Aktien, Germany), assignee. Adhesion inhibition of molds. WO Patent 2003051126, 2003.
[112] T. Sato, T. Watanabe, T. Mikami, T. Matsumoto, Farnesol, a morphogenetic autoregulatory substance in the dimorphic fungus Candida albicans, inhibits hyphae growth through suppression of a mitogen-activated protein kinase cascade, Bio. Pharm. Bull. 27 (5) (2004) 751-752.
[113] N. Suzuki, M. Ozeki, M. Otani, K. Isobe, (Lion Corp., Japan), assignee. Composition for suppressing moldy smell in living rooms. Jp Patent 2004181064, 2004.
[114] Y.J. Hong, B.B. Jun, S. Lee, H.J. Seo, (Amorepacific Corporation, S. Korea). assignee. Fragrance composition having Cymbidium kanran makino flavor. Kr Patent 2002080085, 2002.
[115] S. Rubin, (USA), assignee. Regimen for acne treatment. US Patent 2004185022, 2004.
[116] W.V. Dittrich, (USA). assignee. Compositions containing Cetaphil for treating sunburned skin. US Patent 20050032877, 2005.
[117] G.W. Nam, U.D. Son, W.S. Park, S.H. Kim, C.H. Lee, B.G. Lee, (Amorepacific Corporation, S. Korea), assignee. Dermatological agent composition containing farnesol, skin moisturizing function enhancer and skin drying ameliorant. Kr Patent 2003082826, 2003.
[118] L.M. Patt, (Procyte Corporation, USA), assignee. Compositions and methods using peptide copper complex for treatment of psoriasis. US Patent 2004214749, 2004.
[119] J.-Y. Fang, C.-F. Hung, H.-C. Chiu, J.-J. Wang, T.-F. Chan, Efficacy and irritancy of enhancers on the *in-vitro* and *in-vivo* percutaneous absorption of curcumin, J. Pharm. Pharmacol. 55 (5) (2003) 593-601.
[120] T. Ghafourian, P. Zandasrar, H. Hamishekar, A. Nokhodchi, The effect of penetration enhancers on drug delivery through skin: A QSAR study, J. Control. Release 99 (1) (2004) 113-125.
[121] B.M. Forman, E. Goode, J. Chen, A.E. Oro, D.J. Bradley, T. Perlmann, D.J. Noonan, L.T. Burka, T. McMorris, W.W. Lamph, R.M. Evans, C. Weinberger, Identification of a nuclear receptor that is activated by farnesol metabolites, Cell 81 (5) (1995) 687-693.
[122] K. Hanley, L.G. Komuves, N.M. Bass, S.S. He, Y. Jiang, D. Crumrine, R. Appel, M. Friedman, J. Bettencourt, K. Min, P.M. Elias, M.L. Williams, K.R. Feingold,

Fetal epidermal differentiation and barrier development in vivo is accelerated by nuclear hormone receptor activators, J. Invest. Dermatol. 113 (5) (1999) 788-795.
[123] K. Hanley, L.G. Komuves, D.C. Ng, K. Schoonjans, S.S. He, P. Lau, D.D. Bikle, M.L. Williams, P.M. Elias, J. Auwerx, K.R. Feingold, Farnesol stimulates differentiation in epidermal keratinocytes via PPARalpha, J. Biol. Chem. 275 (15) (2000) 11484-11491.
[124] O.P. Bondar, G. Melnykovych, E.S. Rowe, Effects of farnesol on the thermotropic behavior of dimyristoylphosphatidylcholine, Chem. Phys. Lipids 74 (1) (1994) 93-98.
[125] A.C. Rowat, J.H. Davis, Farnesol-DMPC phase behaviour: A (2)H-NMR study, Biochim. Biophys. Acta 1661 (2) (2004) 178-187.
[126] J.S. LaKind, E.A. McKenna, R.P. Hubner, R.G. Tardiff, A review of the comparative mammalian toxicity of ethylene glycol and propylene glycol, Crit. Rev. Toxicol. 29 (4) (1999) 331-365.
[127] L.A. Goldsmith, Propylene glycol, Int. J. Dermatol. 17 (9) (1978) 703-705.
[128] A.C. Williams, B.W. Barry, Penetration enhancers, Adv. Drug Deliv. Rev. 56 (5) (2004) 603-618.
[129] I. Jelesarov, H.R. Bosshard, Isothermal titration calorimetry and differential scanning calorimetry as complementary tools to investigate the energetics of biomolecular recognition, J. Mol. Recognit. 12 (1) (1999) 3-18.
[130] I. Wadso, R.N. Goldberg, Standards in isothermal microcalorimetry, Pure Appl. Chem. 73 (10) (2001) 1625-1639.
[131] G. Zolotnitsky, U. Cogan, N. Adir, V. Solomon, G. Shoham, Y. Shoham, Mapping glycoside hydrolase substrate subsites by isothermal titration calorimetry, Proc. Natl. Acad. Sci. U. S. A. 101 (31) (2004) 11275-11280.
[132] E. Freire, Isothermal titration calorimetry: Controlling binding forces in lead optimization, Drug Discovery Today: Technologies 1 (3) (2004) 295-299.
[133] A.P. Brogan, W.R. Widger, D. Bensadek, I. Riba-Garcia, S.J. Gaskell, H. Kohn, Development of a technique to determine bicyclomycin-Rho binding and stoichiometry by isothermal titration calorimetry and mass spectrometry, J. Am. Chem. Soc. 127 (8) (2005) 2741-2751.
[134] A.M. Kligman, E. Christophers, Preparation of isolated sheets of human stratum corneum, Arch. Dermatol. 88 (1963) 702-705.
[135] M. Fujii, S. Buyuktimkin, N. Buyuktimkin, J.H. Rytting, Enhancement of skin permeation of miconazole by phospholipid and dodecyl 2-(N,N-dimethyl amino)propionate (DDAIP), Int. J. Pharm. 234 (1-2) (2002) 121-128.
[136] T. Henmi, M. Fujii, K. Kikuchi, N. Yamanobe, M. Matsumoto, Application of an oily gel formed by hydrogenated soybean phospholipids as a percutaneous absorption-type ointment base, Chem. Pharm. Bull. 42 (3) (1994) 651-655.
[137] G.L. Flynn, Y. Shah, S. Prakongpan, K.H. Kwan, W.I. Higuchi, A.F. Hofmann, Cholesterol solubility in organic solvents, J. Pharm. Sci. 68 (9) (1979) 1090-1097.
[138] M. Sznitowska, S. Janicki, A. Williams, S. Lau, A. Stolyhwo, pH-induced modifications to stratum corneum lipids investigated using thermal, spectroscopic, and chromatographic techniques, J. Pharm. Sci. 92 (1) (2003) 173-179.
[139] K. Thoma, R. Klimek, Photostabilization of drugs in dosage forms without protection from packaging materials, Int. J. Pharm. 67 (1991) 169-175.

[140] M. Olcer, G. Hakyemez, Investigations of some physicochemical properties of haloperidol which may affect its activity, J. Clin. Pharm. Ther. 13 (1998) 341-349.
[141] D.C. Montgomery, Design and Analysis of Experiments, John Wiley & Sons Inc, USA, 2001, pp. 223-224.
[142] P.D. Berger, R.E. Maurer, Experimental Design with Applications in Managment, Engineering and Sciences, Duxbury, USA, 2002, pp. 257-258.
[143] X.Y. Liu, P.D. Sawant, Mechanism of the formation of self-organized microstructures in soft functional materials, Adv. Mater. 14 (6) (2002) 421-426.
[144] L.E. Briggner, I. Wadso, Test and calibration processes for microcalorimeters, with special reference to heat conduction instruments used with aqueous systems, J. Biochem. Biophys. Methods 22 (2) (1991) 101-118.
[145] R. Karlsson, K. Lennart, A computer method for simultaneous calculation of equilibrium constants and enthalpy changes from calorimetric data, Chemica Scripta 9 (1976) 54-57.
[146] M.J. Cliff, J.E. Ladbury, A survey of the year 2002 literature on applications of isothermal titration calorimetry, J. Mol. Recognit. 16 (6) (2003) 383-391.
[147] G.A.F. Seber, C.J. Wild, Nonlinear Regression, John Wiley and Sons, USA, 2003, pp. 77-85.
[148] D.A. Schwindt, K.P. Wilhelm, H.I. Maibach, Water diffusion characteristics of human stratum corneum at different anatomical sites in vivo, J. Invest. Dermatol. 111 (3) (1998) 385-389.
[149] K.A. Holbrook, G.F. Odland, Regional differences in the thickness (cell layers) of the human stratum corneum: An ultrastructural analysis, J. Invest. Dermatol. 62 (4) (1974) 415-422.
[150] F. Yamashita, M. Hashida, Mechanistic and empirical modeling of skin permeation of drugs, Adv. Drug Deliv. Rev. 55 (9) (2003) 1185-1199.
[151] H. Schaefer, T.E. Redelmeier, F. Benech-Kieffer, The Skin and its Permeability, Cosmetic Science and Technology Series 19 (1999) 9-49.
[152] NORA. Developing dermal policy based on laboratory and field studies. http://www.cdc.gov/niosh/topics/skin/skinresearch.html. Accessed on May 1, 2005.
[153] D. Fitzpatrick, J. Corish, B. Hayes, Modelling skin permeability in risk assessment - the future, Chemosphere 55 (10) (2004) 1309-1314.
[154] H.K. Vaddi, P.C. Ho, Y.W. Chan, S.Y. Chan, Terpenes in ethanol: Haloperidol permeation and partition through human skin and stratum corneum changes, J. Control. Release 81 (1-2) (2002) 121-133.
[155] J.N. McDougal, J.L. Jurgens-Whitehead, Short-Term dermal absorption and penetration of chemicals from aqueous solutions: Theory and experiment, Risk Anal. 21 (4) (2001) 719-726.
[156] FDA. Part 352 - Sunscreen drug products for Over-The-Counter human use. http://www.accessdata.fda.gov/scripts/cdrh/cfdocs/cfcfr/CFRSearch.cfm?fr=352.10. Accessed on July 1, 2005.
[157] A.R. Pont, A.R. Charron, R.M. Brand, Active ingredients in sunscreens act as topical penetration enhancers for the herbicide 2,4-dichlorophenoxyacetic acid, Toxicol. Appl. Pharmacol. 195 (3) (2004) 348-354.

[158] B.S. Chuah, S.J. Clare, K.R. Franklin, G.C. Hough, G.A. Turner, (Unilever PLC, UK; Unilever NV; Hindustan Lever Limited), assignee. Antiperspirant compositions containing polymers, fatty alcohols and waxes. WO Patent 2001051020, 2001.
[159] D. Digirolamo, assignee. Wax free transparent lipstick composition. US Patent 2002085984, 2002.
[160] S. Momose, Y. Hagiwara, (Kobayashi Kose Co., Ltd., Japan), assignee. Cosmetics containing N-acylamino acid amide-encapsulated powders. Jp Patent 01172312, 1989.
[161] F. Tournilhac, (L'oreal, Fr.), assignee. Cosmetic compositions gelled with a dextrin ester. EU Patent 1386600, 2004.
[162] J.A. Bouwstra, P.L. Honeywell-Nguyen, Skin structure and mode of action of vesicles, Adv. Drug Deliv. Rev. 54 Suppl 1 (2002) S41-55.
[163] S. Engstrom, K. Ekelund, J. Engblom, L. Eriksson, E. Sparr, H. Wennerstrom, The skin barrier from a lipid perspective, Acta Derm. Venereol. Suppl. (Stockh). 208 (2000) 31-35.